การวิเคราะห์สมรรถนะของเซลล์เชื้อเพลิงชนิดออกไซด์แข็งร่วมกับกระบวนการรีฟอร์มมิงเอทานอล

นางสาวชลพรรณ ถนอมจิตร

วิทยานิพนธ์นี้เป็นส่วนหนึ่งของการศึกษาตามหลักสูตรปริญญาวิศวกรรมศาสตรมหาบัณฑิต
สาขาวิชาวิศวกรรมเคมี ภาควิชาวิศวกรรมเคมี
คณะวิศวกรรมศาสตร์ จุฬาลงกรณ์มหาวิทยาลัย
ปีการศึกษา 2554

PERFORMANCE ANALYSIS OF SOLID OXIDE FUEL CELL INTEGRATED WITH ETHANOL REFORMING PROCESS

Miss Chollaphan Thanomjit

A Thesis Submitted in Partial Fulfillment of the Requirements
for the Degree of Master of Engineering Program in Chemical Engineering
Department of Chemical Engineering
Faculty of Engineering
Chulalongkorn University
Academic Year 2011

Thesis Title	PERFORMANCE ANALYSIS OF SOLID OXIDE FUEL CELL INTEGRATED WITH ETHANOL REFORMING PROCESS
By	Miss Chollaphan Thanomjit
Field of Study	Chemical Engineering
Thesis Advisor	Assistant Professor Amornchai Arpornwichanop, D.Eng.

Accepted by the Faculty of Engineering, Chulalongkorn University in Partial Fulfillment of the Requirements for the Master's Degree

…… Dean of the Faculty of Engineering
(Associate Professor Boonsom Lerdhirunwong, Dr.Ing.)

THESIS COMMITTEE

…….. Chairman
(Associate Professor Muenduen Phisalaphong, Ph.D.)

……..……. Thesis Advisor
(Assistant Professor Amornchai Arpornwichanop, D.Eng.)

…….. Examiner
(Assistant Professor Soorathep Kheawhom, Ph.D.)

…….. External Examiner
(Woranee Paengjuntuek, D.Eng.)

ชลพรรณ ถนอมจิตร : การวิเคราะห์สมรรถนะของเซลล์เชื้อเพลิงชนิดออกไซด์แข็งร่วมกับกระบวนการรีฟอร์มมิงเอทานอล. (PERFORMANCE ANALYSIS OF SOLID OXIDE FUEL CELL INTEGRATED WITH ETHANOL REFORMING PROCESS) อ.ที่ปรึกษาวิทยานิพนธ์หลัก: ผศ.ดร.อมรชัย อาภรณ์วิชานพ, 126 หน้า.

งานวิจัยนี้นำเสนอการวิเคราะห์สมรรถนะของเซลล์เชื้อเพลิงชนิดออกไซด์แข็งร่วมกับกระบวนการรีฟอร์มมิงเอทานอลที่แตกต่างกันโดยพิจารณาประสิทธิภาพของระบบทั้งทางไฟฟ้าและทางความร้อน การวิเคราะห์เชิงเทอร์โมไดนามิกส์ของเซลล์เชื้อเพลิงชนิดออกไซด์แข็งที่ดำเนินการที่สภาวะคงตัวจะดำเนินการโดยใช้โปรแกรมจำลองกระบวนการร่วมกับแบบจำลองทางไฟฟ้าเคมีซึ่งพิจารณาค่าศักย์ไฟฟ้าสูญเสียที่เกิดขึ้นภายในเซลล์ทั้ง 3 ชนิด และกระบวนการรีฟอร์มมิงที่ศึกษาได้แก่ กระบวนการรีฟอร์มมิงด้วยไอน้ำ กระบวนการออกซิเดชันบางส่วนด้วยอากาศ และกระบวนการรีฟอร์มมิงแบบออโตเทอร์มัล จากการศึกษาพบว่าการเพิ่มอุณหภูมิของเครื่องรีฟอร์มเมอร์และเซลล์เชื้อเพลิงสามารถเพิ่มประสิทธิภาพทางไฟฟ้าของเซลล์เชื้อเพลิงได้ขณะที่อัตราส่วนเชิงโมลระหว่างไอน้ำต่อเอทานอลและอัตราส่วนเชิงโมลระหว่างออกซิเจนต่อเอทานอลควรมีค่าน้อย เมื่อพิจารณาที่อุณหภูมิรีฟอร์มเมอร์ 700 °C อุณหภูมิเซลล์เชื้อเพลิง 900 °C อัตราส่วนเชิงโมลระหว่างไอน้ำต่อเอทานอล 2 อัตราส่วนเชิงโมลระหว่างออกซิเจนต่อเอทานอล 0.1 พบว่าสมรรถนะของระบบเซลล์เชื้อเพลิงชนิดออกไซด์แข็งร่วมกับกระบวนการรีฟอร์มมิงด้วยไอน้ำมีค่ามากที่สุด เนื่องจากกระบวนการรีฟอร์มมิงด้วยไอน้ำสามารถให้ผลผลิตไฮโดเจนมากที่สุด แต่อย่างไรก็ตาม ในงานวิจัยนี้ได้พิจารณาการเกิดกระบวนการรีฟอร์มมิงด้วยไอน้ำของมีเทนภายในเซลล์เชื้อเพลิงด้วยจึงส่งผลให้สมรรถนะทางไฟฟ้าของทั้งสามระบบแตกต่างกันเพียงเล็กน้อยเท่านั้น

พิจารณาสมรรถนะทางความร้อนของระบบ พบว่าการเพิ่มขึ้นของอัตราส่วนเชิงโมลระหว่างออกซิเจนต่อเอทานอลทำให้ประสิทธิภาพทางความร้อนของระบบเพิ่มขึ้นเพราะการเพิ่มอัตราส่วนเชิงโมลระหว่างออกซิเจนต่อเอทานอลทำให้เกิดปฏิกิริยาออกซิเดชันด้วยอากาศซึ่งเป็นปฏิกิริยาคายความร้อนได้มากขึ้น ทำให้เมื่อเปรียบกันทั้งสามกระบวนการกระบวนการรีฟอร์มมิงแบบออกซิเดชันบางส่วนด้วยอากาศจึงให้ประสิทธิภาพทางความร้อนได้มากที่สุด นอกจากนี้ งานวิจัยนี้ได้นำเสนอการออกแบบโครงข่ายเครื่องแลกเปลี่ยนความร้อนภายในระบบทั้งสามระบบ โดยการวิเคราะห์พินช์ จากการวิเคราะห์พบว่า ทั้งสามระบบสามารถลดการใช้พลังงานความร้อนจากแหล่งภายนอกได้ทั้งหมด

ภาควิชา วิศวกรรมเคมี ลายมือชื่อนิสิต .....

สาขาวิชา วิศวกรรมเคมี ลายมือชื่อ อ.ที่ปรึกษาวิทยานิพนธ์หลัก .....

ปีการศึกษา 2554

5270265021 : MAJOR CHEMICAL ENGINEERING
KEYWORDS : SOLID OXIDE FUEL CELL/ REFORMING PROCESS/ ETHANOL/ PINCH ANALYSIS

CHOLLAPHAN THANOMJIT : PERFORMANCE ANALYSIS OF SOLID OXIDE FUEL CELL INTEGRATED WITH ETHANOL REFORMING PROCESS. ADVISOR: ASST. PROF. AMORNCHAI ARPORNWICHANOP, D.Eng., 126 pp.

This study presents a performance analysis of solid oxide fuel cell (SOFC) integrated with different ethanol reforming processes by considering both the electrical and the thermal performances. Thermodynamic analysis of the SOFC system operated under steady state condition was performed using a flowsheet simulator. Detailed electrochemical model taking into account all voltage losses (i.e., activation, concentration and ohmic losses) was considered. Three different ethanol reforming processes, i.e., steam reforming (SR), partial oxidation (POX) and autothermal reforming (ATR) were studied for hydrogen production. The simulation results showed that increases in reformer and fuel cell operating temperatures can improve the electrical performance of the SOFC system, whereas steam to ethanol ratio and oxygen to ethanol ratio should be minimized. When the reformer and SOFC are operated at temperature of 700 ^{o}C and 900 ^{o}C, steam to ethanol ratio of 2, and oxygen to ethanol ratio of 0.1, the electrical performance of SOFC-SR shows its maximum value because this reforming process gives the highest hydrogen yield. However, since an internal reforming of methane in the SOFC was also considered, the electrical performance of the SOFC system with different reforming systems is slightly different.

The thermal efficiency of SOFC systems can be improved by increasing the oxygen to ethanol ratio because the exothermic oxidation reaction is more pronounced producing more heat to the SOFC system. Furthermore, a design of heat exchanger network based on a pinch analysis was proposed in this study to reduce utility used in the SOFC systems.

Department : Chemical Engineering Student's Signature .....
Field of Study : Chemical Engineering Advisor's Signature .....
Academic Year : 2011

ACKNOWLEDGEMENTS

First and foremost I would like to express my sincerest appreciation to my thesis advisor, Assistant Professor Amornchai Arpornwichanop, for his inspiration and encouragement. He has guided me in both research and non-research areas that enabled me to successfully complete this work.

I am deeply grateful to the other members of my thesis committee, Associate Professor Muenduen Phisalaphong, Assistance Professor Soorathep Kheawhom and Dr. Woranee Paengjuntuek, for their time and useful comments on this thesis.

Financial support from the 90th Anniversary of Chulalongkorn University Fund (Ratchadaphiseksomphot Endowment Fund), the Thailand Research Fund (TRF-MASTER RESEARCH GRANTS) and the Computational Process Engineering Research Group, Special Task Force for Activating Research (STAR), Chulalongkorn University Centenary Academic Development Project is gratefully acknowledged.

I am also grateful to all my friends, colleagues in my research group in the Control and Systems Engineering Research Center and staffs in the Department of Chemical Engineering, Chulalongkorn University for their friendship and assistance.

Finally, I would like to express my gratitude to my beloved family whose invaluable love, sustenance, and patience. Also special thanks go to Mr. Jedsada Thampasato, who has helped, suggested, emboldened, resolved some obstacles and always beside me when I was exhausted. Without their support, my research would not have finished.

CONTENTS

PAGE

CHAPTER PAGE

CHAPTER PAGE

CHAPTER PAGE

LIST OF TABLES

LIST OF FIGURES

FIGURES PAGE

FIGURES PAGE

FIGURES PAGE

FIGURES PAGE

FIGURES PAGE

NOMENCLATURE

$dT_{\min}$	Minimum temperature difference [°C]
$D_{eff,\text{electrode}}$	Electrode effective diffusivity coefficient [$m^2\ s^{-1}$]
E^{OCV}	Open-circuit voltage [V]
E^0	Reversible open-circuit potential at standard temperature and pressure for the H_2 oxidation reaction [V]
$E_{\text{electrode}}$	Activation energy of the exchange current density [kJ mol^{-1}]
F	Faraday's constant [C mol^{-1}]
$F_{i,\text{in}}$	Molar flow rate of component i [kmol h^{-1}]
i	Current density [A m^{-2}]
$i_{0,\text{electrode}}$	Exchange current density [A m^{-2}]
$k_{\text{electrode}}$	Pre-exponential factor of the exchange current density [A m^{-2}]
LHV	Lower heating value [kJ mol^{-1}]
n	Number of electrons participating in the electrochemical reaction
P	pressure [atm]
p_i	Partial pressure of component i in relevant gas channel [bar]
$p_{i,\text{TPB}}$	Partial pressure of component i at relevant three phase boundary [bar]
P_{SOFC}	Power [kW]
Q_{consumed} ,	Consumed energy [kW]
Q_{produced}	Produced energy [kW]
R_{Ohm}	Total cell internal resistance [$\Omega\ m^2$]
$\Re$	Gas constant [kJ $mol^{-1}\ K^{-1}$]
T	Temperature [°C]
U_a	Air utilization
U_f	Fuel utilization

GREEK SYMBOLS

α	Tranfer coefficient
η_{act}	Activation overpotential [V]
η_{conc}	Concentration overpotential [V]
η_{ohm}	Ohmic overpotential [V]
η_{SOFC}	Electrical efficiency [%]
$\eta_{Thermal}$	Thermal efficiency [%]
$\tau_{anode}, \tau_{cathode}$	Anode and cathode thickness [m]
$\tau_{electrolyte}$	Electrolyte thickness [m]
$\sigma_{anode}, \sigma_{cathode}$	Electronic conductivity of the anode and cathode [Ω^{-1} m^{-1}]
$\sigma_{electrolyte}$	Ionic conductivity of the electrolyte [Ω^{-1} m^{-1}]

SUPSCRIPTS

act	Activation
EtOH	Ethanol
conc	Concentration
i	Component
Ohm	Ohmic
TPB	Three-phase boundary

CHAPTER I

INTRODUCTION

1.1 Introduction

In recent years, the demand for energy has continued to increase considerably because of rapid population growth and economic development, particularly in developing countries. In general, electrical energy is normally generated by burning fossil fuels (e.g., coal, oil, and natural gas) which cause the global warming owing to emission of greenhouse gases and air pollutants to the atmosphere. Moreover, fossil fuels are finite resource and nonrenewable energy. Therefore, the seeking for the new alternative energy sources which are renewable, sustainable and eco-friendly is crucial. There are currently alternative energy sources for electricity generation such as solar, wind and geothermal energies. However, these energy sources are limited to the area and the technological development.

Fuel cell is one of the most promising clean technologies for power generation. It can convert chemical energy in fuel directly into electricity and heat without combustion process, thus resulting in high efficiency and low air pollution over conventional internal combustion engines. Among various types of fuel cell, the solid oxide fuel cell (SOFC) has been received much attention due to it provides higher electrical efficiency than other fuel cells. Further, since it is operated at high temperatures (800-1000 ^{o}C), high quality exiting heat can be used as a heat source for cogeneration applications. SOFC also offers the feasibility of using various fuel types.

Currently, methane is the fuel of choice in fuel cell applications mainly in view of its high hydrogen to carbon ratio and readily available (Naidja et al., 2003). However, methane mostly derived from fossil fuel source (natural gas) has been increasingly of concern due to its high price and limited amount. SOFC running on synthesis gas from renewable energy source has drawn a great attention. Ethanol is considered an attractive green fuel for use in SOFC because it can be produced

renewably from various agriculture products. Thus, it is suitable for agricultural country as Thailand. In addition, the ethanol-to-hydrogen system has the significant advantage of being nearly CO_2 neutral, since the carbon dioxide released into the atmosphere during production process of hydrogen is absorbed in the growth of biomass. Therefore, the use of ethanol for energy production is an effective solution for the reduction of CO_2 emissions (Perna, 2007).

In general, technologies for production of hydrogen from ethanol are based on one of the following three major processes: steam reforming (SR), partial oxidation (POX), and autothermal reforming (ATR). The operating condition of each reforming process is different, which affects on hydrogen yield and energy consumption. As a result, there are a number of researchers concerning the hydrogen production from ethanol by using different reforming processes for use in SOFC. An analysis of the effects of important operating conditions such as reformer temperature, steam-to-ethanol ratio, and oxygen-to-ethanol ratio, on the efficiency of SOFC system is also the main topic of interest. Most of the studies focus on SR because it appears to be the most efficiency in terms of hydrogen yield, but it is an endothermic process which requires high energy consumption (Hernandez and Kafarov, 2009; Vourliotakis et al., 2009). Tsiakaras and Demin (2001) found that the use of different ethanol reforming processes in a SOFC system result in different hydrogen yield and thermal management. Similarly, Rabenstein and Hacker (2008) studied the thermodynamic of hydrogen production from ethanol by SR, POX and ATR and showed the total energy demand of each reforming processes is different. Therefore, the selection of ethanol reforming process is a very important and has a significant effect on the performance of SOFC. The previous studies on an ethanol reforming to hydrogen for fuel cells were conducted into two approaches. Firstly, a thermodynamic analysis of ethanol reforming process without SOFC system was proposed (Srisiriwat et al., 2006; Wang and Wang, 2008; Lima da Silva et al., 2009). Secondly, a SOFC system integrated with ethanol processor was analyzed thermodynamically, which SOFC stack model is developed in a programming language, such as FORTRAN, Visual Basic or C++ and linked to AspenPlus or any other commercial simulators as a user defined model or subroutines, whereas other components constituting the system employ existing unit operation models in the program (Riensche et al., 1998; Palsson et al., 2000; Lisbona

et al., 2007; Jamsak et al., 2009). To avoid such a complication, development of SOFC model by using existing functions and unit operation models in a process simulator is an interesting option. For instance, Zhang et al. (2005) simulated of a SOFC stack by using AspenPlus^{TM} unit operation models without linking other programs.

Considering performance improvement of SOFC, there are a few studies regarding a thermal management of SOFC plant. In general, the exhaust gas obtained from the SOFC is often used in cogeneration applications and bottoming cycles to improve the system efficiency, particularly the hybrid system combining a SOFC and a gas turbine (Palsson et al., 2000; Yang et al., 2006; Haseli et al., 2008). In this study, a heat recovery from the exhaust gas for used in the system is focused. Zhang et al. (2005) studied the SOFC integrated with steam reforming process by using natural gas as a fuel and found that a off-gas from an anode was recovered used for mixed with fuel streams and fed into an afterburner in order to produce more heat.

Few works have presented the design of heat exchanger networks for SOFC coupled to ethanol reforming process. Arteaga et al. (2009) studied simulation and heat integration of a SOFC system integrated with ethanol steam reforming process. A design of heat exchanger network of an ethanol fueled SOFC system based on a pinch analysis was proposed. Jamsak et al. (2009) analyzed the performance of a SOFC system integrated with a distillation column (SOFC-DIS) fed by bioethanol and studied the designs of the heat exchanger network for the SOFC-DIS system. As mentioned above, most of them have been based on a steam reforming technology (Arteaga et al., 2009; Jamsak et al., 2009; Casas et al., 2010), whereas few publications deal with autothermal reforming and partial oxidation reforming.

The objective of this work is to study a SOFC system integrated with ethanol processor by using existing AspenPlus functions and unit operation models. Thermodynamic analysis of hydrogen production from ethanol by using three different reforming processes such as SR, POX and ATR, are presented and compared. The effect of SOFC system and reforming operational parameters on the system performance is also considered. Furthermore, the designs of the heat exchanger network for the SOFC integrated with different ethanol reforming process are investigated by using of the pinch technology.

1.2 Objectives

1. To investigate and compare a performance of a SOFC system integrated with different ethanol reforming processes by using Aspen Plus and considering both the electrical and the thermal performances.
2. To design a SOFC system with heat integration by means of pinch analysis.

1.3 Scopes of work

1. A SOFC system integrated with an ethanol reforming process is studied. Simulation of each process is performed from a thermodynamic point of view by using existing AspenPlus functions and unit operation models.
2. Different ethanol reforming processes, i.e., steam reforming, partial oxidation, and autothermal reforming are investigated with respect to different operating parameters, including reforming temperature, steam to ethanol ratio, oxygen to ethanol ratio, and fuel utilization.
3. An appropriate reforming process for ethanol fueled SOFC system is determined by considering a system performance.
4. Heat integration of a SOFC system is considered based on a pinch analysis in order to improve a thermal efficiency of the SOFC system.

1.4 Expected benefits

1. Effects of key operating parameters and different ethanol reforming process on the performance of SOFC systems in terms of hydrogen production and electricity generation can be determined.
2. A suitable ethanol reforming process for a SOFC system is selected.
3. A SOFC system with heat integration to minimize external heat requirement can be designed.

1.5 Methodology of research

1. Study the principle of fuel cell, SOFC, hydrogen production from various reforming processes, and pinch analysis as well as review the literature relating to the thesis.
    - Mathematic model of SOFC including mass and energy balance, and electrochemical model**.**
    - Reactions within SOFC and reforming process (e.g., steam reforming, partial oxidation, and autothermal reforming).
    - Pinch analysis procedure.
2. Study AspenPlus simulator software.
3. Simulate a SOFC system integrated with an ethanol reforming process by using AspenPlus simulator and validate the simulation results with data reported in the literature (Zhang et al., 2005)
4. Investigate the effect of system and reforming operational parameters, i.e., reforming temperature, steam to ethanol ratio, oxygen to ethanol ratio, and fuel utilization for each reforming process, on SOFC system performance and determine an appropriate reforming process for ethanol fueled SOFC system.
5. Examine a heat integration of the SOFC system by means of pinch analysis in order to improve a thermal efficiency.
6. Analyze and summarize the simulation results.
7. Write thesis and prepare a manuscript for publication.

CHAPTER II

LITERATURE REVIEWS

Review of reforming technologies for hydrogen production from ethanol in view of thermodynamic is presented in this chapter. The reviews are focus on the performance of combined system between fuel cell and reforming technology such as steam reforming, partial oxidation and autothermal reforming. In addition, the studies in the thermal management of integrated system to improve the system efficiency are also reviewed in this chapter.

2.1 Modeling of solid oxide fuel cell

There have been several publications focusing on modeling the performance of SOFC. Among several publications, two approaches are presented, i.e., 1) modeling and simulating all process by using mathematical solver or programming language such as Visual Basic, C++, g*PROMS* and MATLAB (Chan et al, 2002; Aguiar et al., 2004; Arpornwichanop et al., 2009) and 2) simulating the system by using a process simulator, i.e., Pro/II, AspenPlus and Hysys (Riensche et al., 1998; Palsson et al., 2000; Zhang et al., 2005; Lisbona et al., 2007; Jamsak et al., 2009).

2.1.1 Mathematical solver-based system

In the former approach, a mathematical solver is used for calculating electrochemical model, mass and energy balance for the entire system. Chan et al. (2002) used Visual Basic program to analyzing SOFC system fed by hydrogen or methane. Mathematical models using in the simulation program consist of the electrochemical model and the heat exchanger model for SOFC. Energy and exergy analysis at the each node of the system were studied. Aguiar et al. (2004) used g*PROMS* to solve mathematical model of planar anode-supported intermediate

temperature SOFC stack with direct internal reforming operating on methane. The model consists of mass and energy balance, and electrochemical model. Arpornwichanop et al. (2009) used MATLAB to simulate of the one-dimensional isothermal SOFC model which composes of mass balance and electrochemical model. The model was validated with the experimental data of Huang et al. (2009) to ensure the simulation result. The simulation result showed that the model prediction agrees well with its corresponding experimental values when the exchange-current densities of anode and cathode and the ionic conductivity of electrolyte are adjusted appropriately.

2.1.2 Process simulator-based system

For the latter approach, a process simulator is used for simulate the SOFC system. It contains extensive and rigorous thermodynamic and physical property database and provides comprehensive built-in process models, thus it offers a convenient and time-saving for study chemical process. However, the SOFC stack has not been included in module of process simulator. Therefore, the SOFC stack model is developed in a programming language, such as FORTRAN, Visual Basic or C++ and linked to commercial simulator as a user defined model or subroutines (Zhang et al., 2005). Riensche et al. (1998) used Pro/II simulator to analyze the SOFC cogeneration power plant fed by natural gas. The process comprises of a pre-reformer, an air pre-heater, boiler, SOFC and afterburner. A SOFC stack is developed by FORTRAN subroutine. The other unit is performed on a process simulator. Palsson et al. (2000) used AspenPlus™ simulator to simulate the SOFC system combined with gas turbine using methane as a fuel. The system consist of an air pre-heater, compressor, mixer, pre-reformer, SOFC, burner, generator and turbine. The SOFC model has been integrated into the process as a user defined model by using FORTRAN, whereas other components constituting the system employ existing unit operation models in program. The SOFC model was compared with similar model found in the literature, the result obtained from the simulation showed that good agreement with the literature result. Similarly, Lisbona et al. (2007) and Jamsak et al.

(2009) that developed the SOFC stack model by using FORTRAN and linked into an AspenPlus™ simulator.

However, from the previous publications indicated that the study of SOFC stack is a complicated and time-consuming. Zhang et al. (2005) proposed a SOFC model by using AspenPlus™ unit operation models without linking other program. The system composes of a general unit, i.e., reformer, heat exchanger and afterburner, but a SOFC stack include an anode and a cathode by utilizing an equilibrium reactor module *Rgibbs* and a separator module *Sep*, respectively. There is no user-subroutine for SOFC stack to avoid an involved programming language. Accordingly, a SOFC stack was proposed by Zhang et al. is an interesting alternative.

2.2 Simulation studies of the ethanol reforming processes

In general, three major methods of ethanol reforming technologies have been proposed for convert ethanol to hydrogen rich gas, namely steam reforming (SR), partial oxidation (POX), and autothermal reforming (ATR). A simulation study of an ethanol reforming process for hydrogen production was presented in two approaches. Firstly, the simulation of ethanol reforming process without SOFC system (Srisiriwat et al., 2006; Wang and Wang, 2008; Lima da Silva et al., 2009) and secondly, the simulation of a SOFC system integrated with fuel/ethanol reforming process (Tsiakaras and Demin, 2001; Zhang et al., 2005; Lisbona et al., 2007; Srisiriwat, 2008; Arteaga-Perez et al., 2009; Hernandez and Kafarov, 2009).The objectives were to analyze the characteristics by performing a thermodynamic analysis and to investigate the optimum operating condition for each process.

2.2.1 Simulation of the ethanol reforming process without SOFC system

There are a number of researches involving a simulation study of the ethanol reforming process without SOFC system. Most of them focus on SR because it appears to be the most efficient in term of hydrogen yield (Garcia and Laborde, 1991; Vasudeva et al., 1996; Mas et al., 2006; Rossi et al., 2009; Lima da Silva et al., 2009). For instance, Lima da Silva et al. (2009) studied thermodynamic of ethanol/water

system using Gibbs energy minimization method in order to contribute to the comprehension of carbon formation conditions during ethanol steam reforming. In this study was preformed considering two different cases: ethanol conversion at very low and high contact times. The result indicated that at very low contact time, a system was highly favorable to carbon formation because ethylene and acetaldehyde were mainly product. On the other hand, carbon activities were much lower than and depended greatly on the inlet steam to ethanol ratio due to ethylene and acetaldehyde were converted into other species. However, a thermodynamic analysis of hydrogen production via POX using Gibbs free energy minimization method was investigated by Wang and Wang (2008). The effect of reaction temperature 500-1400 K, pressure 1-20 atm, oxygen-to-ethanol molar ratio 0-3 and nitrogen-to-ethanol molar ratio 0-100 were studied. The optimal conditions were obtained hydrogen yields of 86.25-94.98% which were 1070-1200 K, oxygen-to-ethanol molar ratio of 0.6-0.8 and 1 atm. Higher pressure and inert gases at nitrogen-to-ethanol molar ratio below 40 had a negative effect on the hydrogen yield, but further increasing the concentration of inert gases increases the hydrogen yield slightly. Coke formation was presented at lower temperature and oxygen-to-ethanol molar ratios. Moreover, there were a few studied on the hydrogen production from different reforming processes. Srisiriwat et al (2006) examined three different fuel processing system such as SR, POX and ATR for hydrogen production from ethanol by performing a thermodynamic analysis. The effect of temperature, steam to carbon molar ratio and air to carbon molar ratio, on the hydrogen yield was studied. The optimum operating conditions giving maximum hydrogen yield for each case was achieved. It was reported that hydrogen yield increase with increasing temperature and steam to carbon ratio for SR. At the optimum condition, the SR system requires the highest total energy whereas the POX system has the lowest ones. However, the SR system gives the maximum hydrogen yield and the ATR system gives the highest hydrogen to carbon monoxide ratio. Likewise, hydrogen production from ethanol by SR, POX and ATR was analyzed thermodynamically by Rabenstein and Hacker (2008). The influences of the process parameters over the following ranges: temperature 200- 1000 ^{o}C, steam to ethanol ratio of 0-10 and oxygen to ethanol ratio of 0-2.5 at atmospheric pressure were investigated. It was found that the favorable conditions of SR were 550-650 ^{o}C and

steam to ethanol ratios more than 4. The operation of POX predicted reasonable a hydrogen yield at oxygen to ethanol ratio below 1.5 and temperature above 600 ^{o}C. For ATR showed no strong effect on the hydrogen yield at increasing oxygen to ethanol ratio from 0-0.75, this method reduces the coke-formation and energy demand for reforming process.

2.2.2 Simulation of a SOFC system integrated with fuel/ethanol reforming process

The thermodynamic analysis of SOFC system fed by product from ethanol processors; SR, CO_2 reforming and POX was carried out by Tsiakaras and Demin (2001). The maximum efficiency of SOFC was calculated in the region of no carbon formation. The result revealed that the maximum SOFC efficiency was achieved at $T < 950$ K and $T > 1000$ K when using preliminary fuel reforming was SR.

Zhang et al. (2005) designed of SOFC stack model in AspenPlus™ using natural gas as fuel which was converted into hydrogen by external SR. The sensitivity analysis of the SOFC operating parameters: overall utilization factor, current density, power output and steam-carbon ratio were considered.

Lisbona et al. (2007) studied a SOFC system of 1 kW nominal focused on thermodynamic model, operated on natural gas. The system includes gases supply, a fuel processor, a heat management system, an after-burner and a power conditioning system. The effect of the deviation from the reference conditions of fuel utilization, gas temperature spring in fuel cell stack, anode off-gas recirculation rate, air inlet temperature and external pre-reforming reaction extent is analyzed.

The high temperature SOFC integrated with autothermal reformer (ATR) was performed from a thermodynamic point of view by Srisiriwat (2008). In this study, the effect of water-gas shift (WGS) reactor on the system performance was investigated. The result showed that the total electric power and overall efficiency of ATR-WGS-SOFC system were higher than ATR-SOFC system. The overall efficiency and electric power of system were increased owing to utilizing exhaust gas from the SOFC as heat source that no need the external energy source and incorporating a gas turbine.

The simulation and heat integration of a SOFC integrated with an ethanol steam reforming system were carried out by Arteaga-Perez et al. (2009). The effect of reforming reactor temperature, water to ethanol molar ratio and fuel utilization coefficient on the plant and HEN design were studied.

Hernandez and Kafarov (2009) designed an integrated process for sustainable electric energy production from bioethanol by steam reforming and SOFC. Three scenarios of process integration were simulated and its efficiencies were calculated to find the best process configuration. The effect of temperature and bioethanol:water molar ratio on process efficiency of the best process configuration were studied by sensitivity analysis. The study showed that the efficiency for the best process configuration was up to 52.6%. Sensitivity analysis indicated that the process efficiency increases with increasing reforming temperature and bioethanol:water molar ratio.

Even though, the simulation of SOFC system integrated with fuel/ethanol reforming process was numerous studied, a few studies on a SOFC system combined with POX or ATR has been carried out.

2.3 Thermal management of fuel cell integrated with reforming process

Fuel cell converts fuel chemical energy into electrical energy and heat as a by-product. SOFC operates at high temperature which the released high temperature off-gas. Usually, off-gas is used to preheat inlet gases, provide heat for external reforming, and use for incorporating a steam/gas turbine. Therefore, to improve the performance of fuel cell and minimize the external energy source to supply the system, thermal management or heat exchanger network (HEN) is the subject of interest. A number of publications are dealing with HEN. For example, Srisiriwat (2008) studied a high temperature SOFC integrated with autothermal reformer (ATR). The effect of water-gas shift (WGS) reactor on the system performance was investigated. The exhaust gas was split in two parts: the first one was to provide heat for cold streams and the second one was to produce electricity by using gas turbine. The result showed that the total electric power and overall efficiency of ATR-WGS-SOFC system were higher than ATR-SOFC system. The hot utilities are no need, the

cold utility can be reduced from 414.2 kW to be 161 kW and the overall efficiency was increased to be 56.6% when incorporating a gas turbine.

Jamsak et al. (2009) designed a thermally integrated bioethanol-fueled SOFC system integrated with distillation column (DIS). Useful heat source in the system, e.g. condenser duty and hot water from the bottom of the column and the cathode recirculation were taken into account to enhance the performance of SOFC-DIS. In addition, the effect of operating conditions on composite curve is also examined and lastly the designs of the heat exchanger network for the SOFC-DIS system are further investigated.

Arteaga-Perez et al. (2009) investigated the simulation and heat integration of a SOFC integrated with an ethanol steam reforming system. The effect of reforming reactor temperature, water to ethanol molar ratio and fuel utilization coefficient on the plant and HEN design were studied. The result showed that two heat exchanger networks were designed considering the influent of fuel utilization coefficient which found that at the fuel utilization coefficient 0.8, the reforming reactor temperature 823 K and water to ethanol molar ratio 1:5.5 reached into the auto-sustainability condition.

Hernandez and Kafarov (2009) designed an integrated process for sustainable electric energy production from bioethanol by steam reforming and SOFC. Three scenarios of process integration were simulated and its efficiencies were calculated to find the best process configuration. The influent of temperature and bioethanol:water molar ratio on process efficiency of the best process configuration were studied by sensitivity analysis. The study showed that the efficiency for the best process configuration was up to 52.6%. This process includes mass and heat integration by a recycle of SOFC anode outlet to steam reformer and heat exchanger network to pre-heat air, bioethanol and water by using post-combustion gas from SOFC. Sensitivity analysis indicated that the process efficiency increases with increasing reforming temperature and bioethanol:water molar ratio.

Most of the studies concerning SR though this process is an endothermic process which energy demending, whereas ATR process is identified to be effective route for hydrogen production as a result of it provides a reasonable compromise between energy efficiency and hydrogen yield.

CHAPTER III

THEORY

In this chapter briefly introduces the principle of fuel cells and type of fuel cells, which focus is on solid oxide fuel cell operation and performance. Ethanol reforming technologies, namely steam reforming, partial oxidation, and autothermal reforming and thermal management by pinch point analysis are also described.

3.1 Fuel Cell Description

3.1.1 Principle of fuel cells

Fuel cells are electrochemical devices that convert chemical energy in fuels into electrical energy (with heat as a byproduct) directly, promising power generation with high efficiency and low environmental impact. The basic physical structure, or building block, of a fuel cell consists of an electrolyte layer in contact with an anode and a cathode on either side as presented in Figure 3.1. Fuel that is continuously fed to the anode and oxidant that is continuously fed to the cathode are consumed. The electrochemical reactions take place at the electrodes, the electrons and ions flow via an external circuit and electrolyte, respectively. The charge carrier can either be an oxygen ion conductor or a hydrogen ion (proton) conductor, the major difference between the two types is the side where the water is produced inside the fuel cell namely the oxidant side in proton-conductor fuel cells and the fuel side in oxygen-ion-conductor ones. Generally, fuel cell reaction can be described by the following reaction:

$$H_2 + 1/2\, O_2 \rightarrow H_2O \qquad (3.1)$$

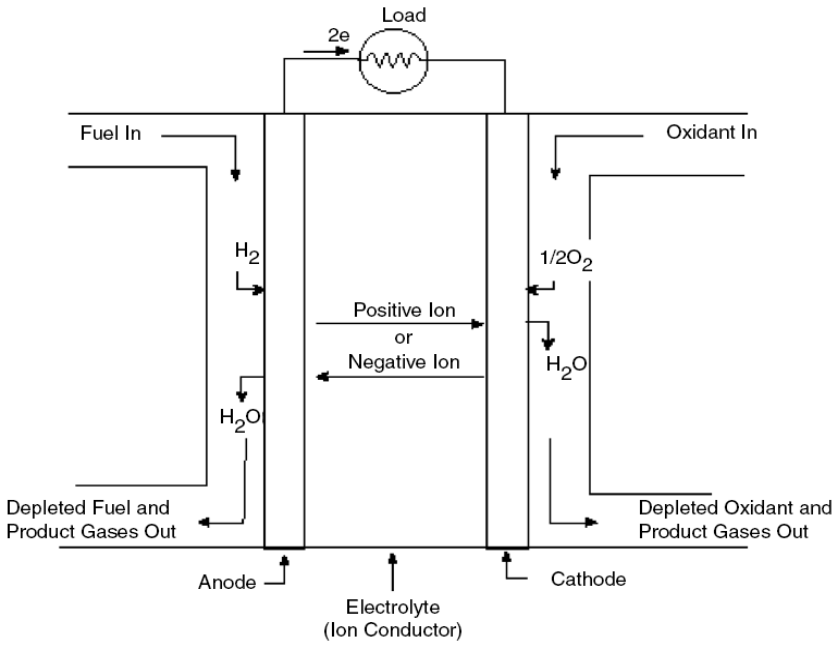

Figure 3.1 Schematic of an Individual Fuel Cell
(EG&G Technical Services, Inc., 2004)

Batteries and fuel cells are similar in term of convert chemical energy from electrochemical reactions directly into electricity. The major difference is that batteries which use the chemical energy stored within the reactants inside the batteries are considered as an energy storage device, whereas fuel cells which convert the chemical energy provided by an external fuel/oxidant mixture into electrical energy are regarded as an energy conversion device. Thus, batteries use chemical energy until the reactants are completely depleted and, at the end of their lifetime, they can either be recharged or thrown away. On the other hand, fuel cells can provide electrical output as long as with feed fuel and oxidant. (Sunggyu et al., 2007)

3.1.2 Type of Fuel Cells

Fuel cells can be classified by type of the electrolyte used in the cell which is significantly related to operating temperature. There are five major types of fuel cells. The information for each type of fuel cell is presented in Table 3.1

1. Polymer exchange membrane fuel cells (PEMFC).
2. Phosphoric acid fuel cell (PAFC).
3. Alkaline fuel cell (AFC).
4. Molten carbonate fuel cell (MCFC).
5. Solid oxide fuel cell (SOFC).

Table 3.1 Fuel Cell Characteristics (Hayre et al., 2006)

Fuel cell	Operating temperature	Charge carrier	Catalyst	Electrolyte	Electrode	Fuel compatibility	Reformer	Advantages	Disadvantages
PEMFC	80 ^{O}C	H^+	Platinum	Polymer membrane	Carbon based	H_2, methanol	External	- Highest power density - Suitable for portable applications - Good start – stop capabilities - Low operating temperature	Requirement for expensive catalysts High sensitivity to fuel impurity
PAFC	200 ^{O}C	H^+	Platinum	Liquid H_3PO_4 (immobilized)	Carbon based	H_2	External	- Low electrolyte cost - Excellent reliability - Mature technology	- Expensive platinum catalyst - Poisoning susceptibility - Corrosive liquid electrolyte
AFC	60 - 200 ^{O}C	OH^-	Platinum, Nickle	Liquid KOH (immobilized)	Carbon based	H_2	External	- Improved cathode performance - Low materials and electrolyte cost - Non-precious metal catalyst	- Must use pure H_2-O_2 Requirement for water removal at anode Expansive removal of CO_2 from fuel and air streams required
MCFC	650 ^{O}C	CO_3^{2-}	Nickle	Molten carbonate (liquid)	Stainless based	H_2, CH_4	External, Internal	- Fuel flexibility - Non-precious metal catalyst - High-quality waste heat	- Lifetime issues - Relatively expensive materials - Corrosive molten electrolyte
SOFC	600 - 1000 ^{O}C	O^{2-}	Perovskites (ceramic)	Ceramic (solid)	Ceramic based	H_2, CH_4,CO	External, Internal	- High efficiency - Variety of fuels - High-quality waste heat - Solid electrolyte - Relatively high power density	- High operating temperature - Sealing issues Relatively expensive cell components/fabrication

3.2 Solid Oxide Fuel Cell (SOFC)

3.2.1 SOFC operation

The SOFC is the least mature technology of fuel cells. The electrolyte in the SOFC is a solid, nonporous ceramic. The most popular SOFC electrolyte material is yttria-stabilized zirconia (YSZ), where ionic conduction by oxygen ions takes place in case of oxygen-ion-conductor fuel cell. Typically, the anode material is nickel-YSZ cermet and the cathode material is strontium-doped lanthanum manganite (LSM). The operating temperature of SOFC is extremely between 600 and 1000 ^{O}C. For this reason, it provides many advantages such as high efficiency, fuel flexibility, and high quality by-product heat for cogeneration or for use in a bottoming cycle. However, the issues of SOFC are sealing, material, and expensive fabrication.

During the SOFC operation, fuel and air are delivered to the anode and the cathode, respectively. At the cathode side, oxygen molecules diffuse into three phase boundary (TPB) and then react with electrons via a reduction reaction to form oxygen ions which then migrate through the ion-conducting electrolyte to the anode/electrolyte interface where react with hydrogen produced by the fuel. At the anode side, hydrogen gases which diffuse into the TPB do oxidation reaction with the oxygen ions to form water and electron as products. While releasing electrons that flow via an external circuit to the cathode/electrolyte interface, establishing direct current from electron flow, and finally react at cathode to form oxygen ions. Operation of SOFC is shown in the Figure 3-2. For a SOFC, the electrochemical reactions are:

Anode: $$H_2 + O^{2-} \rightarrow H_2O + 2e^- \quad (3.2)$$

Cathode: $$\tfrac{1}{2} O_2 + 2e^- \rightarrow O^{2-} \quad (3.3)$$

Overall cell reaction: $$H_2 + \tfrac{1}{2} O_2 \rightarrow H_2O \quad (3.1)$$

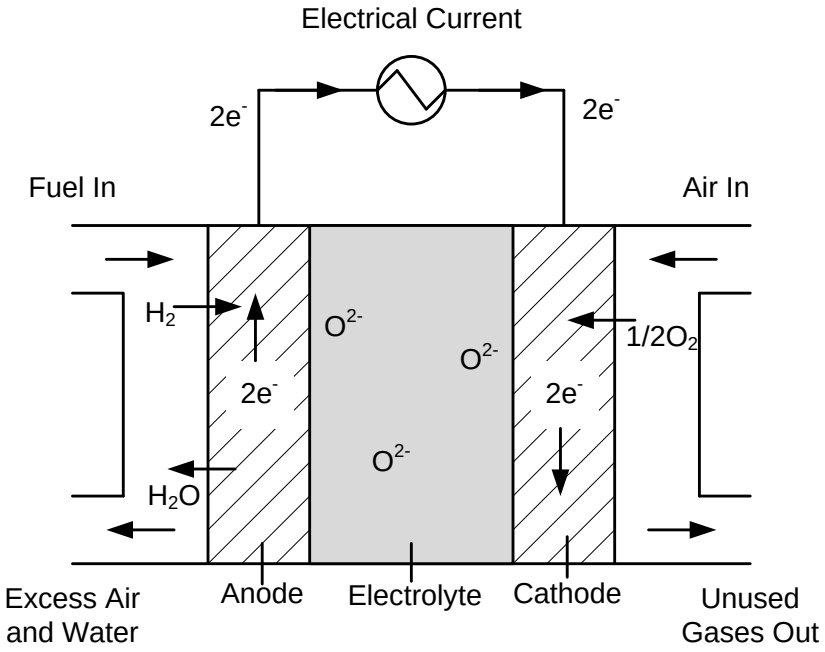

Figure 3.2 Electrochemical reaction within a SOFC

3.2.2 SOFC performance

3.2.2.1 The reversible voltage

The theoretical open-circuit voltage is also known as the "electromotive force" or "reversible cell voltage" or "reversible open-circuit potential (E^{OCV})". E^{OCV} is the maximum voltage that can be achieved by a fuel cell under specific operating conditions and equals to the electrical work done per unit charge on one mole of electrons. For an ideal system, the electrical work is equal to the molar Gibbs free energy of the reaction. E^{OCP} can be calculated by the following equation:

$$E^{\mathrm{OCV}} = -\frac{\Delta G}{nF} \tag{3.4}$$

Where ΔG is Gibbs free energy. n is a number of electrons passing around the circuit per mole of fuel that normally is equal to 2 and F is the Faraday's constant that always equals to 96,485.34 C/mol.

The change in Gibbs free energy is the change between products and reactants. In term of activities of products and reactants in the electrochemical reaction can be calculated as:

$$\Delta G = \Delta G^0 - \Re T \ln\left(\frac{a_{H_2} a_{O_2}^{1/2}}{a_{H_2O}}\right) \tag{3.5}$$

Where ΔG^0 is Gibbs free energy at standard pressure, while a is the activity and defined as the ratio of the partial pressure of the substance to standard reference pressure (P^0) of 1 bar.

$$a_{H_2} = \frac{p_{H_2}}{P^0},\ a_{H_2} = \frac{p_{H_2}}{P^0},\ a_{H_2O} = \frac{p_{H_2O}}{P^0}$$

If equation (3.5) is rewritten

$$\Delta G = \Delta G^0 - \Re T \ln\left(\frac{p_{H_2} p_{O_2}^{1/2}}{p_{H_2O}}\right) \tag{3.6}$$

Substituting the above equation into equation (3.4):

$$E^{OCV} = -\frac{\Delta G^0}{2F} + \frac{\Re T}{2F} \ln\left(\frac{p_{H_2} p_{O_2}^{1/2}}{p_{H_2O}}\right)$$

$$E^{OCV} = E^0 + \frac{\Re T}{2F} \ln\left(\frac{p_{H_2} p_{O_2}^{1/2}}{p_{H_2O}}\right) \tag{3.7}$$

Equation (3.7) is called Nernst equation. It depends on the gas composition and temperature at the electrodes. E^0 is the reversible open-circuit potential at standard temperature and pressure.

3.2.2.2 Actual fuel cell voltage

In real operation, the operating cell voltage (*V*) is always lower than the theoretical open-circuit voltage. As the current is drawn in the fuel cell, the cell voltage falls owing to irreversible losses. These irreversibilities commonly called polarizations or overpotentials cause a voltage drop and are functions of the current density. The current density is the convention used for fuel cells instead of the current and usually in unit of A/cm^2, meaning the current drawn per electrode/active area. There are three dominant overpotentials: ohmic overpotential, activation overpotential and concentration overpotential. The cell voltage can be written as in equation (3.8):

$$V = E^{\mathrm{OCV}} - \eta_{\mathrm{act,anode}} + \eta_{\mathrm{act,cathode}} + \eta_{\mathrm{ohm}} + \eta_{\mathrm{conc,anode}} + \eta_{\mathrm{conc,cathode}} \tag{3.8}$$

where η_{ohm} stands for the ohmic loss, $\eta_{\mathrm{conc,anode}}$ and $\eta_{\mathrm{conc,cathode}}$ represents the concentration overpotentials at the anode and the cathode, respectively, and $\eta_{\mathrm{act,anode}}$ and $\eta_{\mathrm{act,cathode}}$ stand for the activation overpotentials at the anode and the cathode, respectively. More detail of each voltage loss will be explained in the next section.

The actual cell potential is decreased from its equilibrium potential because of irreversible losses as shown in Figure 3.3. The current density is defined as the current produced per unit geometrical area of fuel cell.

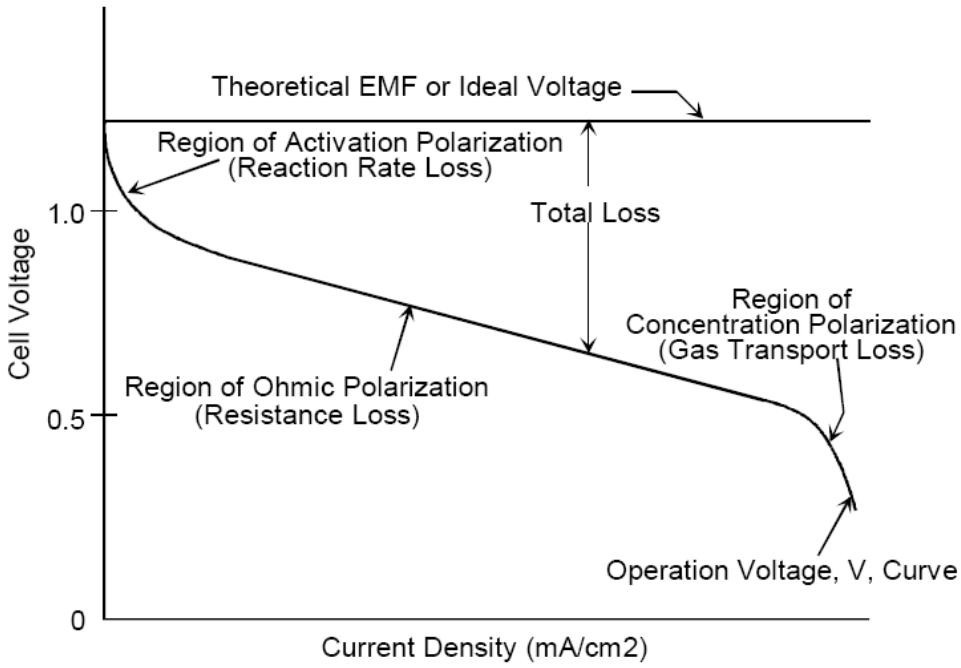

Figure 3.3 Ideal and Actual Fuel Cell Voltage/Current Characteristic (Hirschenhofer et al., 1998)

3.2.2.3 Ohmic loss

Ohmic loss/polarization/overpotential is caused by the resistance to conduction of ions through the electrolyte and electrons through the electrodes and current collectors and by contact resistance between cell components. Therefore, the conductivity of the materials plays a very important role for the ohmic polarization. Nevertheless, the ohmic polarizations are the simplest to understand and model. This loss is proportional to current density following the Ohm's law and can be written as:

$$n_{\text{Ohm}} = iR_{\text{Ohm}} \tag{3.9}$$

where i is the current density, R_{Ohm} is the total cell internal resistance that can be obtained from the measurement of cell resistances or be estimated from the effective distance between the cell components coupled with conductivity data. Here, R_{Ohm} is

calculated from the conductivity of the individual layers (assuming negligible contact resistances, cross-plane charge flow, and series connection of resistances) as given by:

$$R_{\text{Ohm}} = \frac{\tau_{\text{anode}}}{\sigma_{\text{anode}}} + \frac{\tau_{\text{electrolyte}}}{\sigma_{\text{electrolyte}}} + \frac{\tau_{\text{cathode}}}{\sigma_{\text{cathode}}} \tag{3.10}$$

where τ_{anode}, $\tau_{\text{electrolyte}}$ and τ_{cathode} represent the thickness of the anode, electrolyte, and cathode layers, respectively, σ_{anode} and σ_{cathode} is the electronic conductivity of the anode and cathode, and $\sigma_{\text{electrolyte}}$ is the ionic conductivity of the electrolyte.

3.2.2.4 Activation overpotential

Activation overpotential is the voltage loss that relates to the kinetics of reactions taking place on the electrode surface. Activation overpotentials can be computed by the nonlinear Butler-Volmer equation:

$$i = i_{0,\text{electrode}}\left[\exp\left(\frac{\alpha nF}{\Re T}\eta_{\text{act,electrode}}\right) - \exp\left(-\frac{(1-\alpha)nF}{\Re T}\eta_{\text{act,electrode}}\right)\right] \tag{3.11}$$

$\text{electrode} \in \{\text{anode,cathode}\}$

where, α represents the transfer coefficient (usually taken to be 0.5), n is the number of electrons transferred in the single elementary rate-limiting reaction step, and $i_{0,\text{electrode}}$ is the exchange current density at equilibrium condition which depend on the operating temperature as in equation (3.12).

$$i_{0,\text{electrode}} = \frac{\Re T}{nF} k_{\text{electrode}} \exp\left(-\frac{E_{\text{electrode}}}{\Re T}\right) \tag{3.12}$$

$\text{electrode} \in \{\text{anode,cathode}\}$

3.2.2.5 Concentration overpotential

Concentration overpotential is the voltage loss associated with the transport of gaseous reactants through porous electrodes. Due to gradual consumption of the fuel and the oxidant, their fraction will decrease in the fuel and oxidant streams respectively. However, when the current is flowing and concentration gradients develop, the species concentrations at TPB are different from bulk concentrations. In such a case, the corresponding Nernst equation is written as shown in equation (3.13)

$$E_{\mathrm{TPB}}^{\mathrm{OCV}} = E^{0} + \frac{\Re T}{2F}\ln\left(\frac{p_{\mathrm{H_2,TPB}}\, p_{\mathrm{O_2,TPB}}^{1/2}}{p_{\mathrm{H_2O,TPB}}}\right) \tag{3.13}$$

The difference of the reactant concentration at the bulk phase (equation (3.7)) and the electrode-electrolyte interface, TPB (equation (3.13)) results in the concentration overpotential which can be expressed as follows:

$$\eta_{\mathrm{conc}} = E^{\mathrm{OCV}} - E_{\mathrm{TPB}}^{\mathrm{OCV}}$$

$$n_{\mathrm{conc}} = \frac{\Re T}{2F}\ln\left(\frac{p_{\mathrm{H_2O,TPB}}\, p_{\mathrm{H_2}}}{p_{\mathrm{H_2O}}\, p_{\mathrm{H_2,TPB}}}\right) + \frac{\Re T}{4F}\ln\left(\frac{p_{\mathrm{O_2}}}{p_{\mathrm{O_2,TPB}}}\right) \tag{3.14}$$

where the first term on the right-hand side of equation (3.14) refers to the anodic concentration overpotential, $\eta_{\mathrm{conc,anode}}$, the second term refers to the cathodic concentration overpotential, $\eta_{\mathrm{conc,cathode}}$, and $p_{\mathrm{H_2,TPB}}$, $p_{\mathrm{H_2O,TPB}}$, and $p_{\mathrm{O_2,TPB}}$ represent the partial pressures of hydrogen, water, and oxygen at TPB respectively.

3.2.2.6 Fuel cell efficiency

The maximum theoretical work is equal to the change in molar Gibbs free energy of the reaction:

$$\Delta G = \Delta H - T\Delta S \tag{3.15}$$

where ΔH is the enthalpy change or the total energy that can be obtained theoretically, T is the temperature in Kelvin and ΔS is the entropy change by the reaction.

The maximum energy can be converted into electrical energy is the enthalpy change of the reaction denoted as ΔH. In other words, all of the energy that the fuel possesses is converted into electrical energy theoretically. The theoretical voltage (V_{theor}) can be calculated by equation (3.16):

$$V_{\text{theor}} = \frac{\Delta H}{2F} \tag{3.16}$$

Therefore, the fuel cell efficiency can be written according to cell voltage as:

$$\varepsilon = \frac{V}{V_{\text{theor}}} \tag{3.17}$$

However, when a SOFC is running, not all the fuel fed is consumed. Some fuel remains unused. So, the fuel utilization factor can be defined as:

$$U_{\text{fuel}} = \frac{\text{fuel consumed in the cell}}{\text{fuel suplied to the cell}} \tag{3.18}$$

Then, the fuel cell efficiency can be rewritten by adding the fuel utilization factor U_{fuel}:

$$\varepsilon = U_{\text{fuel}} \times \frac{V}{V_{\text{theor}}} \tag{3.19}$$

3.3 Hydrogen reforming technologies

3.3.1 Ethanol

Ethanol, is an alcohol, is a clear, colorless liquid with a characteristic, flammable and high octane number (99.8 % ethanol has an octane number of 113). Ethanol has widespread use as a solvent of substances intended for human contact or consumption, including scents, flavorings, colorings, and medicines. In chemistry, it is both an essential solvent and a feedstock for the synthesis of other products. It has a long history as a fuel for heat and light, and more recently as a fuel for internal combustion engines. It can be mixed with petrol; this increases the octane number of petrol such as gasohol.

In this research, ethanol (EtOH) is considered to be a promising candidate as a source for renewable hydrogen because it can be produced renewably through the fermentation of biomass, waste material from agro-industries, or even organic fraction of municipal solid waste. It presents several advantages over other fuels related to natural availability, easy to store, handle, and transport in a safe way due to its lower toxicity and volatility. The properties of ethanol used as fuel shown in Table 3.2.

Table 3.2 The properties of ethanol used as fuel.

Properties	**Value**
Name	Ethanol or Ethyl Alcohol
Chemical formula	C_2H_5OH
Molecular weight	46.07 g/mol
Density	0.789 g/cm^3
Melting point	-114.3°C
Boiling point	78.4°C
Viscosity	1.20 mPa·s (cP) at 20.0°C
Flash point	13°C
Lower heating value (LHV)	1,230 kJ/mole of ethanol
Higher heating value (HHV)	1,300 kJ/mole of ethanol

3.3.2 Ethanol reforming technologies

Recently, thermo-chemical process as reforming process has received considerable attention due to it is a promising technology for use in commercial. In general, three reforming processes are widely known for converted ethanol into hydrogen such as

- Steam reforming
- Partial oxidation
- Autothermal reforming

Each reforming technology has different of operating method, constraint, advantage, and disadvantage with regard to the economics, environment and other concerns.

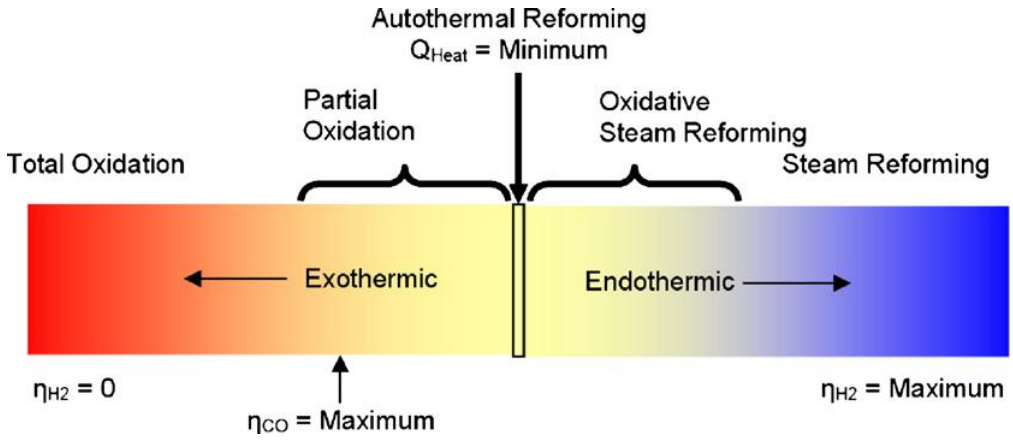

Figure 3.4 Different operating conditions for ethanol reforming. (Rabenstein and Hacker, 2008)

Figure 3.4 discusses the space of operation for a fuel processor for hydrogen production. The operation-mode for the reformer can be very different, with wide implications on the composition of the reformer effluent and the energy demand, necessary to generate the hydrogen-rich gas. (Rabenstein and Hacker, 2008)

3.3.2.1 Steam reforming of ethanol

Ethanol steam reforming is an endothermic process that combines a fuel with steam over catalyst at high temperature, thus ethanol is converted into gaseous mixture of H_2O, CO, CO_2, CH_4 and unreacted EtOH as well as H_2 as main species. The operating temperature is between 700 and 1000 ^{O}C. It is well known that the reaction pathway which describes the ethanol steam reforming is highly dependent on the operating conditions, the catalyst formulation, and the redox characteristic of the support material. (Arteaga-Perez et al., 2009) In practice, the following reactions are usually proposed as the main possible reactions to describe the ethanol steam reforming:

Ethanol steam reforming: $C_2H_5OH + H_2O \leftrightarrow 2\,CO + 4H_2$ (3.20)

Methanation: $CO + 3\,H_2 \leftrightarrow CH_4 + H_2O$ (3.21)

Water gas shift reaction: $CO + H_2O \leftrightarrow CO_2 + H_2$ (3.22)

However, the possible ideal pathway of ethanol steam reforming, which shows the highest hydrogen production, will be occurred when sufficient steam supply as shown in equation (3.23):

$$C_2H_5OH + 3H_2O \leftrightarrow 2\,CO_2 + 6H_2 \quad (3.23)$$

Moreover, undesired pathway such as dehydration, dehydrogenation, and decomposition of ethanol, which produce intermediate products namely ethylene, as well as acetaldehyde, can be occurred during reforming reaction. In order to maximize hydrogen production, it is crucial to ensure sufficient supply of steam and to minimize ethanol dehydration and decomposition. (Ni et al., 2007)

Ethanol steam reforming is the most widely used owing to the higher hydrogen production yield and lower rate of side reactions, but this process has some disadvantages, such as slow start-up, energy-consuming and severe catalyst deactivation.

3.3.2.2 Partial oxidation of ethanol

Ethanol partial oxidation is an exothermic process that a fuel and some oxygen (or air) are combined in proportions to partially combust the fuel into a gaseous mixture of CO and H_2. This process can be carried out catalytically or noncatalytically. The noncatalytic process and catalytic process are operated at high temperatures (1100–1500 ^{O}C) and low temperatures (600–900^{O}C), respectively.

The partial oxidation of ethanol (POE) for hydrogen production involves a complex multiple reaction system, and the purity of the hydrogen product is affected by many undesirable side reactions. Therefore, the yield of hydrogen depends in a complex manner on the process variables such as pressure, temperature, oxygen-to-ethanol molar ratio, etc. (Wang and Wang, 2008). In practice, the following reactions are usually proposed as the main possible reactions to describe the ethanol partial oxidation:

Ethanol partial oxidation:	$C_2H_5OH + \frac{1}{2}O_2 \leftrightarrow 2\,CO + 3H_2$	(3.24)
Methanation:	$CO + 3\,H_2 \leftrightarrow CH_4 + H_2O$	(3.21)
Water gas shift reaction:	$CO + H_2O \leftrightarrow CO_2 + H_2$	(3.22)

The advantages of ethanol partial oxidation are fast start-up time and system complexity because it does not need for external heat source and a water balance. On the other hand, this process has drawback that lowest hydrogen production yield.

3.3.2.3 Autothermal reforming of ethanol

Autothermal reforming, also called oxidative steam reforming, is an exothermic process, which combines the steam reforming and the partial oxidation in a single process. Thus, reactants of this process include fuel, steam, and oxygen (or air). The operating temperature range is between 600 and 900 ^{O}C. Autothermal reforming has received considerable attention since it has the merit of the balance of

specific heat for steam reforming and partial oxidation processes. The total reaction of autothermal reforming of ethanol can be written as:
Ethanol autothermal reforming:

$$C_2H_5OH + 2H_2O + \frac{1}{2}O_2 \leftrightarrow 2\,CO_2 + 5H_2 \quad (3.25)$$

The autothermal reforming can start-up quickly and continue without an addition/external heat supply. The overall hydrogen production yield is lower than steam reforming process.

3.4 Thermal management

It is well-known that fuel cell cannot convert fuel chemical energy into electrical energy totally, energy not converted to electrical energy is dissipated as heat. Especially, SOFC operates at high temperature which the released heat by the system is also high temperature and is often used beneficially. Such as to preheat inlet gases, provide heat for external reforming, and use for incorporating a steam/gas turbine. Therefore, thermal management is used to manage heat among the fuel cell so as to maximize heat recovery. In this study, pinch analysis is used for managing heat in fuel cell.

3.4.1 Pinch analysis

Pinch analysis is a systematic method to optimize the overall heat recovery within a process plant by maximizing heat recovery and reducing the external utility loads based on the First and Second Laws of Thermodynamics. To meet the goal of maximum heat recovery or minimum energy requirement (MER) an appropriate heat exchanger network (HEN) is designed. Steps of pinch analysis can be expressed as follows:

1. Identify hot, cold and utility streams in the system.

- A hot stream is a flowing fluid that needs to be cooled or is available to be cooled, but does not change in composition.
- A cold stream is flowing fluid that needs to be heated but does not change in composition.
- A utility stream is used to heat or cool process stream when heat exchange between process streams is not practical.

2. Determine thermal data for these streams.

For each hot, cold and utility stream identified, thermal data on the streams must be compiled. These data include the following:

- The supply temperature (T_{in}), the initial temperature at which the stream is available before entering a heat excheanger.
- The target temperature (T_{out}), the desired outlet temperature for the stream upon exiting a heat exchanger.
- The heat capacity flow rate ($\dot{m}c_p$), the product of the stream mass flow rate ($\dot{m}$) in kg/s and the specific heat of the fluid in the stream (c_p) in kJ/kg ^{o}C, whereby the specific heat of the fluid is assumed constant over the temperature range. The heat capacity flow rate can be expressed as follows:

$$\dot{m}c_p = \dot{m} \times c_p \tag{3.26}$$

- The change in enthalpy $(d\dot{H})$ in the stream passing through the heat exchanger is given by the First Law of Thermodynamics.

$$d\dot{H} = \dot{Q} + \dot{W} \tag{3.27}$$

Since a heat exchanger performs no mechanical work $(\dot{W} = 0)$ so that

$$d\dot{H} = \dot{Q} = \dot{m} c_p (T_{in} - T_{out}) \tag{3.28}$$

where $\dot{Q}$ represents the flow of heat into or out of stream.

3. Select a minimum acceptable temperature difference ($dT_{\min,set}$) between hot and cold streams.

The design of heat transfer equipment must always base on the Second Law of Thermodynamics that prohibits any temperature crossover between hot and cold stream. Heat may only flow from hot stream to cold stream. As a result, within a heat exchanger, the hot-stream temperature cannot dip below the cold-stream temperature, and a cold stream cannot be heated to temperature higher than the supply temperature of hot stream. A minimum temperature difference ($dT_{\min}$) to drive heat transfer is represented;

$$T_H - T_C \geq dT_{\min} \tag{3.29}$$

where T_H and T_C represents hot-stream and cold-stream temperature respectively.

The minimum temperature difference observed between streams at any length along the heat exchanger referred to as the "pinch point temperature". For the purpose of pinch point analysis, $dT_{\min}$ is often set at desired value, between 3 and 40 ^{o}C, depending on the type of heat exchanger and the application.

4. Construct Composite curves and check $dT_{\min} > dT_{\min,set}$.

Composite curves are temperature-enthalpy diagrams (T-H) which show the change in temperature versus the change in enthalpy for hot and cold composite curves. On the T-H diagram, any stream with a constant c_p is represented by straight line from T_{in} to T_{out}, as illustrated in Figure 3.5.

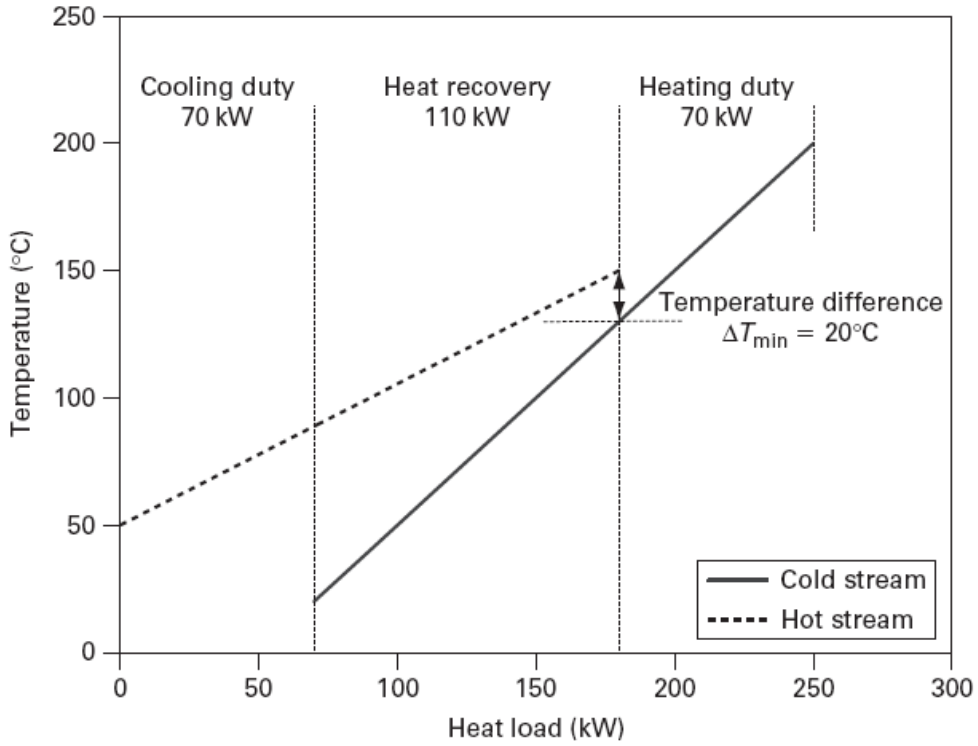

Figure 3.5 Streams plot on T-H diagram with $dT_{\min} = 20^{o}C$ (Ian C Kemp, 2007).

Figure 3.5 shows the hot and cold streams for our example plotted on the T-H diagram. Note that the hot stream is represented by the line with the arrowhead pointing to the left, and the cold stream *vice versa*. For feasible heat exchange between the two, the hot stream must at all points be hotter than the cold stream, so it should be plotted above the cold stream. The heat exchange between the hot and cold streams is equal the stream enthalpy change in equation (3.28), so the inverse of the slope of the curve is heat capacity flow rate. The overlap between the composite curves represents the maximum amount of heat recovery possible within the process. The "overshoot" at the bottom of the hot composite represents the minimum amount of external cooling required and the "overshoot" at the top of the cold composite represents the minimum amount of external heating (Ian C Kemp, 2007).

The pinch design rules to achieve minimum utility targets are:

- Do not transfer heat across the pinch.
- Do not use cold utilities above the pinch.
- Do not use hot utilities below the pinch.

5. If $dT_{min} < dT_{min,set}$ change heat exchanger orientation.

If the actual pinch point temperature is less than $dT_{min,set}$, the hot and cold streams must be reoriented. For the new orientation, a new T-H diagram is developed and the pinch point temperature and location within the heating network are recalculated.

CHAPTER IV

MODELING OF SOFC

A mathematical model is an essential aspect of fuel cell technology design and development process. It facilitates research and development by minimizing the need of repetitive and costly experimentation. The model can provide thorough understanding of the complex reaction and transport processes within fuel cells and be used to examine the effects of operating conditions and design parameters on fuel cell performances. The modeling results can be used to optimize cell and stack designs and select optimal operational conditions. Moreover, the simulation results are validated to ensure the SOFC model with the experimental data of Zhao and Virkar (2005) and simulation data of Zhang et al. (2005).

This chapter presents a solid oxide fuel cell (SOFC) model by using Aspen Plus simulator to simplify in thermodynamics detail and sensitivity analysis on the performance of SOFC. However, this simulation by using Aspen Plus takes the advantage of convenience to expand scope of work including the SOFC and the reforming process and ease for balance of plant. The first Section 4.1 shows the configuration of SOFC system integrated with ethanol reforming process used in this study. Details of an electrochemical model are described in Section 4.2 and Section 4.3 demonstrates the SOFC model and electrochemical model validations. Further, Section 4.4 explains the key parameters used to evaluate the system efficiency.

4.1 Model Configuration

4.1.1 Solid oxide fuel cell system configuration

A schematic of the SOFC system integrated with ethanol steam reforming process (SOFC-SR) in Aspen Plus is shown in Figure 4.1. It consists of three main parts: (1) an ethanol reforming process which ethanol is converted into hydrogen-rich

gas, (2) a SOFC that subsequently generates electricity and (3) an afterburner where the residual fuel from SOFC is combusted in order to supply heat to other heat requiring parts of the SOFC system. The ethanol and reforming agents (steam, air and combined air/steam) provided at 25 ◦C are firstly feed to vaporizer and preheater that are vaporized into gas phase and preheated at 400 ◦C, prior to enter the reformer. The reformer is a reactor, where steam and/or air must be considered, respectively, when steam reforming, partial oxidation or autothermal reforming is the reforming process, in order to produces a hydrogen-rich gas and then feeding into a SOFC. SOFC generates the electrical power and steam by the electrochemical reaction between hydrogen and oxygen in air, which is preheated at 800 ◦C before feeding to cell. In general, SOFC cannot electrochemically utilize 100 % of the fuel, therefore unreacted fuel is sent to the afterburner where the unreacted fuel is combusted with part of the excess air. The exhaust gas from afterburner is produced more heat that can be thermally utilized for other heat-requiring parts of the SOFC system. The models of the ethanol reforming process, SOFC and afterburner are discussed separately.

The assumptions are considered to simulate the SOFC system as show in the following:

- Steady state operation is considered.
- The SOFC stack model is equilibrium.
- All gaseous components behave as an ideal gas.
- Hydrogen is only electrochemically oxidized.
- SOFC is configured to be planar.
- Pressure drop is negligible.
- Heat loss from all units in the system is negligible.
- SOFC has a uniform temperature.

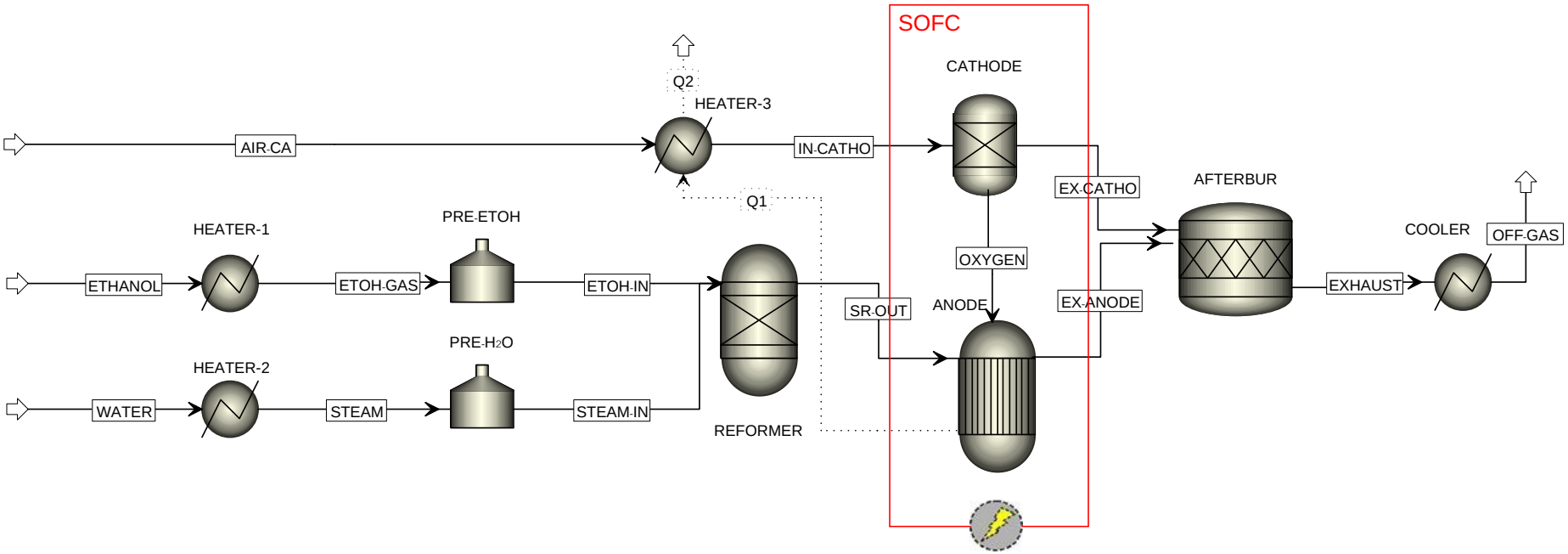

Figure 4.1 A schematic of the SOFC system integrated with ethanol steam reforming process**.**

4.1.2 Ethanol reforming process

Ethanol reforming process where ethanol is converted into gaseous mixture of H_2O, CO, CO_2, CH_4 and unreacted EtOH as well as H_2 as main species. Other hydrocarbon compounds such as acetaldehyde and ethylene are considered intermediate products, which are quickly converted to more simple molecules at high contact times and temperatures (>673 K) (Arteaga et al., 2009). A SOFC system integrated with different ethanol reforming processes (i.e., steam reforming, partial oxidation and autothermal reforming) was evaluated. A reforming process is generally comprised of a preheater and a reformer reactor. The ethanol and reforming agents (steam, air and combined air/steam) are vaporized and heated up before enter a reformer ("REFORMER") which uses the equilibrium reactor module *Rgibbs*. The reactor is supposed to be operated isothermal conditions. The reactions are assumed that occur at equilibrium condition. The direct minimization of the Gibbs free energy is used to compute the equilibrium composition of synthesis gas. The equation of state used in the calculation was based on the Peng-Robinson (PEN-ROB) method. The main reactions are ethanol steam reforming and ethanol oxidation whereas methane steam reforming, methane oxidation, water gas shift (WSGR) and methanation reactions are considered as side reactions. The reactions occured in reformer for each process can be summarized as:

SOFC-SR

Ethanol SR:	$C_2H_5OH + 3H_2O \rightarrow 6H_2 + 2CO_2$	(R1a)
	$C_2H_5OH + H_2O \rightarrow 2H_2 + CO_2 + CH_4$	(R1b)
Methane SR:	$CH_4 + H_2O \leftrightarrow CO + 3H_2$	(R2)
WGSR:	$CO + H_2O \leftrightarrow CO_2 + H_2$	(R3)

SOFC-POX

Ethanol POX: $C_2H_5OH + \frac{1}{2}O_2 \rightarrow 3H_2 + 2CO$ (R4a)

$C_2H_5OH + 3O_2 \rightarrow 3H_2O + 2CO_2$ (R4b)

Methanation: $CO + 3H_2 \leftrightarrow CH_4 + H_2O$ (R5)

Methane POX: $CH_4 + \frac{1}{2}O_2 \leftrightarrow CO + 2H_2$ (R6)

WGSR: $CO + H_2O \leftrightarrow CO_2 + H_2$ (R3)

SOFC-ATR

Ethanol SR: $C_2H_5OH + 3H_2O \rightarrow 6H_2 + CO_2$ (R1a)

$C_2H_5OH + H_2O \rightarrow 2H_2 + CO_2 + CH_4$ (R1b)

Methane SR: $CH_4 + H_2O \leftrightarrow CO + 3H_2$ (R2)

Ethanol POX: $C_2H_5OH + \frac{1}{2}O_2 \rightarrow 3H_2 + 2CO$ (R4a)

$C_2H_5OH + 3O_2 \rightarrow 3H_2O + 2CO_2$ (R4b)

Methane POX: $CH_4 + \frac{1}{2}O_2 \leftrightarrow CO + 2H_2$ (R6)

WGSR: $CO + H_2O \leftrightarrow CO_2 + H_2$ (R3)

It is noted that in this study, the products of ethanol reforming are predicted based on a thermodynamic analysis without considering the effects of catalyst used. There are a number of researches concerning about the synthesis and study of catalysts for ethanol reforming (Fierro et al., 2005; M. de Lima et al., 2008; Cai et al., 2008; Srisiriwat et al, 2009).

4.1.3 Solid oxide fuel cell

Hydrogen required for SOFC operation is produced from ethanol in "REFORMER" unit. The simulation of SOFC unit is separated into two parts; the first one is "ANODE" in which the reactions occur inside the cell and the second one is "CATHODE" which supplies oxygen as an oxidant to the anode side as represented by the separator module *Sep*. SOFC operates at high temperature between 600 and 1000 °C. Therefore, direct oxidation of the CO and CH_4 contained in the reformate gas is feasible in the SOFC without a catalyst, but it is less favoured than the water gas shift of CO to H_2 and reforming of CH_4 to H_2 (EG&G Technical Services, 2000). In this study, however, was assumed that hydrogen is the only fuel electrochemically reacting because the more readily oxidized fuel. An anode is represented by the equilibrium reactor module *Rgibbs*. The reactions considered in this block are:

Electrochemical:	$H_2 + \frac{1}{2}O_2 \rightarrow H_2O$	(R7)
Methane SR:	$CH_4 + H_2O \leftrightarrow CO + 3H_2$	(R2)
WGSR:	$CO + H_2O \leftrightarrow CO_2 + H_2$	(R3)

The three reactions above are specified to reach thermodynamic equilibrium at a given temperature to simplify the simulation. Although the electrochemical reaction is not represented as a reversible reaction, the simulation results will closely simulate the electrochemical conversion because of the very high temperature conditions, which result in an extremely large equilibrium constant, K, for reaction (R7) (Zhang et al., 2005). Hydrogen produced from methane internal steam reforming (R2) and water gas shift reactions (R3) at the anode participates in the electrochemical reaction (R7). Hydrogen is consumed by oxidation reaction at the anode side, and releases electrons to the external circuit. Simultaneously, oxygen in air accepts electrons from the external circuit that is reduced into oxygen ion at the cathode side and it through electrolyte to react with hydrogen to form as water and electron at anode side. The direct-current electricity is generated by electron flow from anode side to cathode side.

4.1.4 Afterburner

After undergoing the electrochemical and chemical reactions in the SOFC, the unreacted fuel gases from an anode side enter the afterburner in order to combust the remaining hydrogen and carbon monoxide (EX-ANODE stream) by reacted with the excess oxygen from a cathode side (EX-CATHODE stream). The exhaust gas from afterburner is high temperature and heat that can be thermally utilized for other heat-requiring parts of the SOFC system. An afterburner model is represented by the reactor module *Rstoic* and set at adiabatic condition. The reactions specified in this block are assumed that reaching complete combustion (100% conversion). The combustion reactions occurring in afterburner are shown as follows:

Hydrogen combustion: $H_2 + \frac{1}{2}O_2 \rightarrow H_2O$ (R7)

Carbon monoxide combustion: $CO + \frac{1}{2}O_2 \rightarrow CO_2$ (R8)

4.2 Model Equation

4.2.1 Electrochemical model

A generalized steady-state model is considered (Perna et al., 2007; Arteaga-Perez et al., 2009) in order to investigate the performance of a SOFC system integrated with reforming process. An electrochemical model equation relates the fuel and air composition, cell temperature, pressure, current density and cell parameters such as active area and electrode thickness.

The theoretical open-circuit potential is the difference between the thermodynamic potentials of the electrode reactions. It is also known as the "reversible cell voltage" (E^{OCV})" that can be expressed by the Nernst equation:

$$E^{OCV} = E^0 + \frac{\Re T}{2F} \ln\left(\frac{p_{H_2} p_{O_2}^{\frac{1}{2}}}{p_{H_2O}} \right) \quad (4.1)$$

E^0 is the reversible open-circuit potential at standard pressure and is a function of the operating temperature as can be given by the following equation:

$$E^0 = 1.253 - 2.4516 \times 10^{-4} T \tag{4.2}$$

However, the actual voltage (V) is always less than the open-circuit voltage because internal resistance and overpotential losses, which mainly occurs due to concentration, activation and ohmic overpotentials.

$$V = E^{OCV} - \eta_{\text{act,anode}} + \eta_{\text{act,cathode}} + \eta_{\text{ohm}} + \eta_{\text{conc,anode}} + \eta_{\text{conc,cathode}} \tag{4.3}$$

where η_{ohm} stands for the ohmic loss, $\eta_{\text{conc,anode}}$ and $\eta_{\text{conc,cathode}}$ represents the concentration overpotentials at the anode and the cathode, respectively, and $\eta_{\text{act,anode}}$ and $\eta_{\text{act,cathode}}$ stand for the activation overpotentials at the anode and the cathode, respectively.

The activation overpotential is related to the electrode kinetics at the reaction site and the relationship between overpotential-current density can be expressed by the nonlinear Butler–Volmer equation as follow:

$$i = i_{0,\text{electrode}} \left[\exp\left(\frac{\alpha n F}{\Re T} \eta_{\text{act,electrode}} \right) - \exp\left(-\frac{(1-\alpha) n F}{\Re T} \eta_{\text{act,electrode}} \right) \right] \tag{4.4}$$

$$\text{electrode} \in \{\text{anode,cathode}\}$$

where α represents the transfer coefficient, n is the number of electrons transferred in the single elementary rate-limiting reaction step, and $i_{0,\text{electrode}}$ is the exchange current density. In general, the transfer coefficient of the SOFC (α) is 0.5 and transferred electrons in the electrochemical reaction is 2, so the activation overpotential for a typical SOFC is expressed as (Ni et al., 2007)

$$\eta_{\text{act,electrode}} = \frac{\Re T}{F} \ln\left[\frac{i}{2i_{0,\text{electrode}}} + \sqrt{\left(\frac{i}{2i_{0,\text{electrode}}}\right)^2 + 1}\right] \tag{4.5}$$

$\text{electrode} \in \{\text{anode,cathode}\}$

The exchange current density ($i_{0,\text{electrode}}$) depends on the operating temperature, as shown in equation (4.6). The pre-exponential factor and the activation energy of the anode and cathode is used for calculation of $i_{0,\text{electrode}}$, given by Aguiar et al. (2004) as shown in Table 4.1

$$i_{0,\text{electrode}} = \frac{\Re T}{nF} k_{\text{electrode}} \exp\left(-\frac{E_{\text{electrode}}}{\Re T}\right) \tag{4.6}$$

$\text{electrode} \in \{\text{anode,cathode}\}$

The ohmic overpotential is caused by the resistance along the flow of ions through the electrolyte and electrons through the electrodes and current collectors and by contact resistance between cell components. This loss obey Ohm's law that can be expressed by

$$n_{\text{Ohm}} = iR_{\text{Ohm}} \tag{4.7}$$

where *i* is the current density, R_{Ohm} is the internal electrical resistance, that calculated from the conductivity of the individual layers (assuming negligible contact resistances, cross-plane charge flow, and series connection of resistances) as given by:

Table 4.1 Pre-exponential factor and activation energy.

Anode		***Cathode***	
k_{anode}	$6.54\times10^{11}\ \ \Omega^{-1}m^{-2}$	k_{cathode}	$2.35\times10^{11}\ \ \Omega^{-1}m^{-2}$
E_{anode}	$140\ \ kJ\ mol^{-1}$	E_{cathode}	$137\ \ kJ\ mol^{-1}$

$$R_{\text{Ohm}} = \frac{\tau_{\text{anode}}}{\sigma_{\text{anode}}} + \frac{\tau_{\text{electrolyte}}}{\sigma_{\text{electrolyte}}} + \frac{\tau_{\text{cathode}}}{\sigma_{\text{cathode}}} \tag{4.8}$$

where τ_{anode}, $\tau_{\text{electrolyte}}$ and τ_{cathode} represent the thickness of the anode, electrolyte, and cathode layers, respectively, σ_{anode} and σ_{cathode} is the electronic conductivity of the anode and cathode, and $\sigma_{\text{electrolyte}}$ is the ionic conductivity of the electrolyte.

The concentration overpotential is the voltage loss associated with the transport of gaseous reactants through porous electrodes. It can be determined from the difference in the open-circuit potential calculated based on the reactant and product concentrations at three-phase boundaries (TPB) and the bulk concentrations. The concentration overpotential (n_{conc}) is determined as:

$$n_{\text{conc}} = \frac{\Re T}{2F}\ln\left(\frac{p_{\text{H}_2\text{O,TPB}}\, p_{H_2}}{p_{\text{H}_2\text{O}}\, p_{\text{H}_2\text{,TPB}}}\right) + \frac{\Re T}{4F}\ln\left(\frac{p_{\text{O}_2}}{p_{\text{O}_2\text{,TPB}}}\right) \tag{4.9}$$

where the first term on the right-hand side refers to the anodic concentration overpotential ($\eta_{\text{conc,anode}}$) and the second term to the cathodic concentration overpotential ($\eta_{\text{conc,cathode}}$), $p_{\text{H}_2\text{O,TPB}}$, $p_{\text{H}_2\text{,TPB}}$, and $p_{\text{O}_2\text{,TPB}}$, are the partial pressures of H_2, H_2O, and O_2 at the three-phase boundaries, respectively. Their diffusion transport in a porous electrode can be described by Fick's model as given by

$$p_{\text{H}_2\text{,TPB}} = p_{\text{H}_2\text{,f}} - \frac{\Re T \tau_{\text{anode}}}{2F\overline{D}_{\text{eff,anode}}} i \tag{4.10}$$

$$p_{\text{H}_2\text{O,TPB}} = p_{\text{H}_2\text{O,f}} + \frac{\Re T \tau_{\text{anode}}}{2F\overline{D}_{\text{eff,anode}}} i \tag{4.11}$$

$$p_{\text{O}_2\text{,TPB}} = P - (P - p_{\text{O}_2\text{,a}})\exp\left(\frac{\Re T \tau_{\text{cathode}}}{4F\overline{D}_{\text{eff,cathode}} P} i\right) \tag{4.12}$$

Table 4.2 Physical parameters of cell components. (Arpornwichanop et al., 2009)

Anode thickness, τ_{anode}	$500\mu m$
Cathode thickness, $\tau_{cathode}$	$50\mu m$
Electrolyte thickness, $\tau_{electrolyte}$	$20\mu m$
Anode electrical conductivity, σ_{anode}	$80 \times 10^3\ \Omega^{-1}m^{-1}$
Cathode electrical conductivity, $\sigma_{cathode}$	$8.4 \times 10^3\ \Omega^{-1}m^{-1}$
Electrolyte ionic conductivity, $\sigma_{electrolyte}$	$33.4 \times 10^3 \exp(-10{,}300/T)\ \Omega^{-1}m^{-1}$
Anode diffusion coefficient, $D_{eff,anode}$	$33.4 \times 10^{-5}\ m^2s^{-1}$
Cathode diffusion coefficient, $D_{eff,cathode}$	$1.37 \times 10^{-5}\ m^2s^{-1}$
Active cell surface, A	$100\ m^2$

Although the gas-diffusion coefficient ($\overline{D_{eff,i}}$) increases with increasing temperature, the effect of increased diffusion rate on the concentration overpotential is less pronounced (Ni et al., 2007). Therefore, the gas-diffusion coefficient is assumed to be constant in this study. Table 4.2 gives the values of physical parameters of cell components used in this work.

4.3 System Performance

4.3.1 Basic definitions

4.3.1.1 Fuel utilization

Fuel utilization is the fraction of the total fuel inlet that is electrochemically reacted to produce electricity in the cell. As above, CH_4, CO and H_2 are considered as inlet fuel and H_2 is only electrochemically oxidized. Therefore, the fuel utilization is defined by:

$$U_f = \frac{F_{H_2,react}}{(F_{H_2,in} + F_{CO,in} + 4F_{CH_4,in})} \quad (4.13)$$

where $F_{i,in}$ represent molar flow rate of component i (CH_4, CO and H_2)

4.3.1.2 Air utilization

Air utilization is the ratio of the total oxygen inlet used to react in electrochemical reaction. It can be expressed by:

$$U_a = \frac{F_{O_2,react}}{F_{O_2,inlet}} \quad (4.14)$$

4.3.2 Performance index

The process effectiveness and efficiencies are computed using different criteria. Generally, process effectiveness of reforming process is assessed by hydrogen yield (H_2 yield). The performance indexes of system are evaluated by the electrical efficiency (η_{SOFC}) and thermal efficiency ($\eta_{Thermal}$).

4.3.2.1 Hydrogen yield

Hydrogen yield (H_2 yield) is the fraction of the total inlet fuel that is converted into hydrogen defined by Equation (4.15). Ethanol is used as a fuel in this study.

$$H_2 \text{ yield} = \frac{F_{H_2}}{F_{EtOH,in}} \quad (4.15)$$

4.3.2.2 Electrical efficiency

The electrical efficiency (η_{SOFC}) is evaluated by the ratio of fuel cell electric power and the energy that could be produced if the hydrogen entering into the cell is completely burned:

$$\eta_{SOFC} = \frac{P_{SOFC}}{F_{EtOH,in} \cdot LHV_{EtOH}} \times 100 \tag{4.16}$$

where P_{SOFC}, $F_{EtOH,in}$ and LHV_{EtOH} is the power, ethanol inlet molar flow rate, and lower heating value of ethanol (1230 kJ/mole of ethanol).

4.3.2.3 Thermal efficiency

Thermal efficiency ($\eta_{Thermal}$) is related to the produced and consumed energy in the process equipment, the following equation is used:

$$\eta_{Thermal} = \frac{Q_{produced} - Q_{consumed}}{F_{EtOH,in} \cdot LHV_{EtOH}} \tag{4.17}$$

where $Q_{produced}$ is an energy content of the exhaust gas converted to low temperature (200 °C) and $Q_{consumed}$ is consumed energy which is heat required for ethanol and water vaporizations, ethanol and steam pre-heating, and reforming process.

4.4 Model Validation

To ensure that the electrochemical model as proposed in previous section can reliably predict the SOFC performance. This model was validated the simulation results with experiment data of Zhao and Virkar (2005). In their experiment, the inlet fuel consists of 97% H_2 and 3% H_2O and inlet oxidant comprises of 21% O_2. The thickness of anode, cathode, and electrolyte were 1000, 20 and 8 μm, respectively. The current–voltage curve of the SOFC was characterized at temperatures of 1023 K, 1073 K, and 1123 K and a pressure of 1 bar. The comparison of the model prediction and experimental data in terms of cell voltage at different current densities and operating temperatures is shown in Figure 4.2. It indicated that the model prediction shows good agreement with experimental data in the literature.

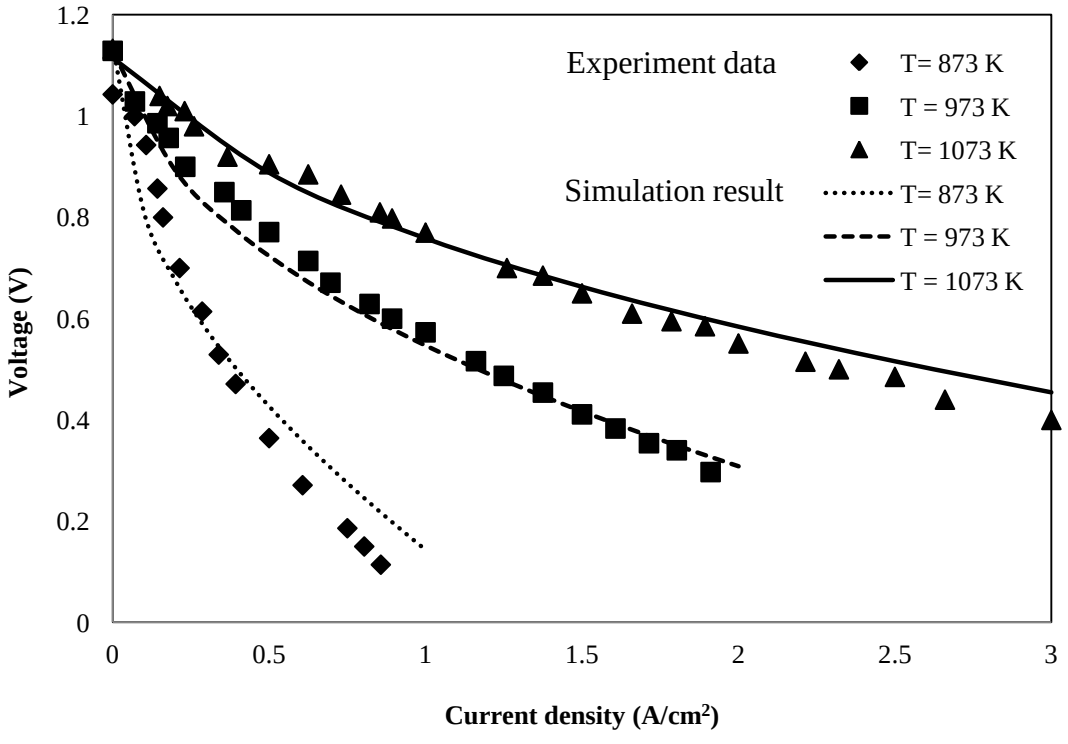

Figure 4.2 Comparison of cell characteristics between simulation results and experimental data (Zhao and Virkar, 2005).

CHAPTER V

SOLID OXIDE FUEL CELL INTEGRATED WITH ETHANOL REFORMING PROCESS

In this chapter, the performance of SOFC using different ethanol reforming process, such as steam reforming, partial oxidation, and autothermal reforming, is investigated via thermodynamic analysis to determine the most suitable reforming process. The performance in term of hydrogen yield and fuel cell efficiency is analyzed with respect to the effect key operating parameters such as reformer temperature, cell temperature, steam to ethanol ratio, and oxygen to ethanol ratio.

5.1 Introduction

Typically, a SOFC system consists of three main parts: (1) a fuel processor which converts a hydrogen containing raw fuel such as ethanol into a hydrogen-rich gas, (2) a SOFC stack that subsequently generates electricity and (3) an afterburner where the unreacted fuel from SOFC is burnt to generate more heat in order to supply heat to other heat requiring parts of the SOFC system. There are many processes for hydrogen production. Recently, thermo-chemical process as reforming process has received considerable attention due to it is a promising technology for use in commercial. In general, three reforming processes are widely known such as steam reforming (SR), partial oxidation (POX), and autothermal reforming (ATR) (Hayre et al, 2006), that has a significant effect on the operating condition and the efficiency. Most of the studies focus on SR because it appears to be the most efficiency in terms of hydrogen yield, but it is an endothermic process which requires high energy consumption (Hernandez and Kafarov, 2009; Vourliotakis et al., 2009). To avoid or reduce energy consumption, partial oxidation is an interesting option owing to POX is an exothermic, so no need an external heat source for the reactor. However, it gives less hydrogen yield than SR and low partial pressure of H_2 that the nitrogen dilution of

the hydrogen containing effluent. This nitrogen dilution is deteriorating fuel cell operation, because increased nitrogen content lowers the open-circuit voltage of the fuel cell (Rabenstein et al., 2008). In order to circumvent such problems, autothermal reforming uses the partial oxidation to provide the heat and steam reforming to increase the hydrogen production resulting in the process improvement. Tsiakaras and Demin (2001) and Rabenstein and Hacker (2008) found that the implementation of reforming process was difference, resulting in the different fraction of gas and thermal management in system. Therefore, the selection of ethanol reforming process is a very important and has a significant effect on the performance of SOFC.

When ethanol is considered as a raw fuel for the fuel processor, most of the studies focus on ethanol steam reforming process. (Garcia and Laborde, 1991; Vasudeva et al., 1996; Mas et al., 2006; Rossi et al., 2009; Lima da Silva et al., 2009) The previous studies on an ethanol reforming to hydrogen for fuel cells were conducted into two approaches. A thermodynamic analysis of ethanol reforming process without SOFC system was firstly proposed (Tsiakaras and Demin, 2001; Srisiriwat et al., 2006; Wang and Wang, 2008; Lima da Silva et al., 2009). Moreover, a SOFC system integrated with ethanol processor was analyzed thermodynamically, which SOFC stack model is developed in a programming language, such as FORTRAN, Visual Basic or C++ and linked to AspenPlus or any other commercial simulators as a user defined model or subroutines, whereas other components constituting the system employ existing unit operation models in the program (Riensche et al., 1998; Palsson et al., 2000; Lisbona et al., 2007; Jamsak et al., 2009). To avoid such a complication, development of SOFC model by using existing functions and unit operation models in a process simulator is an interesting option.

Although the advantages and disadvantages of the use of each reforming process have been widely reported, the determination of a suitable reforming process integrated with an SOFC system by using Aspen Plus is investigated in this study. Thermodynamic analysis is performed to compare the relevant performance in term of hydrogen yield and electrical efficiency of the SOFC systems with different reforming process. The key operating parameters, namely reformer temperature, cell temperature, steam to ethanol ratio, and oxygen to ethanol ratio are investigated.

5.2 SOFC system configurations

In this study, three ethanol reforming process integrated with SOFC system are considered, i.e. SOFC using steam reforming process, SOFC using partial oxidation process and SOFC using autothermal reforming process. The schematic diagram of a SOFC system with ethanol steam reforming process (SOFC-SR) in Aspen Plus simulator is illustrated in Figure 5.1. This process consists of vaporizers, preheaters, a reformer reactor, a SOFC stack that is separated into two electrode sides such as anode and cathode, an afterburner and a cooler. The ethanol and reforming agents (steam, air and combined air/steam) provided at 25 ◦C are vaporized into gas phase and preheated at 400 ◦C, prior to enter the reformer. Within the reformer, chemical reactions, namely; ethanol steam reforming, water gas shift and methane steam reforming occur to convert fuel into hydrogen. Hydrogen-rich gas enters an anode in order to electrochemically react with oxygen as an oxidant from the cathode, which generate the electrical power and steam. The heat released from SOFC is used for air preheating at entering the cathode in order to maintain the cell operating temperature at isothermal condition. The residual fuel from anode and cathode is burnt in an afterburner. The exhaust gas from afterburner is produced more heat that can be thermally utilized for other heat-requiring parts of the SOFC system. The outlet temperature in system is fixed at 200 ◦C. To achieve the cell operating temperature for all system, the requested air flow can be determined by using an AspenPlus™ *Design-spec* satisfying the heat released from the cell. Figure 5.2 and Figure 5.3 show the plant configuration for the SOFC integrated with partial oxidation (SOFC-POX) and autothermal reforming (SOFC-ATR), respectively. The components of the systems are similar to SOFC-SR system but three systems use different reforming agents, which are SOFC-SR system using steam as the reforming agent, SOFC-POX system using air as the reforming agent and SOFC-ATR system using both air and steam as the reforming agents. The reformer and cell operating temperatures in all systems are kept to be 700 and 800 ◦C, respectively. Moreover, the fuel utilization is set equal to 85%.

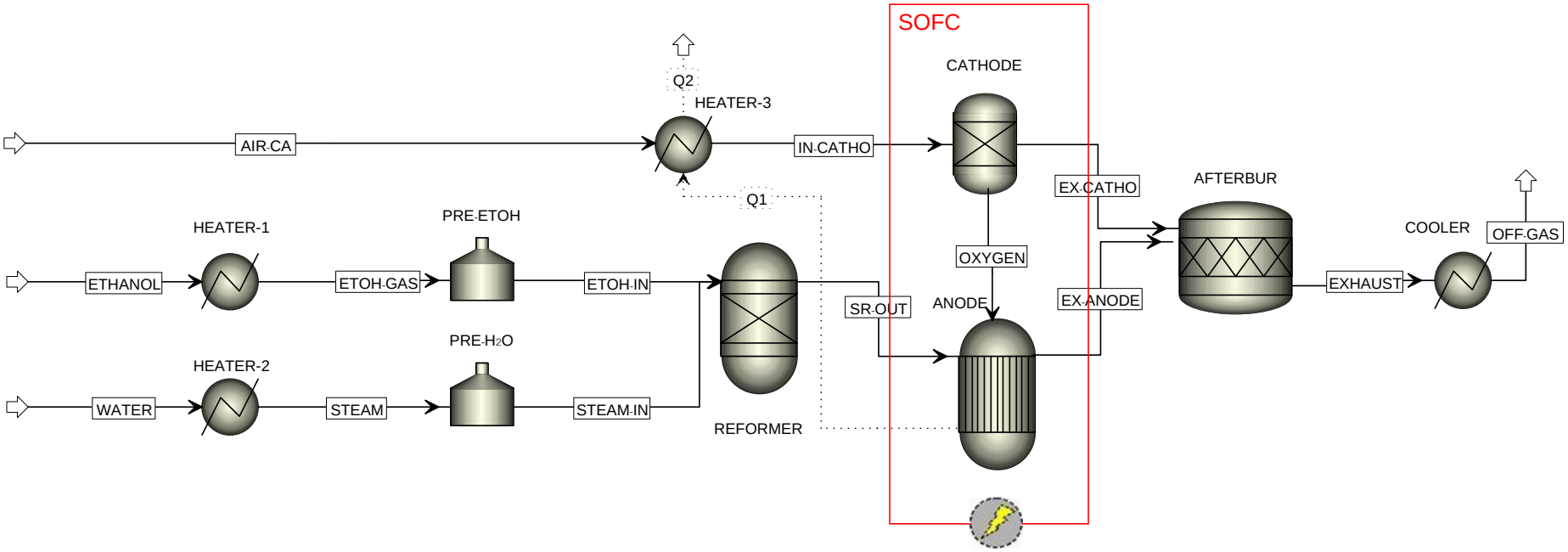

Figure 5.1 Schematic diagram of a SOFC system with ethanol steam reforming process (SOFC-SR).

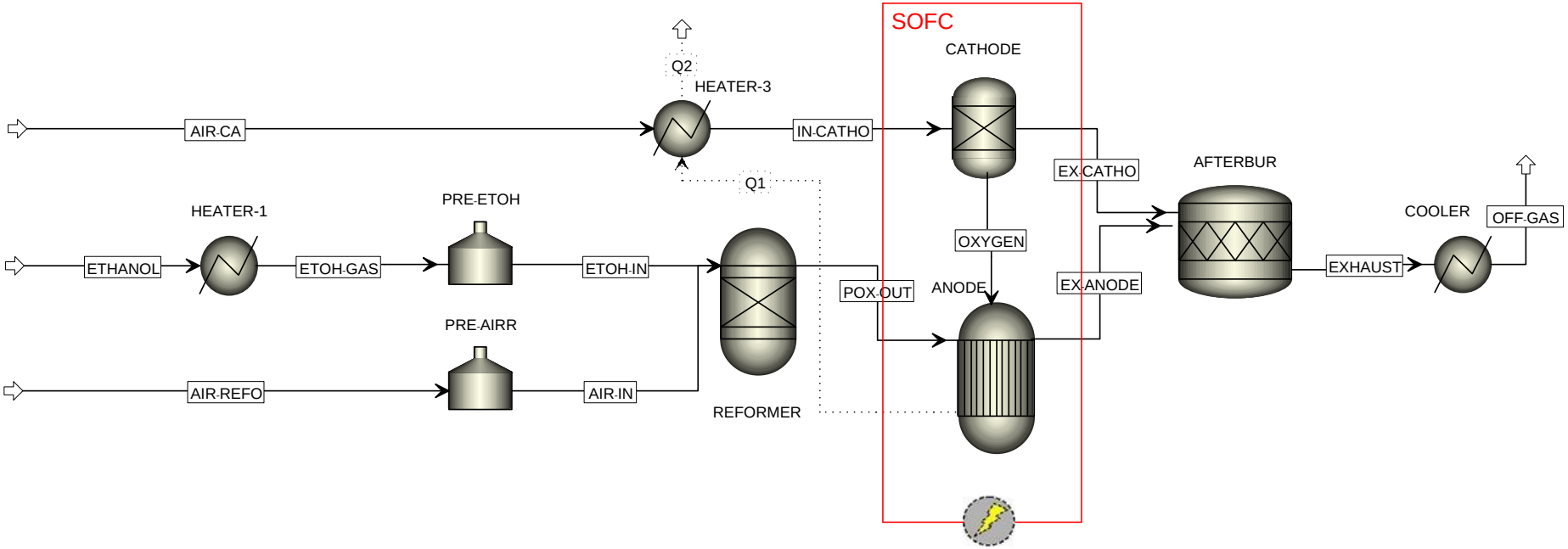

Figure 5.2 Schematic diagram of a SOFC system with ethanol partial oxidation process (SOFC-POX).

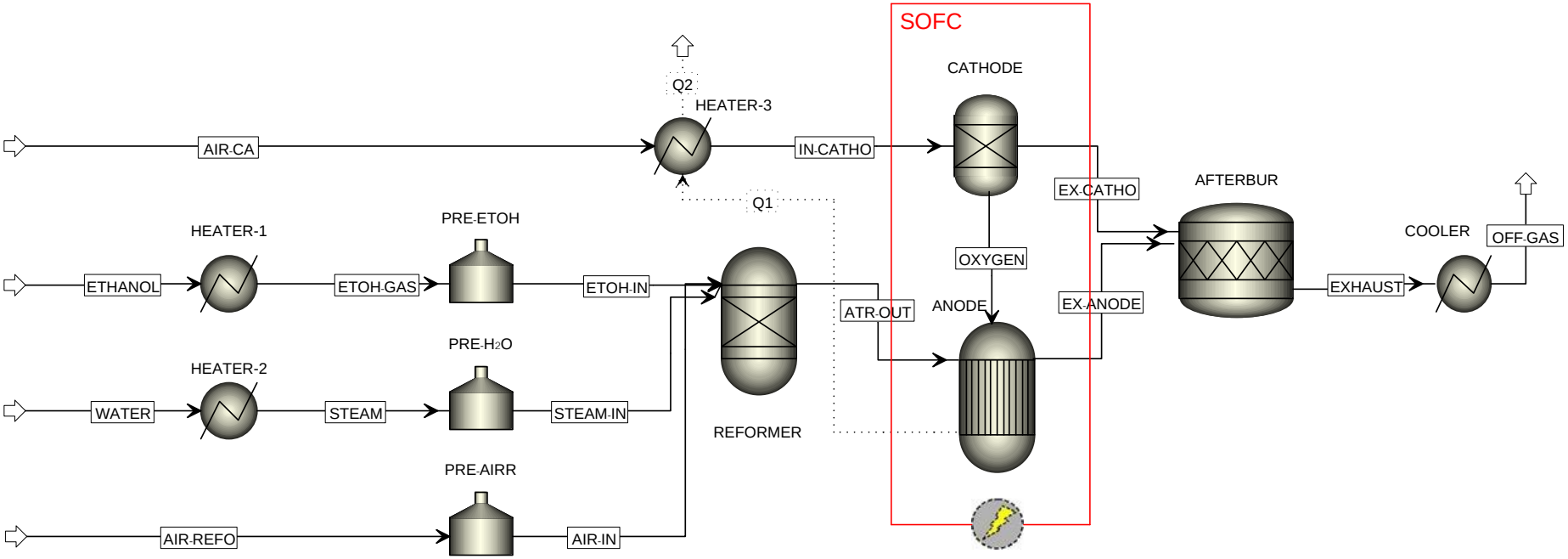

Figure 5.3 Schematic diagram of a SOFC system with ethanol autothermal reforming process (SOFC-ATR).

5.3 Results and discussion

Thermodynamic analysis of SOFC integrated with ethanol reforming process, namely; steam reforming, partial oxidation, and autothermal reforming, by using Aspen Plus is studied using steady-state fuel cell model and a detailed electrochemical taking into account all various voltage losses (i.e., activation, ohmic and concentration losses). The impact of important operating parameters such as, reformer temperature, cell temperature, steam to ethanol ratio, and oxygen to ethanol ratio. The minimization of the Gibbs free energy was used to determine the equilibrium compositions. The equation of state used in the calculation was based on the Peng-Robinson (PEN-ROB) method. The gas compositions considered are C_2H_5OH, H_2O, H_2, O_2, N_2, CH_4, CO and CO_2 whereas C_2H_4 and C_2H_4O can be considered as intermediates of an incomplete reforming reaction and are in fact no thermodynamically stable products (Rabenstein et al., 2008). No carbon formation under this operating condition is assumed. This study presents the equilibrium compositions of ethanol-reforming as a function of the reformer temperature (400–1000 °C), stack temperature (600–1000 °C), steam to ethanol ratio (S/E) (2.0–10.0), and oxygen to ethanol ratio (O/E) (0.1–0.9) at atmospheric pressure. The standard operating condition used for each system is listed in Table 5.1.

Table 5.1 Standard operating conditions

	SOFC-SR	SOFC-POX	SOFC-ATR
Ethanol molar feed flow rate (l/min)	0.962	0.962	0.962
Water molar feed flow rate (l/min)	0.604	-	0.604
Air molar feed flow rate (l/min)	-	970.3	970.3
Reforming temperature (°C)	700	700	700
Stack exhaust temperature (°C)	800	800	800
Fuel utilization (%)	85	85	85
Voltage (V)	0.834	0.855	0.839
Current density (mA/cm^2)	273.39	227.82	227.82
Gross AC efficiency (LHV) (%)	66.71	57.23	55.93

5.3.1 The SOFC integrated with ethanol steam reforming process (SOFC-SR)

In this section, a thermodynamic analysis of ethanol steam reforming process is presented. At the standard conditions, the inlet molar flow rate of ethanol is 1 kmol/h and steam to ethanol ratio (S/E) is 2.

5.3.1.1 Effect of reformer temperature and steam to ethanol ratio.

The thermodynamically predicted equilibrium conversion of ethanol in this system is always at 100% as noted in Figure 5.4. Figure 5.4 shows the changing of the equilibrium compositions distribution over changing steam reforming temperature from 400 ˚C to 1000 ˚C at S/E = 2. The simulation result demonstrates that mole fraction of H_2 and CO increase with increasing reformer temperature whereas mole fraction of CO_2, CH_4 and H_2O decrease concurrently. Especially, at reformer temperature T_{Ref} < 700 ˚C the H_2 content is rapidly increasing. This is because the methane steam reforming reaction (R2) is favored and the reverse water gas shift reaction (R3) is more pronounced at the aforementioned temperature, which is the endothermic reactions. The maximum concentrate of H_2 reaches at 800 ˚C which the mole fraction of gases obtained at this reformer temperature are 60.95%H_2, 0.32% CH_4, 24.03%CO, 4.41% CO_2 and 10.29% H_2O. Increasing S/E also has influence on H_2 content in the reformer effluent as showed in

Figure 5.5. When raising S/E increases the water in the system that pronounces more water gas shift reaction (R3) according the thermodynamically equilibrium and thus, molar flow of H_2 is increasing. However, the unreacted steam leads to the dilution effect of H_2 that causes mole fraction of H_2 decrease. Moreover, the concentration of H_2 affects the cell efficiency so that the choice of the S/E should be carefully considered.

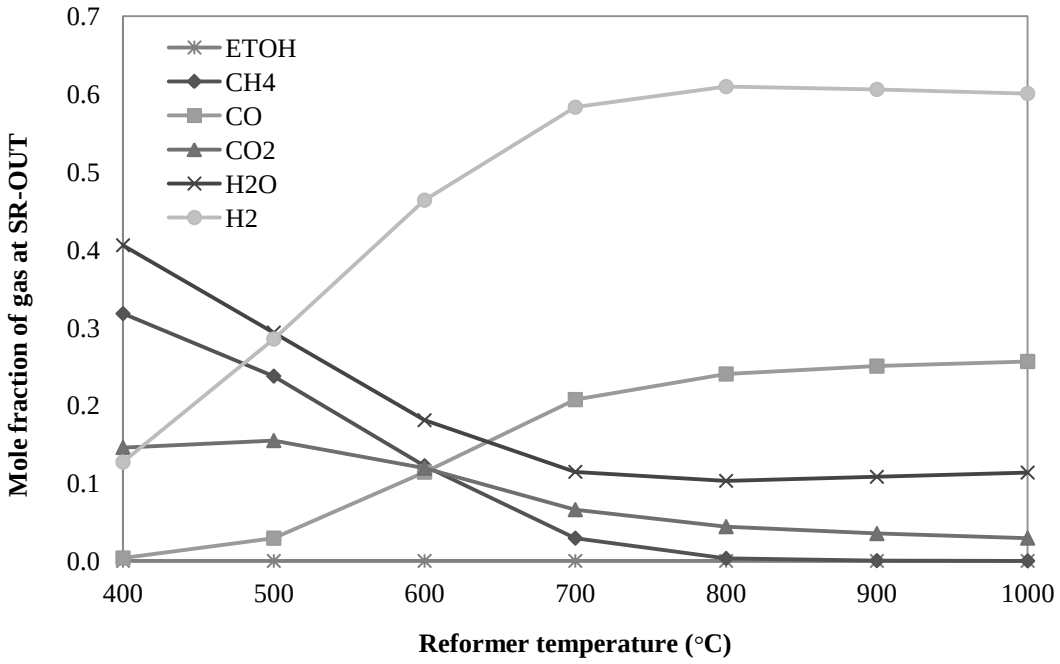

Figure 5.4 Effect of reformer temperature on equilibrium compositions at the reformer outlet with S/E = 2 in SOFC-SR system.

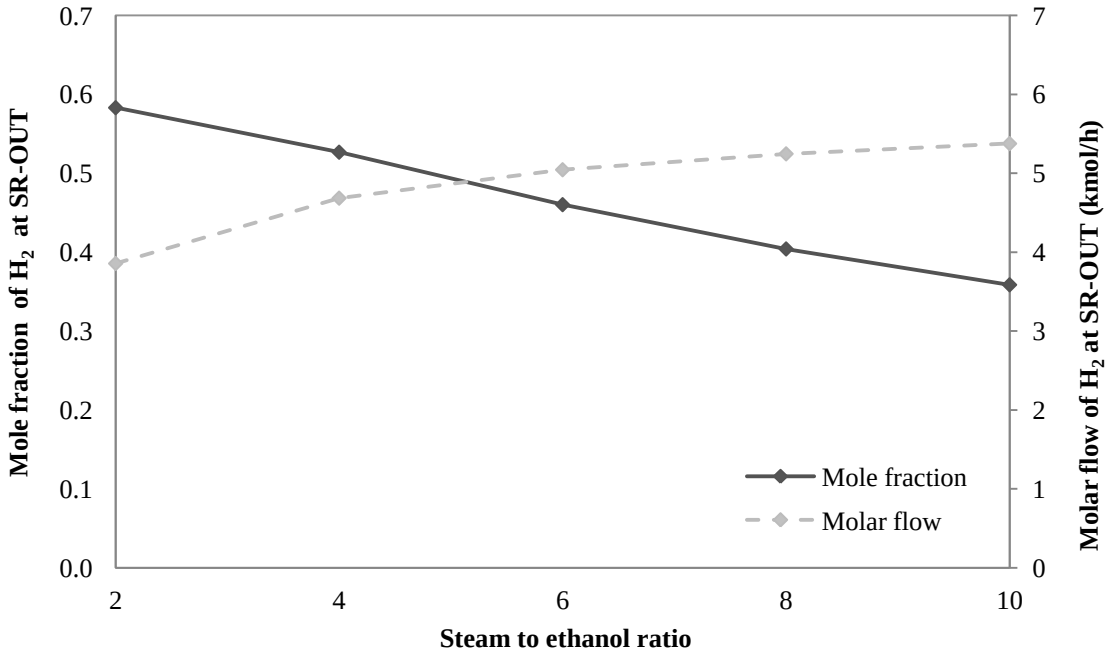

Figure 5.5 Effect of steam to ethanol ratio on mole fraction and molar flow of H_2 at T_{Ref} = 700 ˚C in SOFC-SR system.

The influences of steam to ethanol ratio and reformer temperature on the hydrogen yield (H_2 yield) of steam-reforming of ethanol are shown in Figure 5.6. It is found that an increase of both reformer temperature and S/E can improve the H_2 yield . Owing to the steam reforming reaction and the water gas shift reaction are supported. However, the H_2 yield very slight reduction is occurring for increasing the reformer temperature around 800-1000 ˚C, which is effected by the reverse water–gas-shift reaction. The maximum H_2 yield approaches 5.37 at T_{Ref} = 700 ˚C and S/E = 10.

Figure 5.7 shows the effect of reformer temperature on all voltage overpotentials at S/E = 2 in SOFC-SR system. When the reformer temperature is raised the anode concentration overpotential (CONCAN) decreases slightly whereas the cathode concentration overpotential (CONCCA), the activation overpotential and the ohmic loss (OHM) are constant. This is due to the mole fraction of H_2 and H_2O in the reformer effluent that the anode concentration overpotential is calculated based on H_2 and H_2O concentrations.

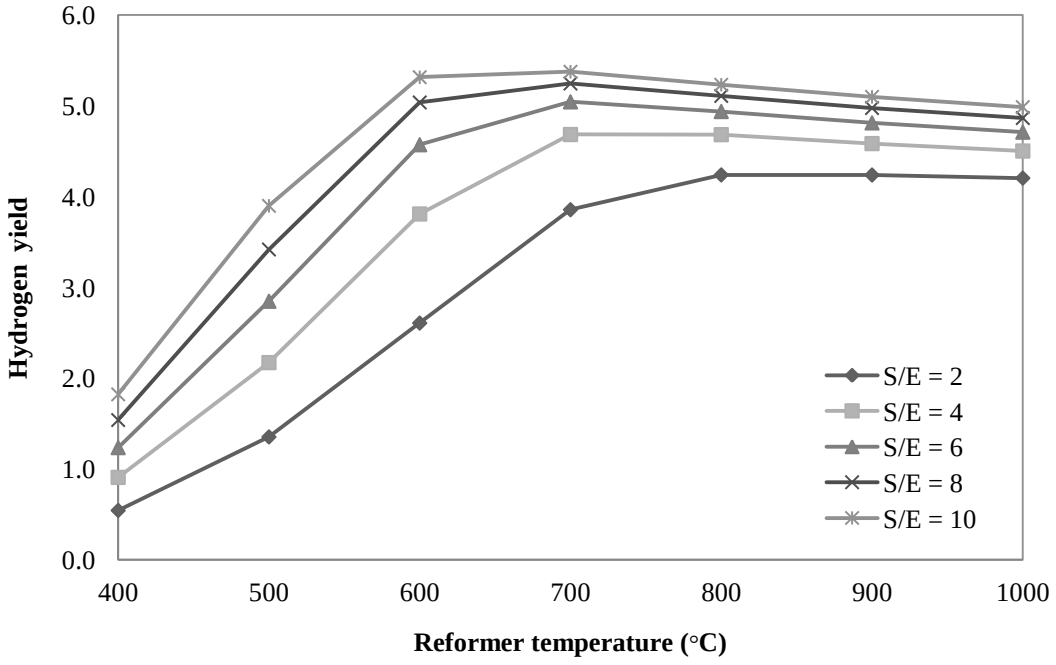

Figure 5.6 Effect of reformer temperature and steam to ethanol ratio on hydrogen yield in SOFC-SR system.

Moreover, it is noted that the cathode activation overpotential (ACTCA) is more than the anode activation overpotential (ACTAN) because an exchange current density of cathode is less than anode. On the contrary, the anode concentration overpotential is more than the cathode concentration overpotential due to an anode thickness is thicker than a cathode one. However, increasing S/E at constant reformer temperature also has influence on all voltage losses as showed in the same trend except the anode concentration overpotential.

Figure 5.8 shows the influent of steam to ethanol ratio and reformer temperature on the electrical efficiency (η_{SOFC}). Raising the reformer temperature around 400 – 700 ◦C the η_{SOFC} is strongly increasing, since this means increasing of H_2 concentration in the reformer effluent makes the cell voltage increases. On the other hand, when increasing the S/E the η_{SOFC} is decreasing. The maximum η_{SOFC} reaching at T_{Ref} = 800 ˚C and S/E = 2 is 67.04%.

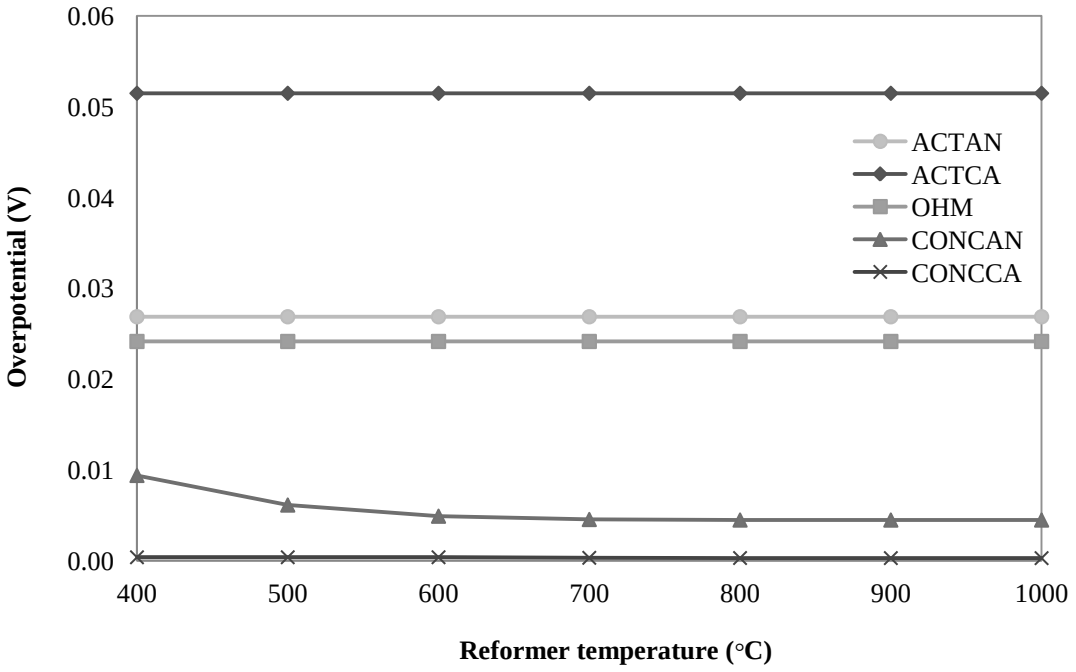

Figure 5.7 Effect of reformer temperature on all voltage overpotentials at S/E = 2 in SOFC-SR system.

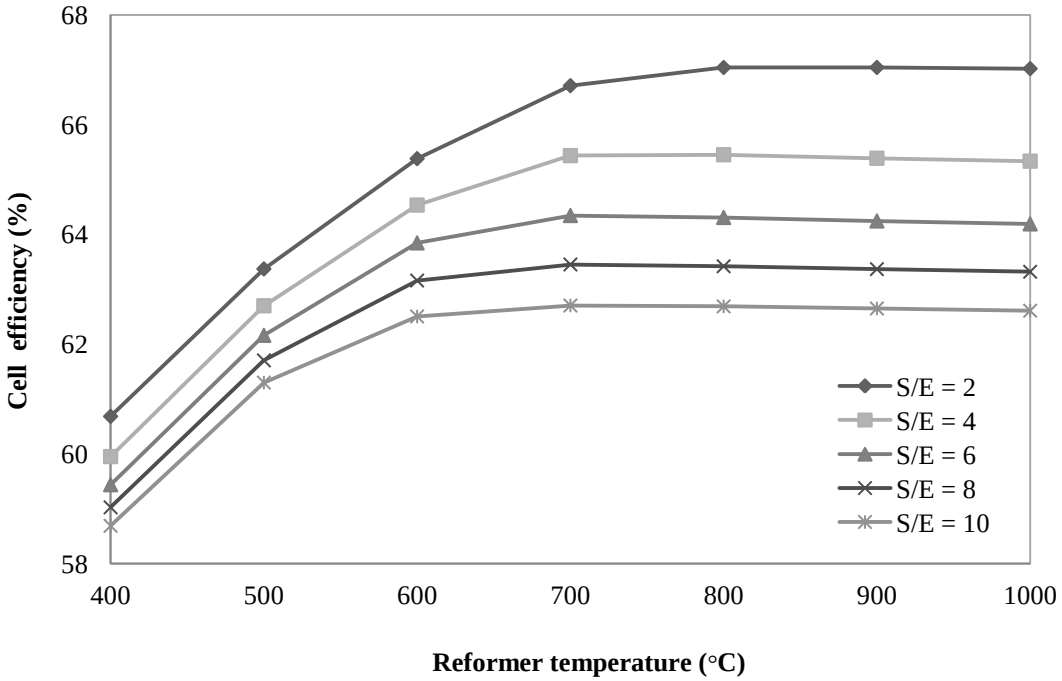

Figure 5.8 Effect of reformer temperature and steam to ethanol ratio on cell efficiency in SOFC-SR system.

5.3.1.2 Effect of SOFC temperature and steam to ethanol ratio.

The effect on the anode equilibrium compositions effluent at different cell operating temperatures is analyzed as shown in Figure 5.9. The results indicate that the amount of H_2O and CO increase with increasing temperatures from 600 °C to 1000 °C, whereas the opposite trend is observed for H_2 and CO_2. This effect is explained by an electrochemical reaction (R7) and the reverse water gas shift reaction (R3) increase. Moreover, an internal reforming of methane occurred at the anode is always at 100% owing to CH_4 is not found at an anode effluent in all range of SOFC temperature studied. Considering the mole fraction and molar flow of H_2 and H_2O at the anode effluent against the steam to ethanol ratio is shown in Figure 5.10. Within the range of the S/E, the mole fraction and molar flow of H_2O increase with increasing S/E, but the concentration of H_2 reduce. This can be explained by raising S/E leads to less fraction of H_2 in an anode effluent, resulting in the decreased rate of the electrochemical reaction.

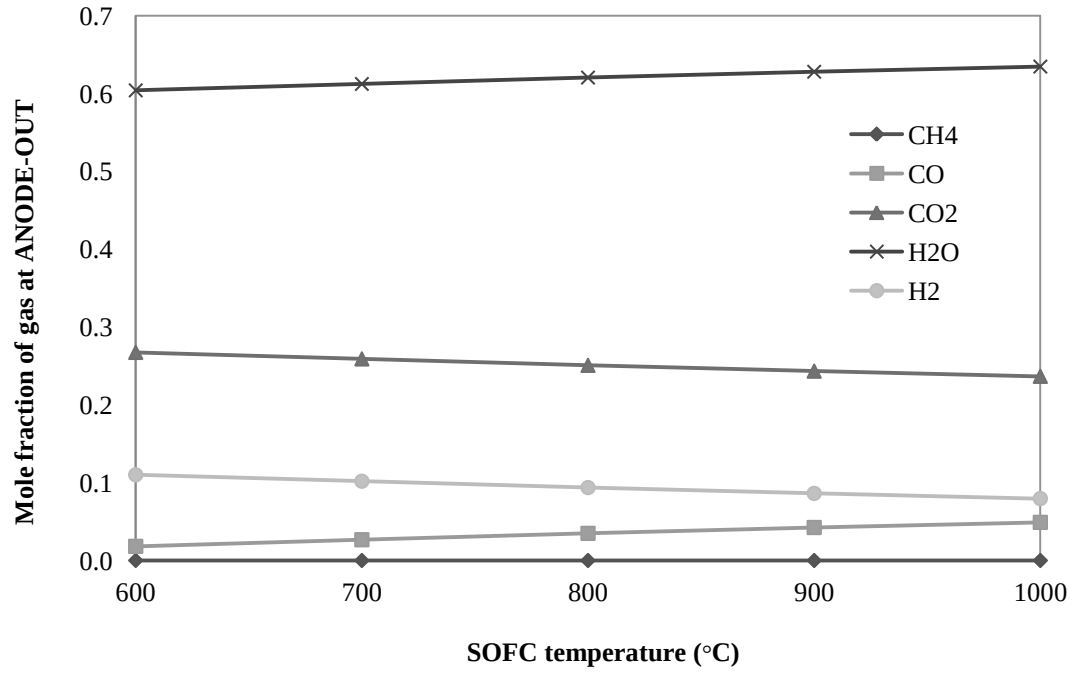

Figure 5.9 Effect of SOFC temperature on equilibrium compositions at the anode outlet with T_{Ref} = 700 ◦C and S/E = 2 in SOFC-SR system.

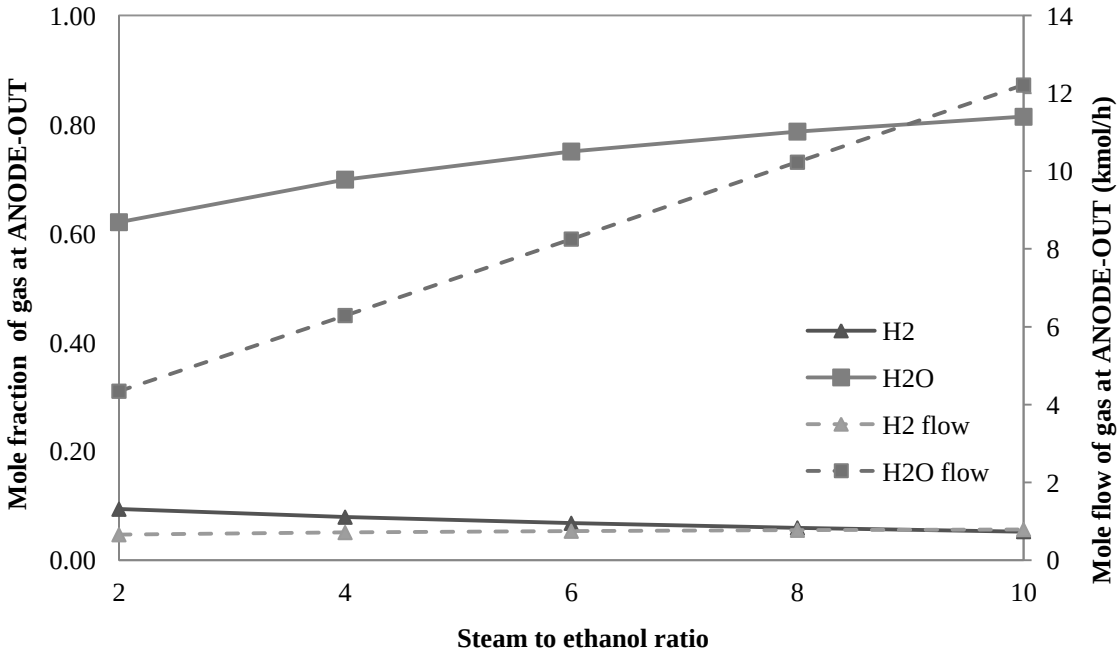

Figure 5.10 Effect of steam to ethanol ratio on mole fraction and molar flow of H_2 and H_2O at T_{Ref} = 700 ◦C and T_{SOFC} = 800 ◦C in SOFC-SR system.

Figure 5.11 shows the effect of SOFC temperature on all voltage overpotentials at T_{Ref} = 700 ◦C and S/E = 2 in SOFC-SR system. It is noted that the activation overpotential and ohmic loss reduce rapidly at SOFC temperature around 600 – 900 ◦C. This result from an increasing of the exchange-current density that effects on the activation overpotential. Likewise, the ohmic loss decreases because of the reduction of the specific resistance (R_{ohm}) that the electrolyte conductivity is a function of SOFC temperature; therefore, its value increase when the SOFC temperature is raised. Conversely, the variation of composition in anode effluent, shown in Figure 5.9, results in an increased slightly the concentration overpotential.

Figure 5.12 shows the electrical efficiency (η_{SOFC}) as a function of SOFC operating temperature and steam to ethanol ratio. An increase in SOFC operating temperature can improve the η_{SOFC}. This implied that an increase in SOFC temperature pronounces more electrochemical reaction and reduces the activation overpotential and ohmic loss and thus the η_{SOFC} is enhanced. However, raising S/E causes less fraction of H_2 in an anode effluent, resulting in the decreased rate of the electrochemical reaction; therefore, the η_{SOFC} reduces slightly. The maximum η_{SOFC} reaching at T_{SOFC} = 900 ◦C and S/E = 2 is 69.59%.

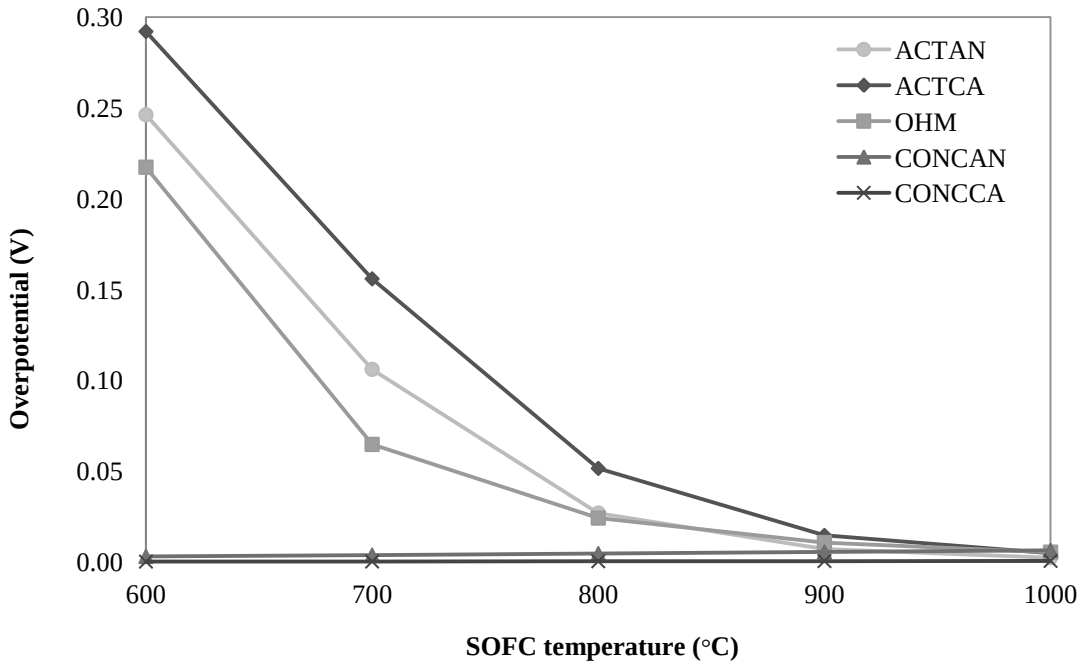

Figure 5.11 Effect of SOFC temperature on all voltage overpotentials at S/E = 2 in SOFC-SR system.

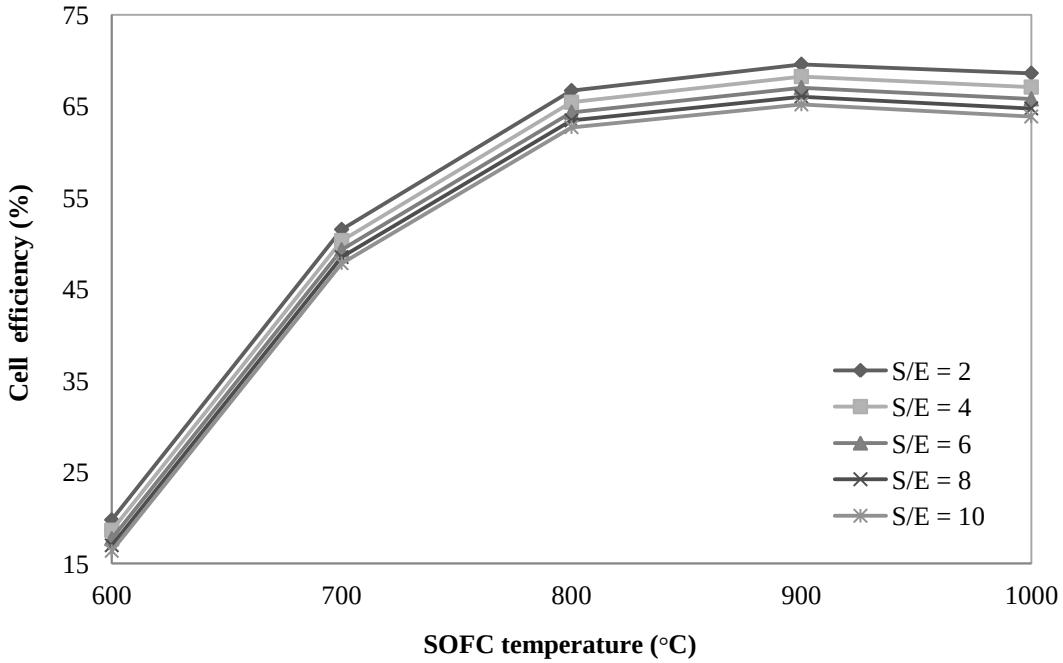

Figure 5.12 Effect of SOFC temperature and steam to ethanol ratio on cell efficiency in SOFC-SR system.

5.3.2 The SOFC integrated with ethanol partial oxidation process (SOFC-POX)

In this section, a thermodynamic analysis of ethanol partial oxidation process is presented. At the standard conditions, the inlet molar flow rate of ethanol is 1 kmol/h and oxygen to ethanol ratio (O/E) is 0.5.

5.3.2.1 Effect of reformer temperature and oxygen to ethanol ratio.

The influent of reformer temperature on the equilibrium compositions in reformer effluent at O/E = 0.5 as illustrated in Figure 5.13. Raising the reformer temperatures increases both the mole fraction of H_2 and CO whereas mole fraction of CO_2, CH_4 and H_2O are shown in the opposite trends. Particularly, at equilibrium condition, ethanol is completely consumed in all the temperature ranges considered. It is noted that the CH_4 content is high at T_{Ref} = 400 ˚C due to the ethanol partial oxidation reaction (R4a) and methanation reaction (R5) are supported at as above temperature that H_2O is observed. However, an increasing in reformer temperature pronounces more the reverse methanation reaction, so the CH_4 content decreases. The maximum concentrate of H_2 reaches at 1000 ˚C which the mole fraction of gases obtained at this reformer temperature are 43.24%H_2, 0.19% CH_4, 28.93%CO, 0.06% CO_2, 0.14% H_2O and 27.44%N_2.

Figure 5.14 shows the effect of oxygen to ethanol ratio on mole fraction and molar flow of H_2 in the reformer effluent at T_{Ref} = 700 ˚C in SOFC-POX system. It is found that the increase of O/E around 0.1 – 0.3 can enhance more the partial oxidation reaction (R4a), so H_2 content is increased. However, the increase of O/E above 0.3 leads to occur the complete oxidation reaction (R4b) and contain more N_2 gas in the system, thus H_2 concentration is reduced. Moreover, from the simulation results, no oxygen exists in the reforming gas at all operating conditions. This indicates that oxygen reacts completely with ethanol.

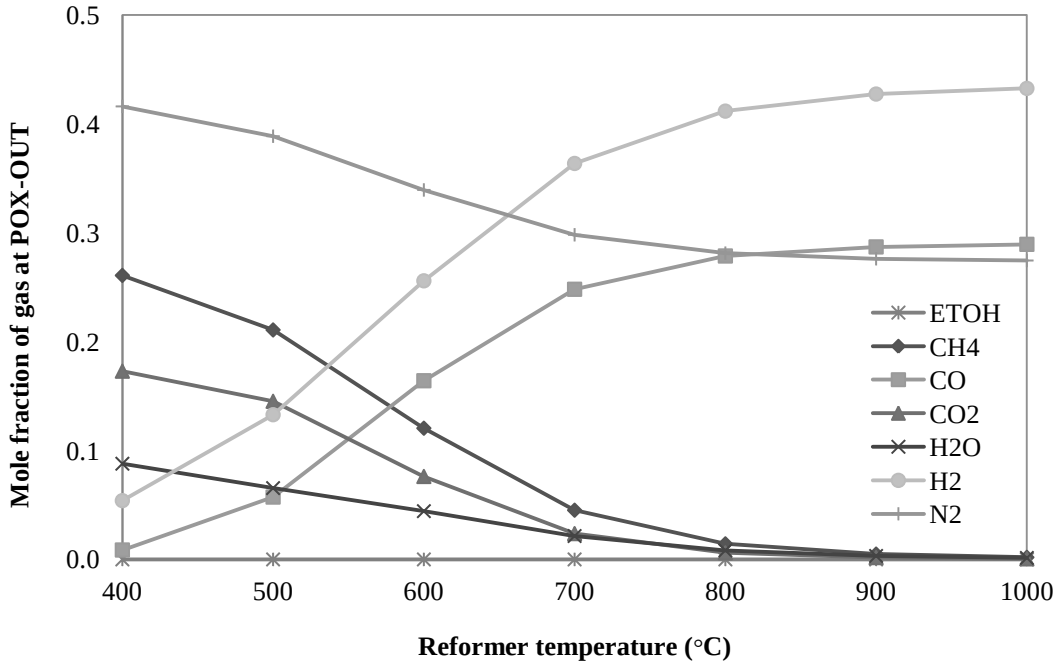

Figure 5.13 Effect of reformer temperature on equilibrium compositions at the reformer outlet with O/E = 0.5 in SOFC-POX system.

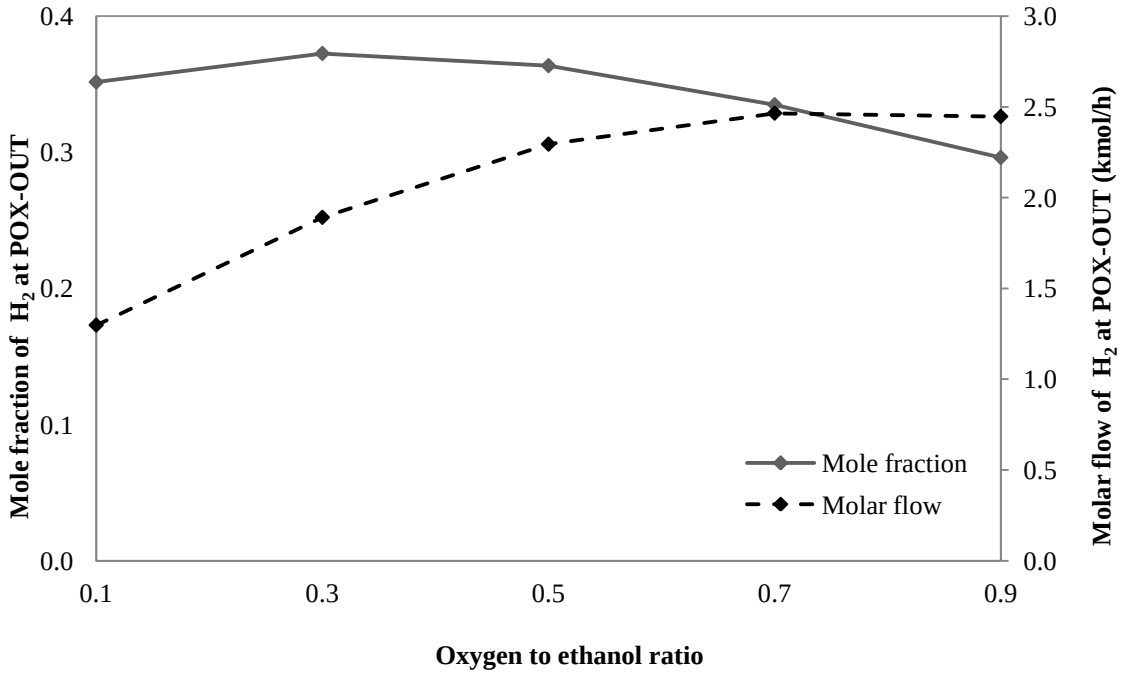

Figure 5.14 Effect of steam to ethanol ratio on mole fraction and molar flow of H_2 at T_{Ref} = 700 ˚C in SOFC-POX system.

Figure 5.15 presents the hydrogen yield (H_2 yield) as a function of reformer temperature and oxygen to ethanol ratio. The simulation result demonstrates that an increase in reformer temperature from 400 ˚C to 1000 ˚C and O/E from 0.1 to 0.5 can improve the H_2 yield. However, at T_{Ref} > 800 ˚C and O/E above 0.5, the H_2 yield is slightly reduced, since the complete oxidation reaction (R4b) is occurring. The maximum H_2 yield of partial oxidation operation is 2.96 at T_{Ref}=1000 ˚C and O/E=0.5.

The effect of reformer temperature on all voltage overpotentials at O/E = 0.5 in SOFC-POX system as presented in Figure 5.16. Although the reformer temperature is raised, the cathode concentration overpotential (CONCCA), the activation overpotential and the ohmic loss (OHM) are constant. Only the anode concentration overpotential (CONCAN) decreases slightly with increasing reformer temperature. A similar trend is also observed in SOFC-SR system. It is noted that the major losses are the cathode activation overpotential (ACTCA), the anode activation overpotential (ACTAN) and ohmic loss, respectively. Moreover, increasing O/E at constant reformer temperature also has influence on all voltage losses that an all voltage losses reduce slightly because the current density and the exchange-current density decrease.

Figure 5.17 presents the electrical efficiency (η_{SOFC}) at the reformer temperature varying from 400 ˚C to 1000 ˚C and the oxygen to ethanol ratio varying from 0.1 to 0.9. The reformer temperature is raised the η_{SOFC} increases, since the cell voltage increases. On the contrary, the η_{SOFC} decreases with increasing the O/E. The maximum η_{SOFC} is found at T_{Ref} = 1000 ˚C and O/E = 0.1 that equal to 64.72%.

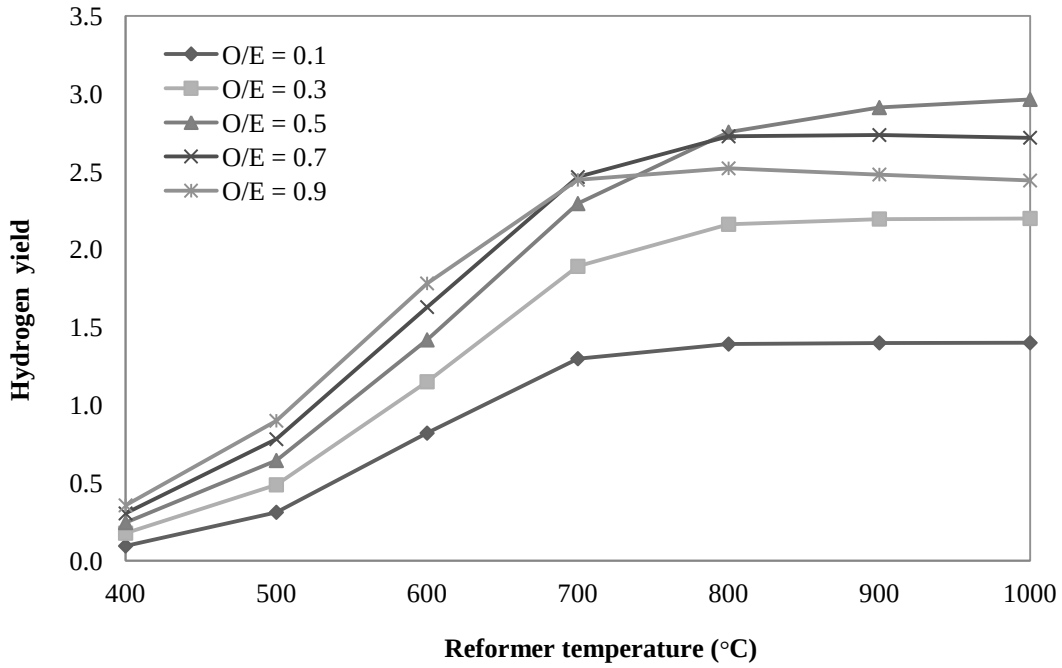

Figure 5.15 Effect of reformer temperature and oxygen to ethanol ratio on hydrogen yield in SOFC-POX system.

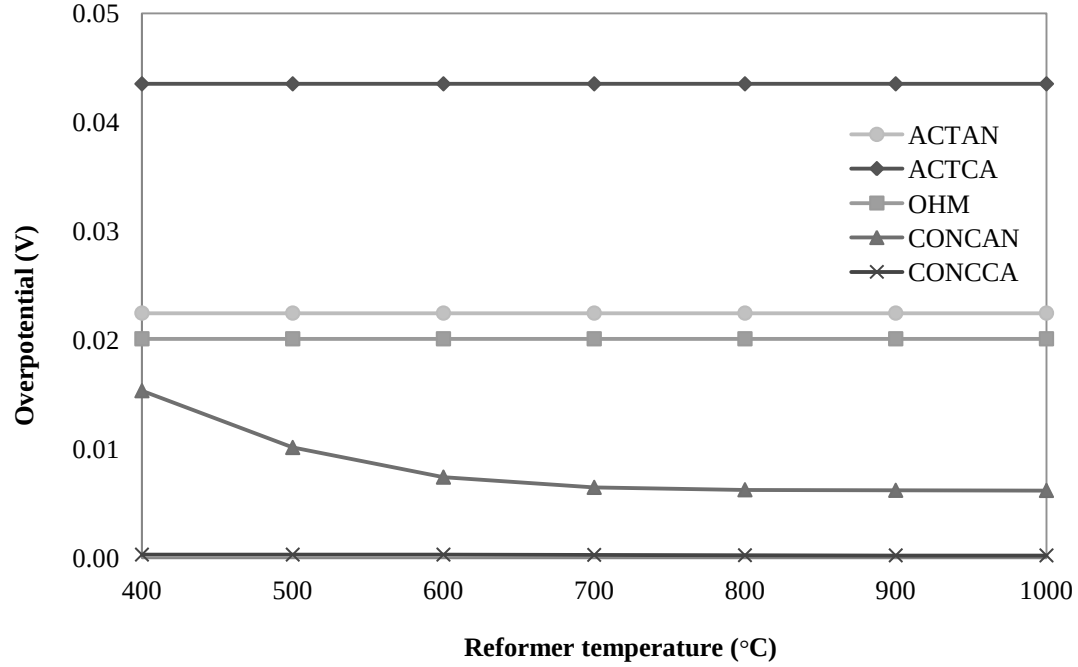

Figure 5.16 Effect of reformer temperature on all voltage overpotentials at O/E = 0.5 in SOFC-POX system.

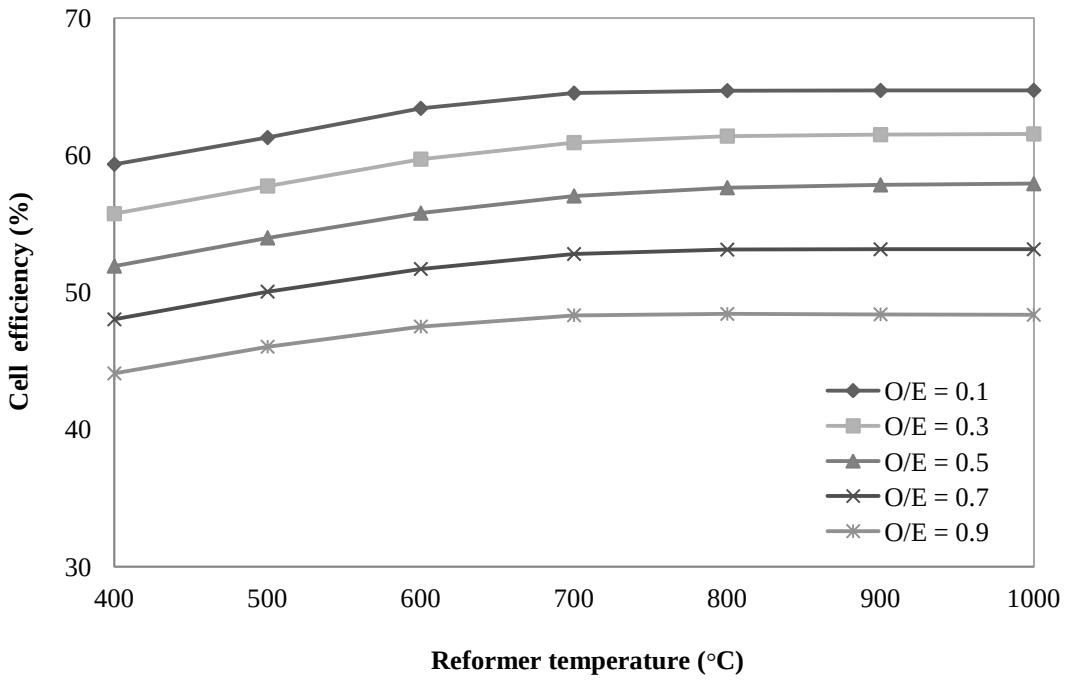

Figure 5.17 Effect of reformer temperature and oxygen to ethanol ratio on cell efficiency in SOFC-POX system.

5.3.2.2 Effect of SOFC temperature and oxygen to ethanol ratio.

In this study, the impact of cell operating temperatures on the equilibrium compositions at the anode outlet is investigated. Figure 5.18 demonstrates that at high SOFC temperature, the amount of H_2O and CO increase with increasing temperatures whereas the H_2 and CO_2 contents degrade. This can be explained by rising the cell temperature pronounces more the electrochemical reaction (R7) and the reverse water gas shift reaction (R3). It should be noted that the fraction of gases at the anode outlet in this system are less than the SOFC-SR system. This results from N_2 dilution which contents in the air as a reforming agent. However, the flow of H_2O at the anode effluent increases insignificantly with the increased O/E as shown in Figure 5.19. This is because oxygen that is reforming agent in partial oxidation operation is completely consumed in the reformer and thus it is not effect on the reactions in SOFC.

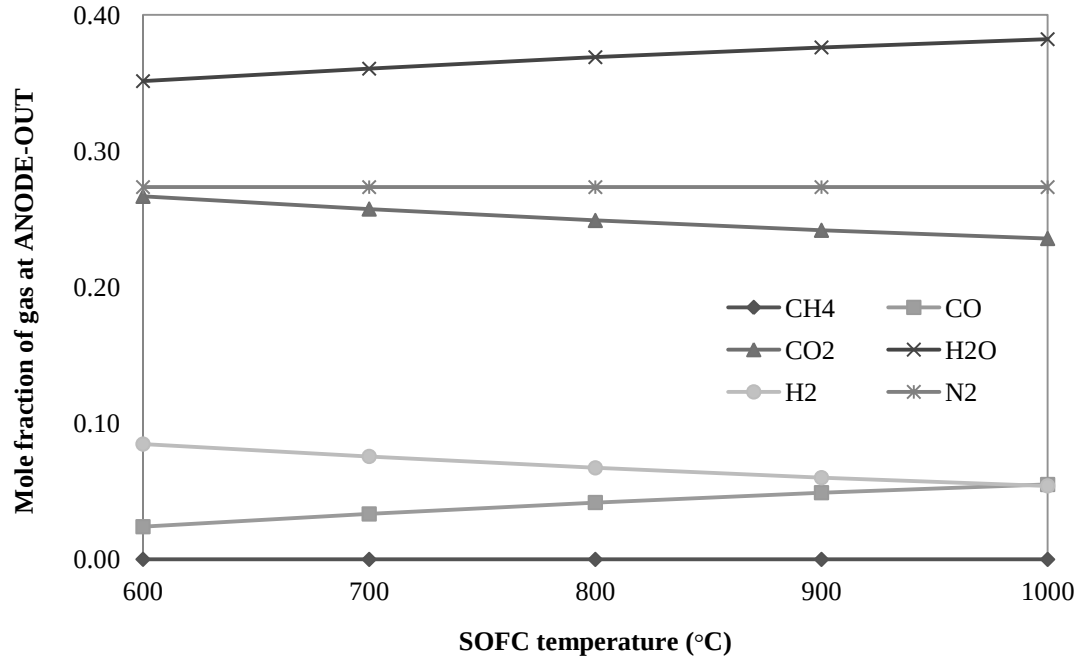

Figure 5.18 Effect of SOFC temperature on equilibrium compositions at the anode outlet with T_{Ref} = 700 °C and O/E = 0.5 in SOFC-POX system.

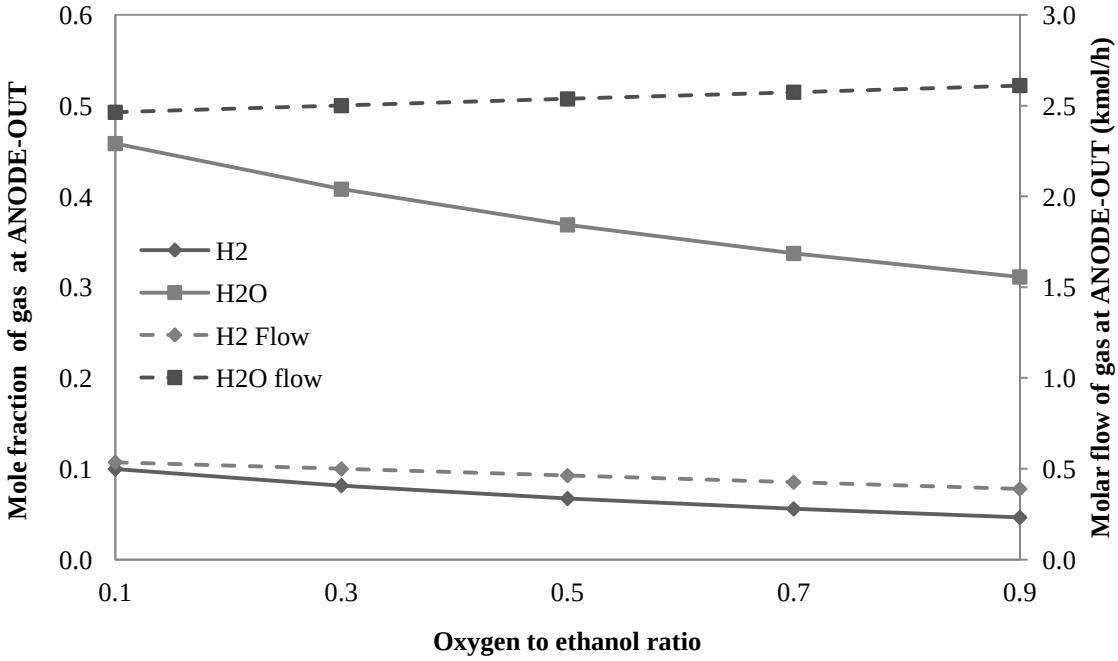

Figure 5.19 Effect of oxygen to ethanol ratio on mole fraction and molar flow of H_2 and H_2O at T_{Ref} = 700 °C and T_{SOFC} = 800 °C in SOFC-POX system.

Considering the effect of SOFC temperature on all voltage overpotentials at T_{Ref} = 700 ◦C and O/E = 0.5 in SOFC-POX system as shown in Figure 5.20. The activation overpotential and ohmic loss reduce rapidly at SOFC temperature around 600 – 900 ◦C. This can be explained by an increased the exchange-current density and decreased the specific resistance (R_{ohm}). On the other hand, the concentration overpotential increases slightly, since the variation of gas composition in reformer and anode effluents.

Figure 5.21 shows the electrical efficiency (η_{SOFC}) at SOFC operating temperature varying from 600 ◦C to 1000 ◦C and the oxygen to ethanol ratio varying from 0.1 to 0.9. An increase in SOFC operating temperature can improve the η_{SOFC}. This is because at high SOFC temperature, the electrochemical reaction rate is increased. Nevertheless, raising O/E causes the molar flow of CH_4 and CO in the reformer effluent lessen, resulting in the decreased H_2, which can be converted from the methane steam reforming and the water gas shift reactions in the cell, participates in the electrochemical reaction; therefore, the current is decreased that cause the η_{SOFC} reduces. The maximum η_{SOFC} is 67.24% at T_{SOFC} = 900 ◦C and O/E = 0.1.

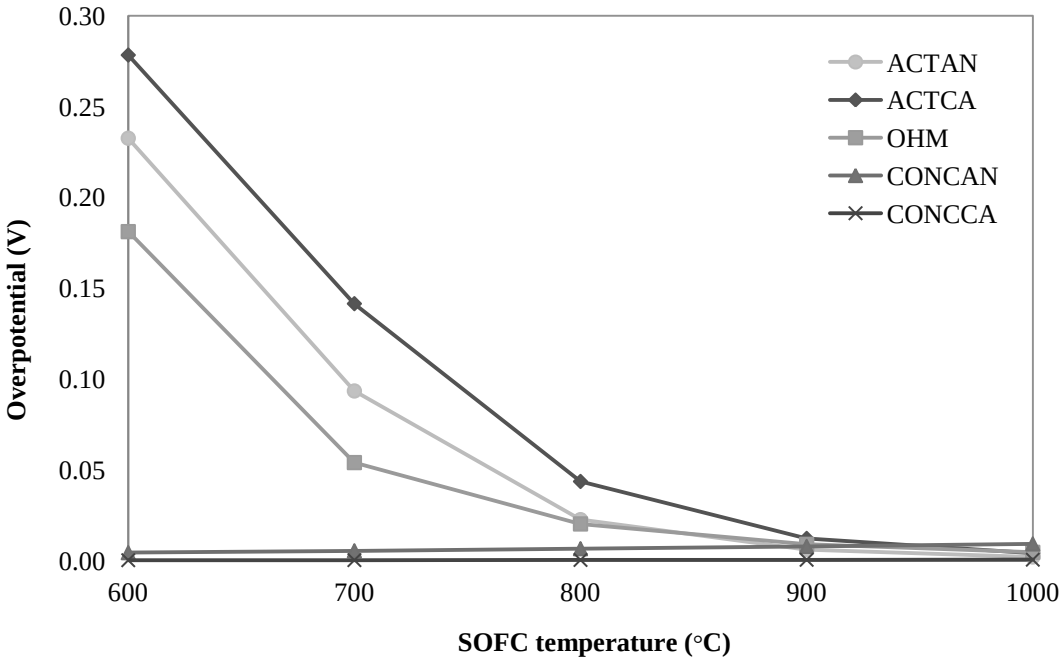

Figure 5.20 Effect of SOFC temperature on all voltage overpotentials at O/E = 0.5 in SOFC-POX system.

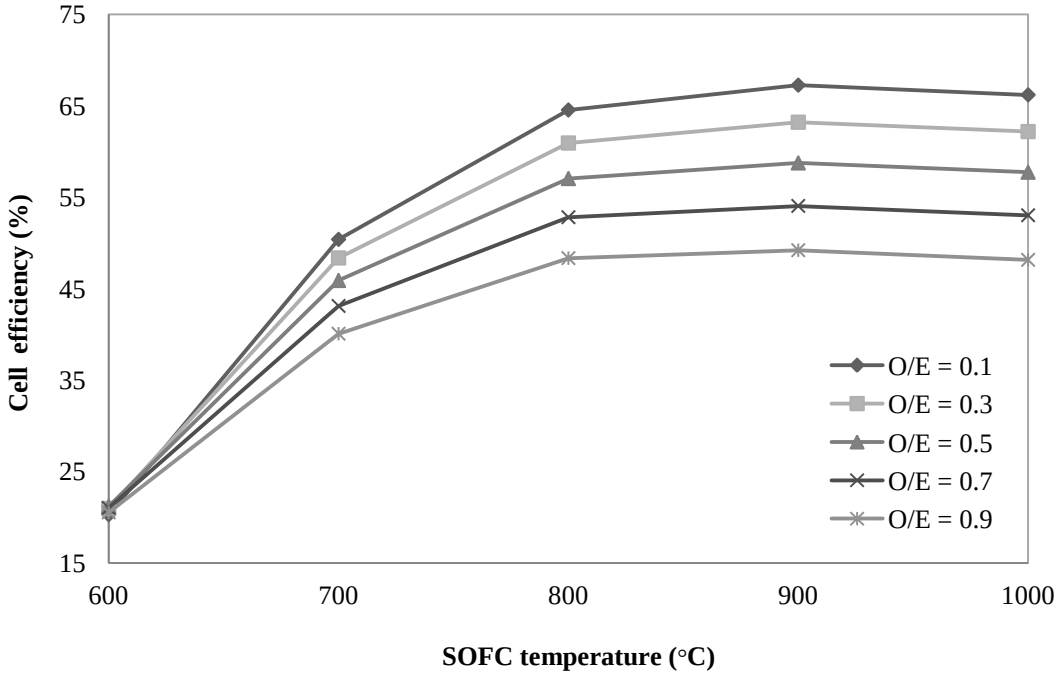

Figure 5.21 Effect of SOFC temperature and oxygen to ethanol ratio on cell efficiency in SOFC-POX system.

5.3.3 The SOFC integrated with autothermal reforming process (SOFC-ATR)

In this section, a thermodynamic analysis of ethanol autothermal reforming process is presented. At the standard conditions, the inlet molar flow rate of ethanol is 1 kmol/h, steam to ethanol ratio (S/E) is 2 and oxygen to ethanol ration (O/E) is 0.5.

5.3.3.1 Effect of reformer temperature, steam to ethanol ratio and oxygen to ethanol ratio.

The equilibrium composition of reformate gas in autothermal reforming operation is analyzed by increasing the reformer temperature form 400 °C to 1000 °C at S/E = 2 and O/E = 0.5. As can be seen in Figure 5.22, the H_2 and CO contents increase with increasing reformer temperature. This is caused by the steam reforming and partial oxidation reactions of ethanol (R1a, R4a) are more pronounced which are the endothermic reactions and favored at high temperatures. On the contrary, the CO_2, CH_4 and H_2O contents decrease at high temperatures because the steam reforming and partial oxidation reactions of methane (R2, R6) are supported. The equilibrium conversion of ethanol in this system is always at 100%. A similar trend is also observed in both the SOFC-SR and the SOFC-POX systems. The approached maximum H_2 content in the reformer effluent at 700 °C consist of 40.86%H_2, 0.52% CH_4, 13.95%CO, 8.28% CO_2, 14.99% H_2O and 21.40% N_2. Considering at reformer temperature 700 °C, when raising O/E increases the oxygen in the system that pronounces more the complete oxidation reaction (R4b); therefore, the molar flow of H_2 is decreasing. Moreover, an increasing in O/E also increases the nitrogen in the system that the nitrogen dilution leads to H_2 concentration decrease. Likewise, the H_2 concentration decrease with increasing S/E. However, increased S/E supports more the steam reforming and the water gas shift reactions and thus, the molar flow of H_2 is increased as shown in Figure 5.23.

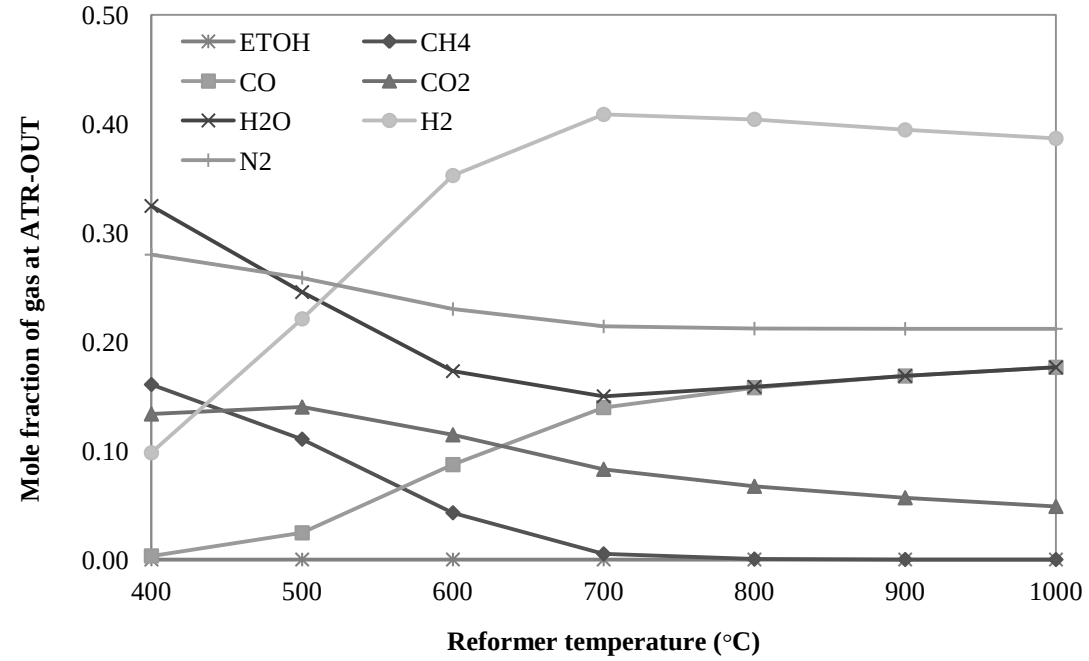

Figure 5.22 Effect of reformer temperature on equilibrium compositions at the reformer outlet with S/E = 2 and O/E = 0.5 in SOFC-ATR system.

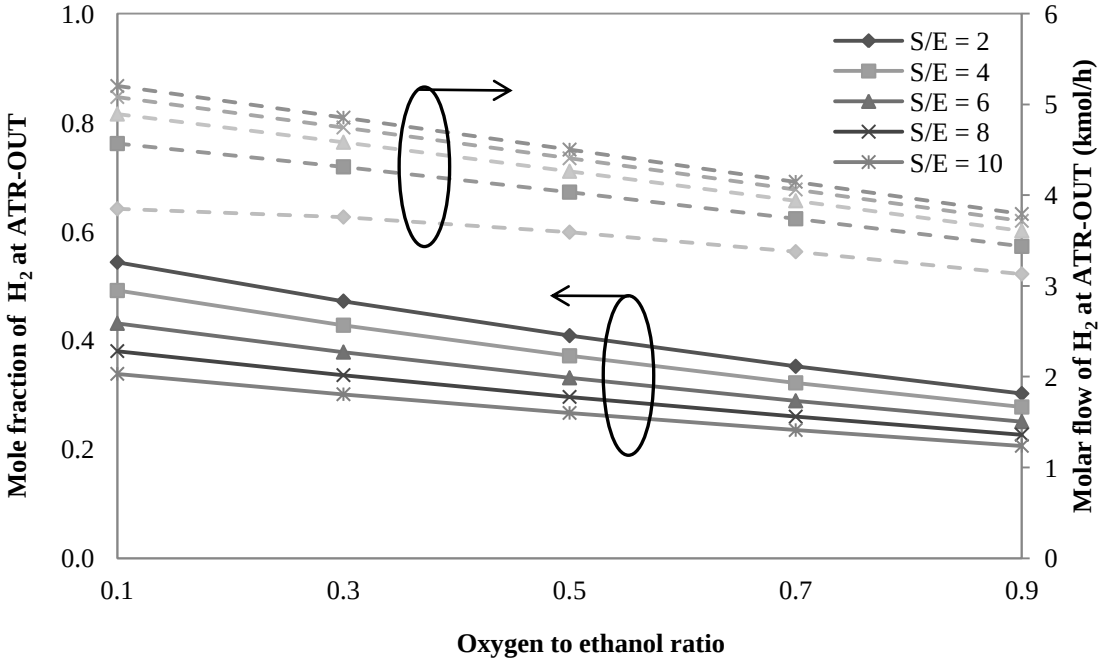

Figure 5.23 Effect of steam to ethanol ratio and oxygen to ethanol on mole fraction and molar flow of H_2 at T_{Ref} = 700 °C in SOFC-ATR system.

Figure 5.24 and Figure 5.25 show the hydrogen yield (H_2 yield) as a function of reformer temperature, steam to ethanol ratio and oxygen to ethanol ratio. According to Figure 5.24, It can be seen that an increase of both S/E and reformer temperature also has the effect on increasing the H_2 yield. This implies that an increase the H_2 yield owing to the increased SR reaction in the reformer which is the endothermic reaction and favored at high temperatures and an excess steam is used to overcome the equilibrium limitation of SR reaction, enhancing the extent of hydrogen produced (Ashrafi et al., 2008). From the Figure 5.25, an increase in reformer temperature from 400 ◦C to 1000 ◦C can improve the H_2 yield, since the rate of possible reactions occurred in this system are supported. Considering increased of the O/E, the H_2 yield is increased insignificantly at T_{Ref} < 600 ◦C. However, the H_2 yield decrease with varying in O/E from 0.1 to 1.0 at T_{Ref} > 600 ◦C. This is because the increased amount of oxygen favors the POX reaction and suppresses the SR, resulting in the depleted H_2 yield. From both Figure 5.24 and Figure 5.25, it is noted that the maximum H_2 yield of autothermal reforming operation is 4.56 at T_{Ref} = 1000 ◦C, S/E = 10 and O/E=0.5.

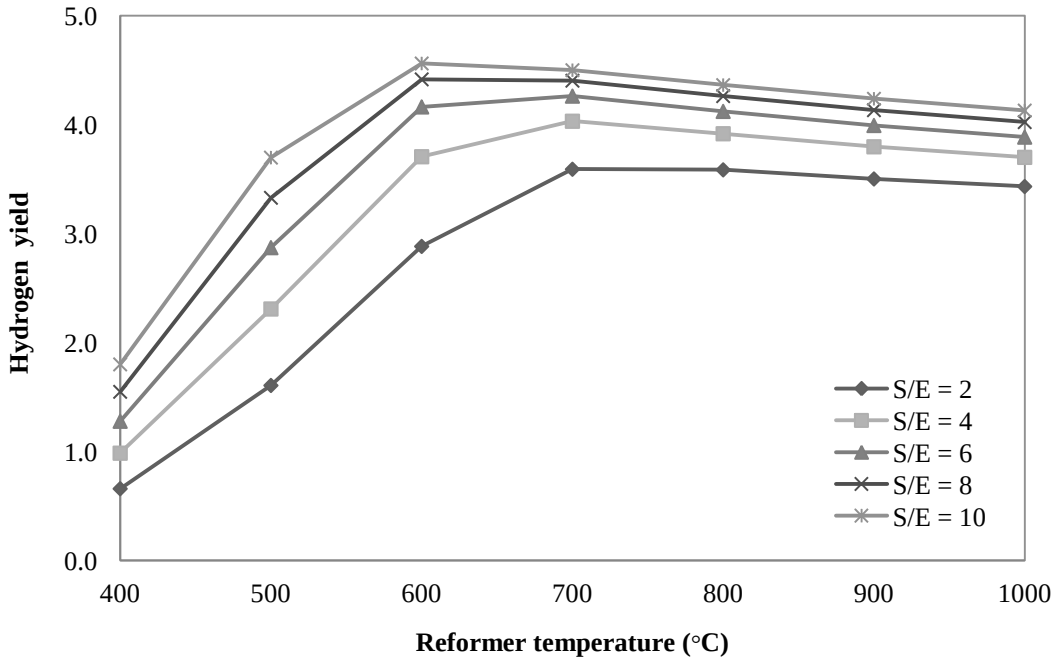

Figure 5.24 Effect of reformer temperature and steam to ethanol ratio on hydrogen yield in SOFC-ATR system.

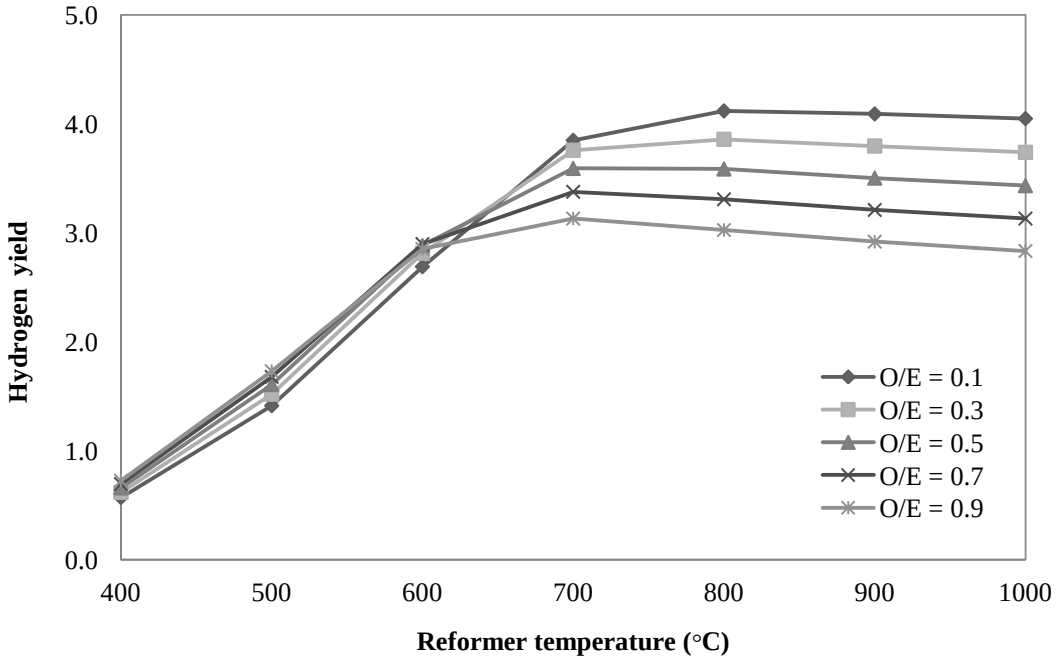

Figure 5.25 Effect of reformer temperature and oxygen to ethanol ratio on hydrogen yield in SOFC-ATR system.

Figure 5.26 presents the effect of reformer temperature on all voltage overpotentials at S/E = 2 and O/E = 0.5 in SOFC-ATR system. It is found that the major losses are the cathode activation overpotential (ACTCA), the anode activation overpotential (ACTAN) and ohmic loss, respectively. An increased the reformer temperature only has effects on decreasing the anode concentration overpotential (CONCAN) slightly. A similar trend is also observed in SOFC-SR and SOFC-POX systems.

The electrical efficiency (η_{SOFC}) at the reformer temperature, the steam to ethanol ratio and the oxygen to ethanol ratio are shown in Figure 5.27 and Figure 5.28. An increasing the reformer temperature around 400 – 700 °C the η_{SOFC} is increasing because increasing of H_2 concentration in the reformer effluent makes the cell voltage increases. On the contrary, the η_{SOFC} decreases with increasing the S/E and the O/E. This causes by the reduction of H_2 concentration. The η_{SOFC} reaches a maximum value as 64.83% at T_{Ref} = 800 °C, S/E = 2 and O/E = 0.1.

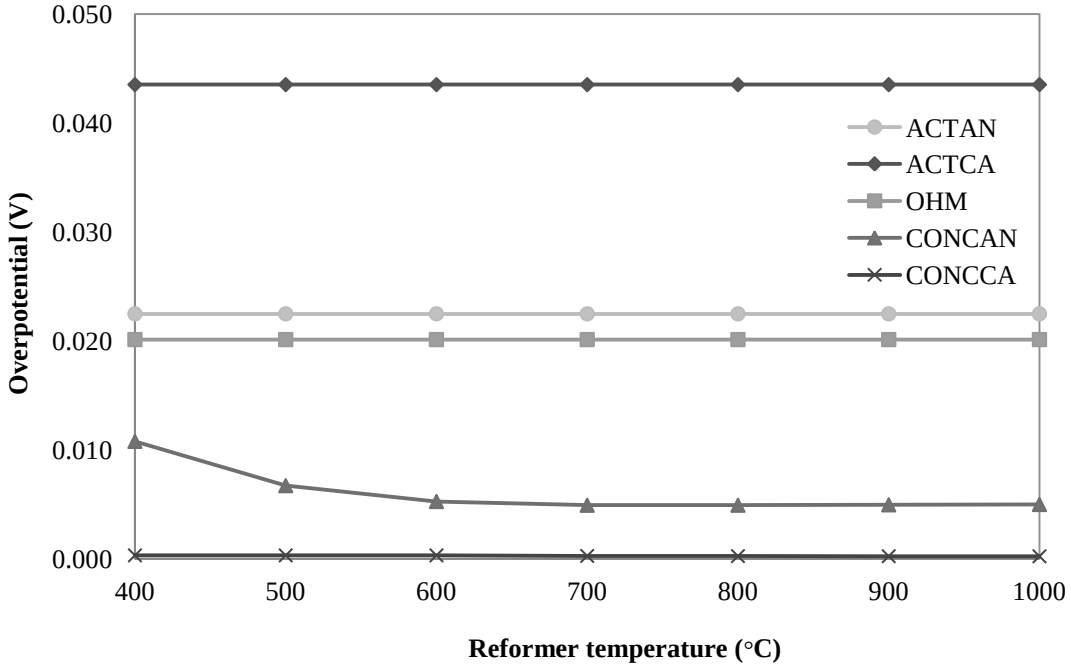

Figure 5.26 Effect of reformer temperature on all voltage overpotentials at S/E = 2 and O/E = 0.5 in SOFC-ATR system.

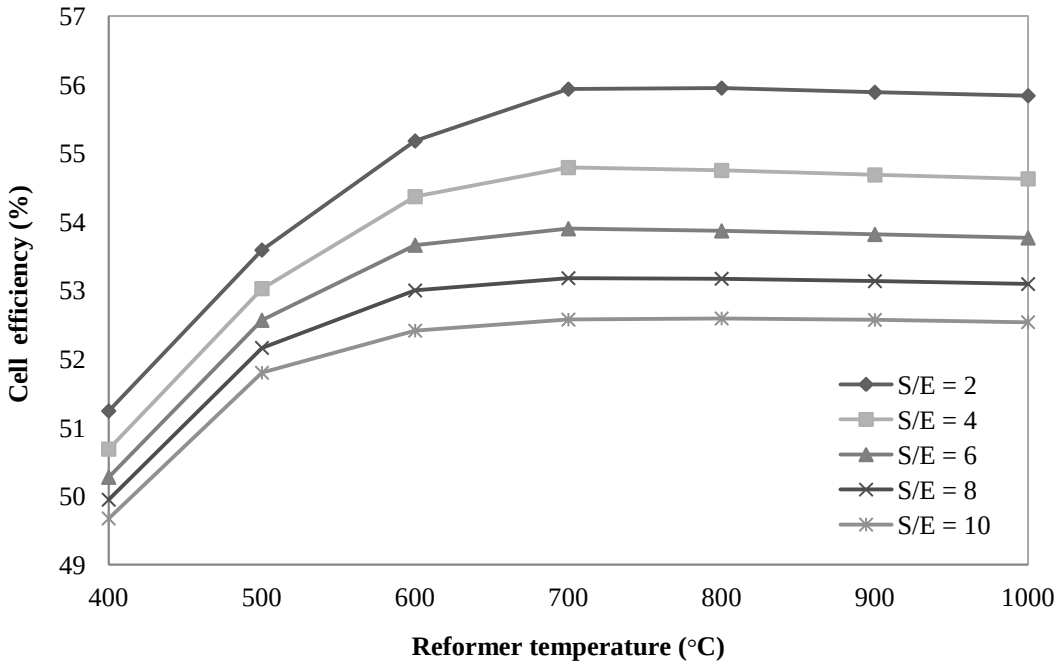

Figure 5.27 Effect of reformer temperature and steam to ethanol ratio on cell efficiency at O/E = 0.5 in SOFC-ATR system.

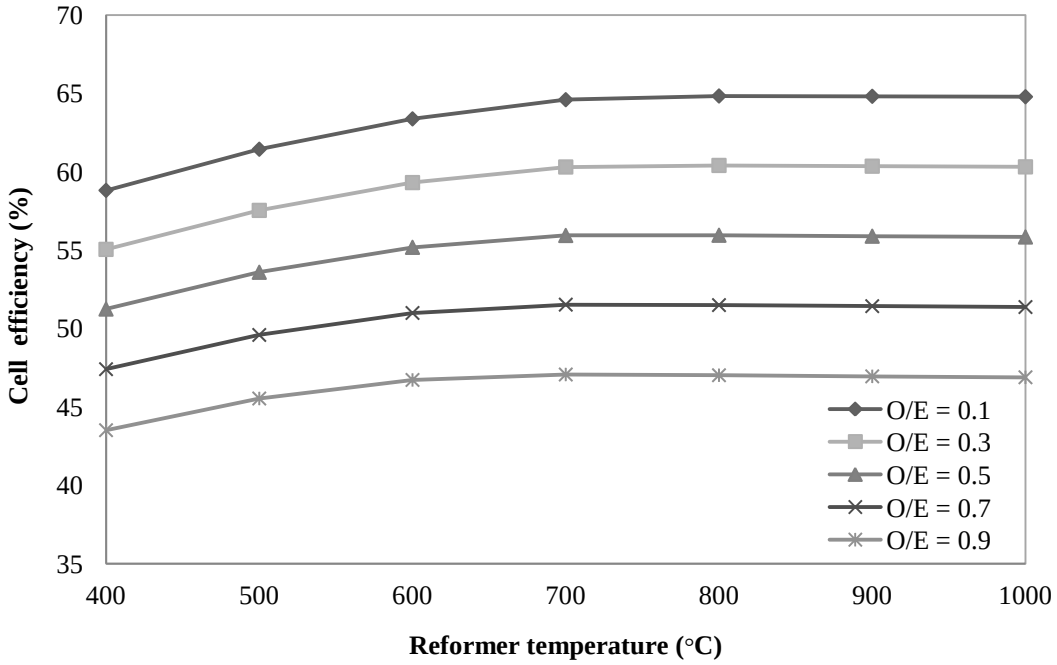

Figure 5.28 Effect of reformer temperature and oxygen to ethanol ratio on cell efficiency at S/E = 2 in SOFC-ATR system.

5.3.3.2 Effect of SOFC temperature, steam to ethanol ratio and oxygen to ethanol ratio.

The effect on the anode equilibrium compositions effluent at different cell operating temperatures is analyzed as shown in Figure 5.29. The results demonstrate that at all SOFC temperature range studied, the amount of H_2O and CO increase slightly with increasing temperatures whereas the H_2 and CO_2 contents degrade insignificantly. Although an increased the cell temperature pronounces more the electrochemical reaction and the reverse water gas shift reaction, the fuel utilization is fixed and thereby the compositions of gas in the anode effluent change slightly.

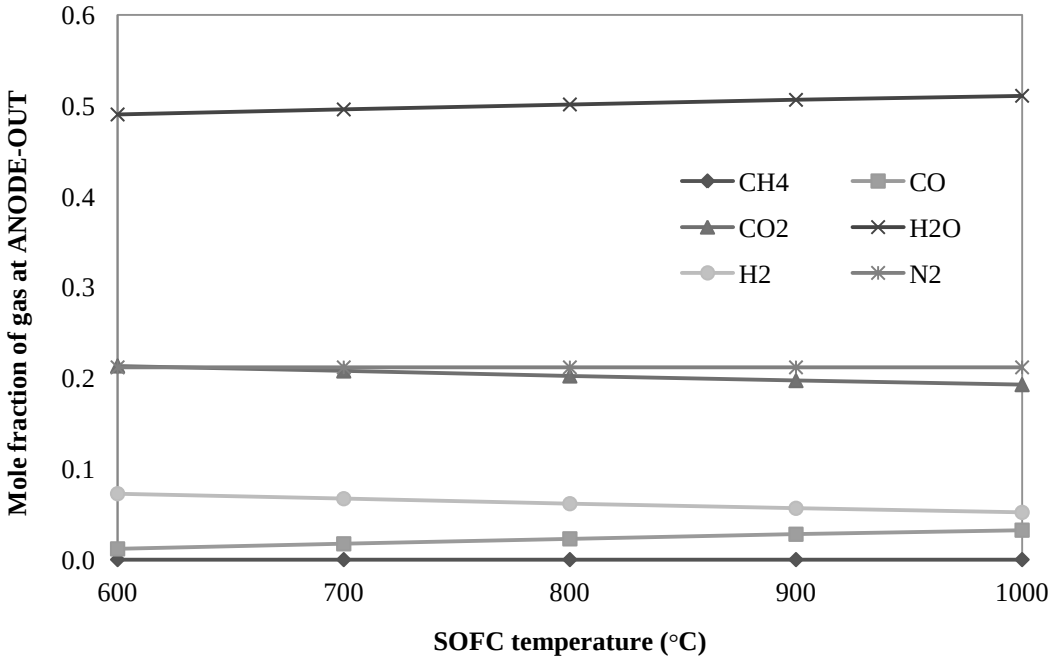

Figure 5.29 Effect of SOFC temperature on equilibrium compositions at the anode outlet with T_{Ref} = 700 °C, S/E = 2 and O/E = 0.5 in SOFC-SR system.

The mole fraction and molar flow of H_2 and H_2O at the anode effluent against the steam to ethanol ratio and the oxygen to ethanol ratio are shown in Figure 5.30 and Figure 5.31, respectively. According to the Figure 5.30, raising S/E the water content increase, results in the reduction of H_2 concentration in an anode effluent. However, H_2 concentration is slightly decreased because increased water pronounces steam reforming reaction of methane inside the cell; therefore, a bit of H_2 molar flow is increased. Similarly, increasing O/E, that increase N_2 content in the system causes reduced fraction of H_2 and H_2O. Despite increased oxygen in this system, an anode has no result due to an oxygen is depleted in the reformer. Therefore, the flow of H_2O at the anode effluent increases insignificantly with the increased O/E whereas the flow of H_2 reduces as shown in Figure 5.31.

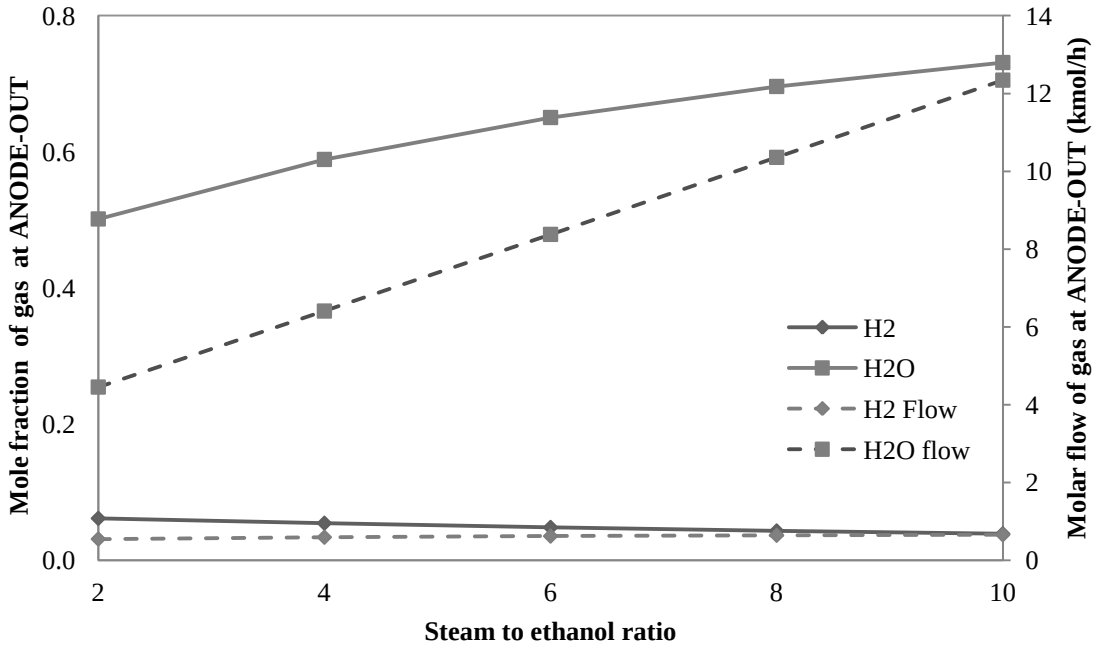

Figure 5.30 Effect of steam to ethanol ratio on mole fraction and molar flow of H_2 and H_2O at T_{Ref} = 700 ℃, T_{SOFC} = 800 ℃ and O/E = 0.5 in SOFC-ATR system.

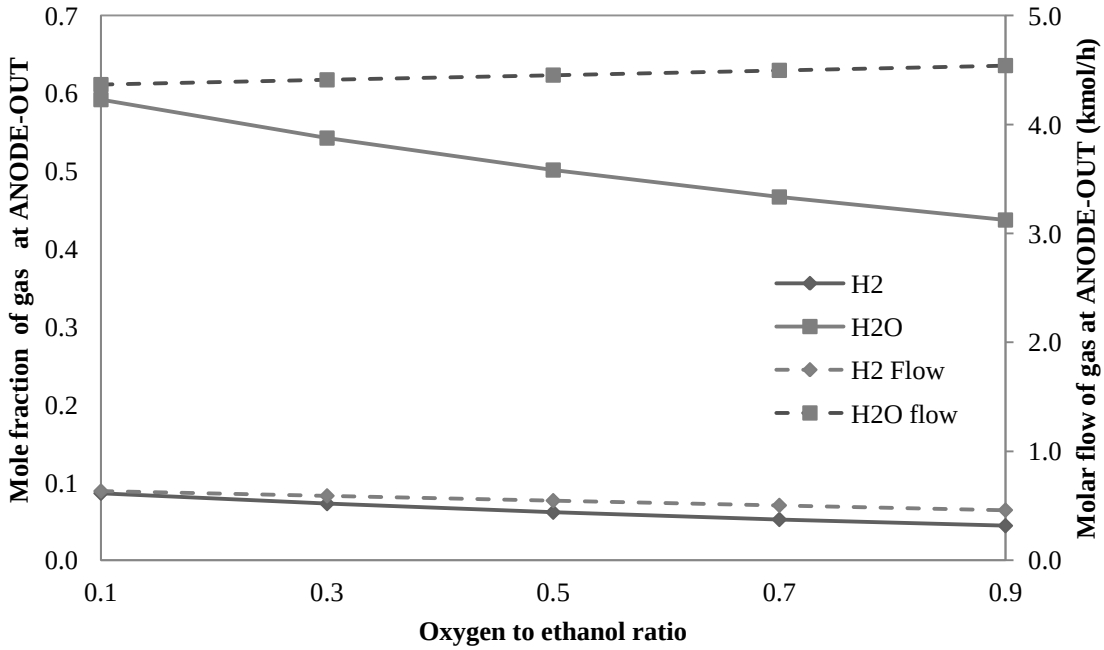

Figure 5.31 Effect of oxygen to ethanol ratio on mole fraction and molar flow of H_2 and H_2O at T_{Ref} = 700 ℃, T_{SOFC} = 800 ℃ and S/E = 2 in SOFC-ATR system.

Figure 5.32 shows the influent of SOFC temperature on all voltage overpotentials at S/E = 2 and O/E = 0.5 in SOFC-ATR system. At SOFC temperature from 600 ◦C to 900 ◦C, the activation overpotential and ohmic loss reduce rapidly whereas the concentration overpotential is insignificant effect. A similar trend is also observed in SOFC-SR and SOFC-POX systems.

Figure 5.33 and Figure 5.34 present the electrical efficiency (η_{SOFC}) of SOFC at different cell operating temperature, the steam to ethanol ratio and the oxygen to ethanol ratio. The η_{SOFC} is enhanced with increasing in SOFC operating temperature. This is because the electrochemical reaction is more supported. Nevertheless, raising the S/E, as shown in Figure 5.33, and O/E, as shown in Figure 5.34, lead to the η_{SOFC} reduces owing to decreased rate of the electrochemical reaction and dilution of N_2 in the cell. The maximum η_{SOFC} is 67.21% at T_{SOFC} = 900 ◦C, S/E = 2 and O/E = 0.1.

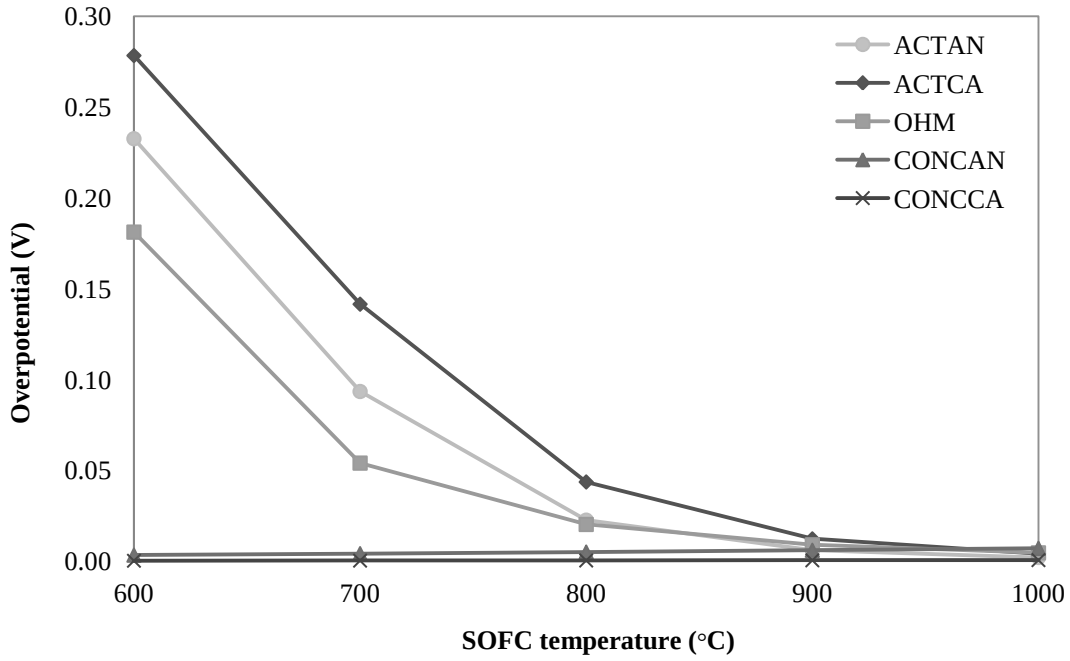

Figure 5.32 Effect of SOFC temperature on all voltage overpotentials at S/E = 2 and O/E = 0.5 in SOFC-ATR system.

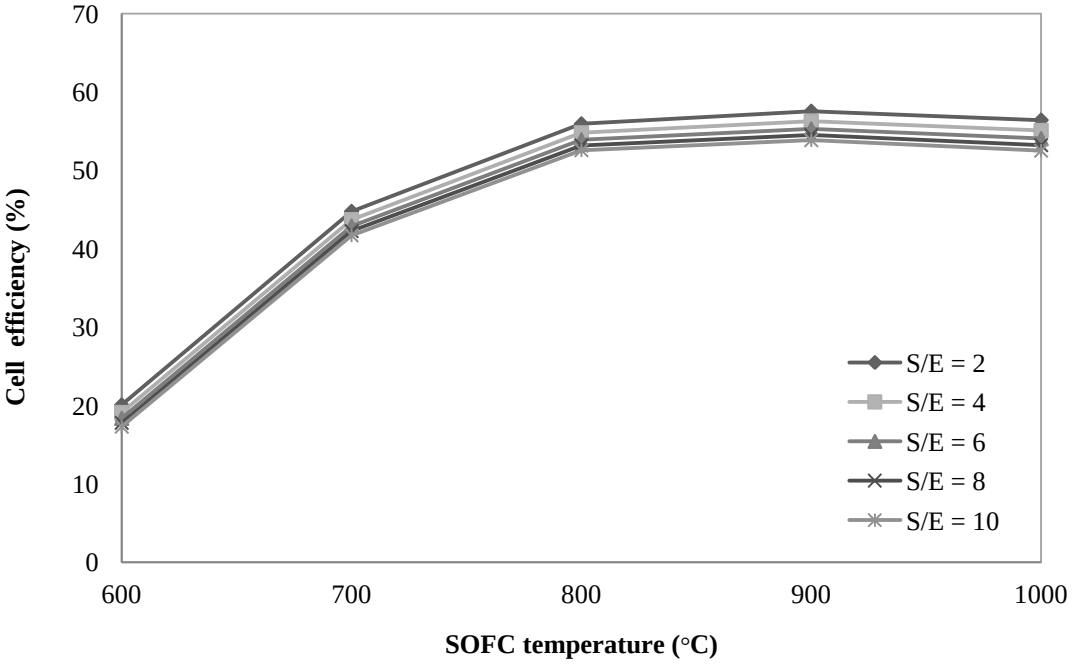

Figure 5.33 Effect of SOFC temperature and steam to ethanol ratio on cell efficiency in SOFC-ATR system.

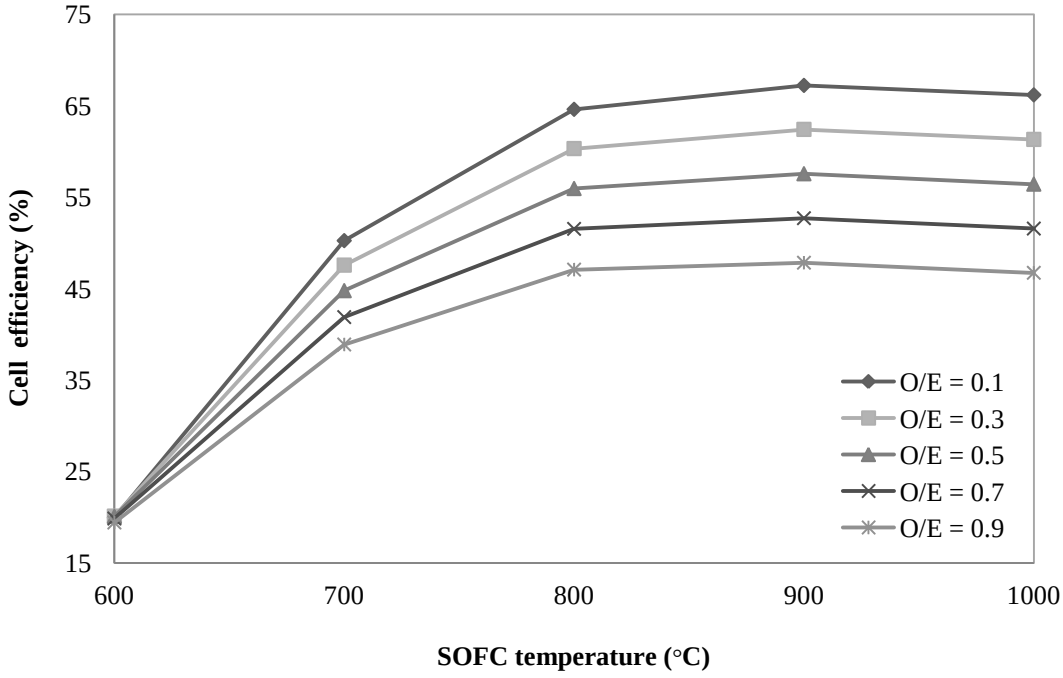

Figure 5.34 Effect of SOFC temperature and oxygen to ethanol ratio on cell efficiency in SOFC-ATR system.

5.4 Conclusions

In this study, the performance analysis of SOFC using different ethanol reforming process, such as steam reforming, partial oxidation, and autothermal reforming was performed by using Aspen Plus. An anode supported SOFC under isothermal condition based on steady state model associated with a detail of electrochemical model taking into account all voltage losses (i.e., activation, concentration and ohmic losses) was employed. At this condition, the reformer temperature of 700 ℃, cell temperature of 900 ℃ steam to ethanol ratio of 2 and oxygen to ethanol ratio of 0.1, the maximum electrical performance for each system is predicted. The simulation result shows that the electrical efficiency of the SOFC-SR, SOFC-POX and SOFC-ATR systems are 69.59%, 67.24% and 67.21%, respectively. Interestingly, it is shown that the electrical performance of the SOFC system with different reforming systems is slightly different because an internal reforming of methane was considered in this work. The effect of key operating parameters, i.e., reformer temperature, SOFC operating temperature, steam to ethanol ratio and oxygen to ethanol ratio are also presented. It is found that the electrical performance is enhanced with increasing in reformer and cell temperatures and decreasing steam to ethanol ratio and oxygen to ethanol ratio. Although the hydrogen yield increases with increasing steam to ethanol ratio, the increased amount of water suppresses the thermodynamically equilibrium electrochemical reaction and thus the electrical performance increases. The addition of oxygen to the reformer is an important factor having the direct impact on a hydrogen yield. The increased exceed amount of oxygen favors the complete oxidation reaction, resulting in hydrogen yield is reduced. From the simulation results, no oxygen exists in the reforming gas at all operating conditions, so an anode has no result from oxygen.

CHAPTER VI

THERMAL ANALYSIS OF SOFC SYSTEM

The objectives of this chapter are to examine the thermal performance of SOFC system cooperating with ethanol reforming process and to design the SOFC system with heat integration by means of pinch analysis in order to reduce an external utility used in the system. Three different reforming processes were used steam reforming (SR), partial oxidation (POX) and autothermal reforming (ATR). Similar to chapter 5, the effect of operating parameters, i.e., reformer temperature, cell operating temperature, steam to ethanol ratio, and oxygen to ethanol ratio, are considered. Thermodynamic analysis of all systems is performed on Aspen Plus.

6.1 Introduction

As mentioned earlier, the electrical performance of the SOFC system integrated with ethanol reforming process was presented. Most of the studies about SOFC system, the electrical performance are significantly considered regardless of the energy consumption within the system, especially energy consumption in the reforming process that is different the energy demand for each process. Considering for the real application, the energy consumption in the system is an important factor. However, the SOFC operates at high temperature (600-1000 ◦C), so the waste heat from SOFC can be thermally utilized for other heat-requiring parts of the SOFC system. In general, the exhaust gas obtained from the SOFC is often used in cogeneration applications and bottoming cycles to improve the system efficiency, particularly the hybrid system combining a SOFC and a gas turbine (Palsson et al., 2000; Yang et al., 2006; Haseli et al., 2008). In this study, a heat recovery from the exhaust gas for used in the system is focused. A number of researches have been concentrated on a heat recovery from the exhaust gas. Zhang et al. (2005) studied the SOFC integrated with steam reforming process by using natural gas as a fuel and

found that a off-gas from an anode was split into two streams; the first one was recycle gas stream that the unreacted fuel was mixed with fuel streams and the second one was to feed into an afterburner in order to produce more heat, similar to Lisbona's work (2007).

Few works have presented the design of heat exchanger networks for SOFC coupled to ethanol reforming process. Arteaga et al. (2009) studied simulation and heat integration of a SOFC system integrated with ethanol steam reforming process. A design of heat exchanger network of an ethanol fueled SOFC system based on a pinch analysis was proposed. Jamsak et al. (2009) analyzed the performance of a SOFC system integrated with a distillation column (SOFC-DIS) fed by bioethanol and studied the designs of the heat exchanger network for the SOFC-DIS system.

As above, a few investigations on ethanol-fed SOFC system have previously been published. Most of them have been based on a steam reforming technology (Arteaga et al., 2009; Jamsak et al., 2009; Casas et al., 2010), whereas few publications deal with autothermal reforming and partial oxidation reforming. Therefore, thermal performance of SOFC system couple with ethanol reforming process; i.e., steam reforming, partial oxidation and autothermal reforming is proposed. The designs of the heat exchanger network for the SOFC integrated with different ethanol reforming process are further investigated by using of the pinch technology.

6.2 Results and discussion of thermal analysis

Thermal analysis of a SOFC system cooperating with ethanol reforming process is presented. The minimization of the Gibbs free energy was used to determine the heat duty of unit in the system, which positive heat duty shows heat demand and negative heat duty presents heat produced from unit. An operating condition used for all units is assumed to operate under isothermal condition based on steady state model, unless an afterburner operates at adiabatic condition that heat duty is set to zero. In general, the electrochemical reaction within a SOFC is an exothermic reaction so air excess feed into SOFC in order to maintain a cell operating temperature. For all simulations, the inlet feed temperature are kept constant at 25 ◦C.

The operational ranges examined in this study are at the reformer temperature from 400 ˚C to 1000 ˚C, stack temperature from 600 ˚C to1000 ˚C, steam to ethanol ratio (S/E) from 2.0 to 10.0, and oxygen to ethanol ratio (O/E) from 0.1 to 0.9 at atmospheric pressure. The operating temperature for each unit in the system is shown in Table 6.1.

Table 6.1 The operating temperature for each unit in the system

Unit	Temperature (˚C)
Vaporizer (HEATER1,2)	100
Preheater	400
Reformer	700
Cell stack	800
Cooler	200
Preheater air to cathode (HEATER3)	800

6.2.1 The SOFC integrated with ethanol steam reforming process (SOFC-SR)

A thermodynamic analysis of ethanol steam reforming process is presented. At the standard conditions, the inlet molar flow rate of ethanol is 1 kmol/h and steam to ethanol ratio (S/E) is 2. The positive and negative values represent heat consumption and heat production from a system, respectively.

The effect of reformer temperature at S/E = 2, T_{SOFC} = 800 ˚C on heat duty of the SOFC-SR system is shown in Figure 6.1. The simulation result shows that the reformer temperature is raised the heat duty of reformer (Q_{SR}) increases. Reasonable the steam reforming reaction which is the endothermic reaction is more pronounced at high reformer temperature, so heat demand in reformer increases. Whereas the heat duty of air inlet to cathode preheating ($Q_{PAIR-CA}$) decreases because hydrogen yield increases with increasing reformer temperature, resulting in the electrochemical reaction in an anode is supported the heat duty of SOFC is more produced; therefore, air inlet at cathode side is no need to preheat. However, an air inlet at cathode is

increased when the produced heat from a SOFC is high and thus the heat duty of cooler (Q_{COOL}) is increased. It is noted that at reformer temperature of 400 ˚C, Q_{SR} produces a heat because the water gas shift reaction is more pronounced the CO content in reformer effluent reduces, as shown in Figure 5.4. In addition, an increased reformer temperature has no effect on the feed flow rate, the vaporizer and preheater heat duty of ethanol (Q_{H1}, Q_{PETOH}) and water (Q_{H2}, Q_{PH2O}) are constant. Considering the total heat duty of the system (Q_{TOTAL}) found that Q_{TOTAL} reduces with raising the reformer temperature.

Figure 6.2 shows the heat duty at different steam to ethanol ratio at T_{REF} = 700˚C, T_{SOFC} = 800 ˚C. According to the Figure 6.2, it can be seen that raising S/E increases the water in the system that supports more the steam reforming reaction according the thermodynamically equilibrium, so the vaporizer and preheater heat duty of water (Q_{H2}, Q_{PH2O}) and the reformer duty (Q_{SR}) are increased. The cooler (Q_{COOL}) duty is also increased because amount of water in the system increases. So the heat duty in the system increases, the total heat duty (Q_{TOTAL}) is decreased.

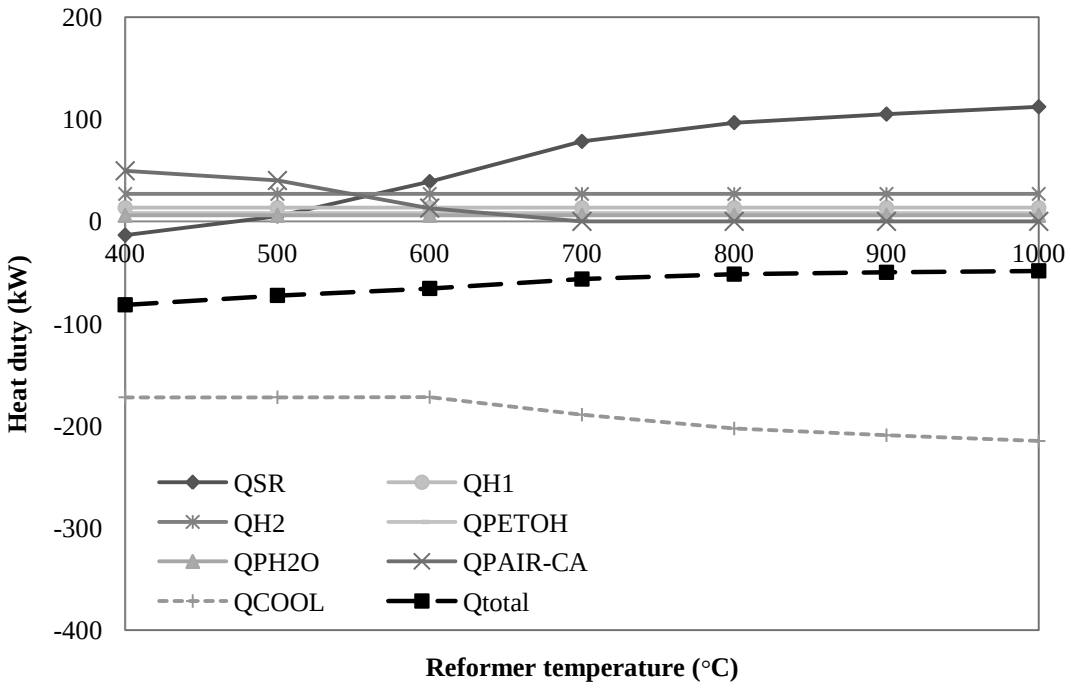

Figure 6.1 Effect of reformer temperature at S/E = 2, T_{SOFC} = 800 ˚C on heat duty of the SOFC-SR system.

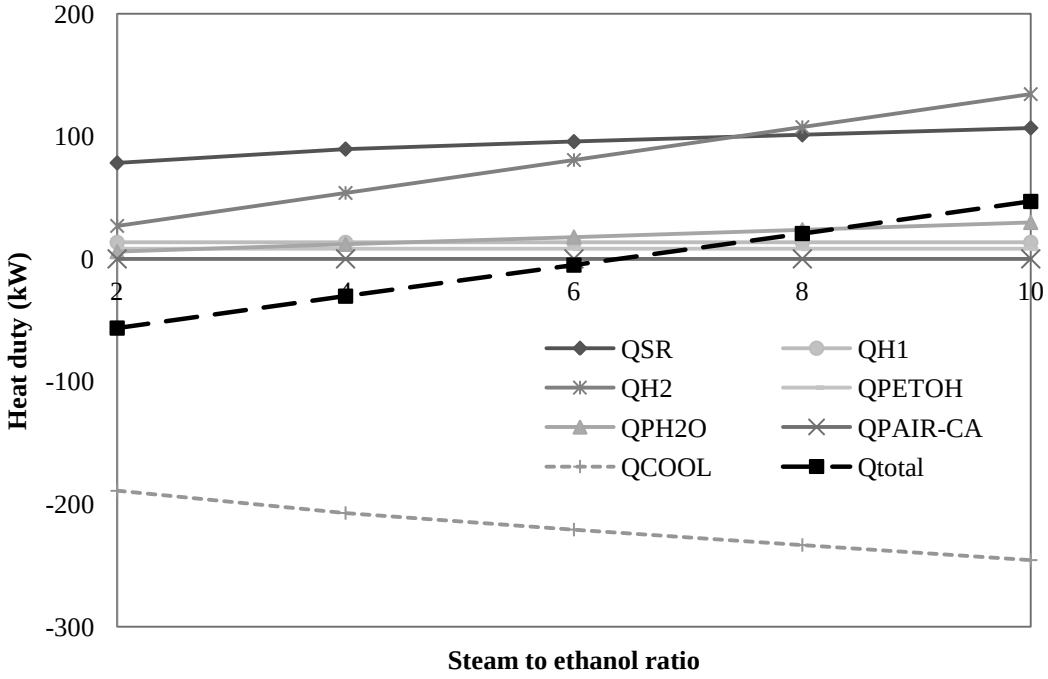

Figure 6.2 Effect of steam to ethanol ratio at T_{REF} = 700 ˚C, T_{SOFC} = 800 ˚C on heat duty of the SOFC-SR system.

The effect of SOFC temperature at S/E = 2, T_{REF} = 700 ˚C on heat duty of the SOFC-SR system is illustrated in Figure 6.3. Although an increase in cell operating temperature increases the rate of electrochemical reaction and the reverse water gas shift reaction; the heat duty of anode is reduced and thus air flow into the cell in order to control cell operating temperature also decreases, resulting in the heat duty of cooler (Q_{COOL}) is decreased. Therefore, the total heat duty (Q_{TOTAL}) decreases with decreasing the SOFC operating temperature.

Figure 6.4 and Figure 6.5 show thermal efficiency ($\eta_{Thermal}$) of the SOFC-SR system as a function of reformer temperature, SOFC operating temperature and steam to ethanol ratio. A decrease in reformer temperature, SOFC operating temperature and S/E can improve the $\eta_{Thermal}$. This is because the energy demand in the system increases such as the vaporizer and preheater heat duty of water (Q_{H2}, Q_{PH2O}) and the reformer duty (Q_{SR}) are increased that causes the total heat duty (Q_{TOTAL}) decreases. Therefore, the $\eta_{Thermal}$ reduces. It is noted that at S/E = 8 and 10 with reformer temperature, the value of $\eta_{Thermal}$ is negative. This implies that less the $\eta_{Thermal}$ is due to the energy consumption is higher than the energy production.

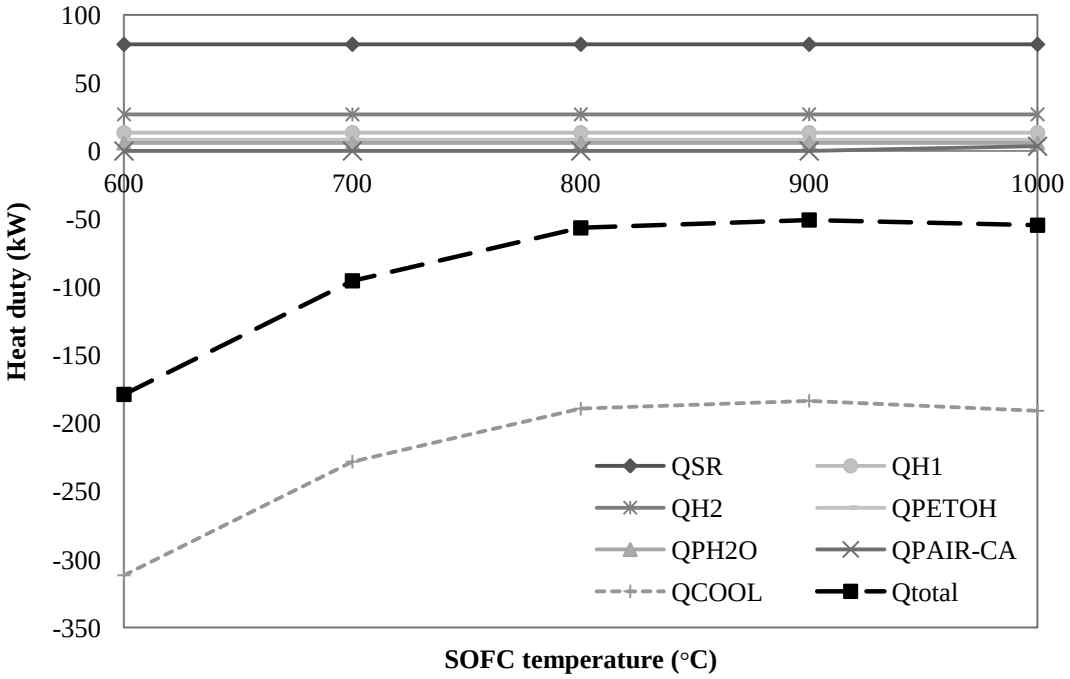

Figure 6.3 Effect of SOFC temperature at S/E = 2, T_{REF} = 700 ˚C on heat duty of the SOFC-SR system.

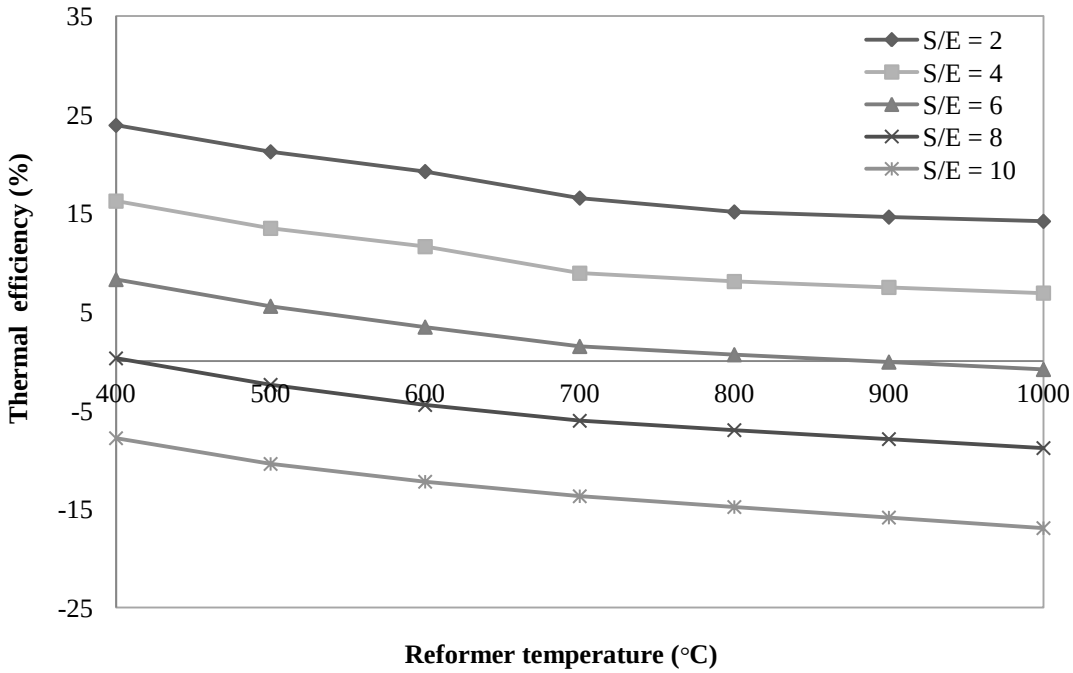

Figure 6.4 Effect of reformer temperature and steam to ethanol ration on thermal efficiency of the SOFC-SR system.

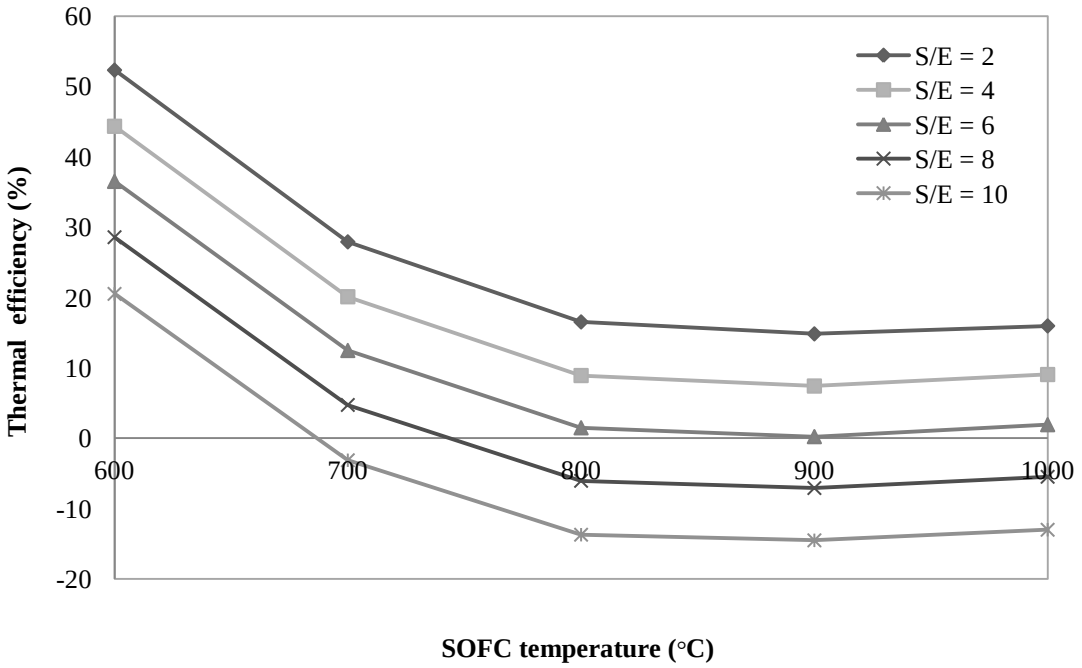

Figure 6.5 Effect of SOFC temperature and steam to ethanol ration on thermal efficiency of the SOFC-SR system.

6.2.2 The SOFC integrated with ethanol partial oxidation process (SOFC-POX)

In this section, a thermodynamic analysis of ethanol partial oxidation process is presented. At the standard conditions, the inlet molar flow rate of ethanol is 1 kmol/h and oxygen to ethanol ratio (O/E) is 0.5. The positive and negative values represent heat consumption and heat production from a system, respectively.

The effect of reformer temperature at O/E = 0.5, T_{SOFC} = 800 ˚C on heat duty of the SOFC-POX system is shown in Figure 6.6. The result indicates that the increasing reformer temperature results in the constant of vaporizer duty of ethanol (Q_{H1}), preheater of ethanol (Q_{PETOH}) and preheater of air (Q_{AIRR}). Because of the amount of the inlet are unchanging. However, the reformer duty (Q_{POX}) is raised. The temperature interval of 400 ˚C to 700 ˚C, the Q_{POX} is a negative value since the complete oxidation reaction (R4b) which is high exothermic reaction (-1368 kJ/mol) (Rabenstein and Hacker, 2008). It points that the fraction of H_2O and CO_2 leaving the reformer is increasing (shown in Figure 5.13). In the other hand, the complete

oxidation reaction is inhibited whereas the partial oxidation reaction is pronounced at the temperature higher than 700 ◦C. Since the partial oxidation reaction of ethanol is slightly endothermic. It is noted that heat duty of air inlet to cathode preheating ($Q_{PAIR-CA}$) decreases with increasing reformer temperature because hydrogen yield increases; therefore, the heat duty of SOFC is also increased. For this reason, the cooler duty (Q_{COOL}) increase that causes the total heat duty (Q_{TOTAL}) is decreased.

The heat duty at varying oxygen to ethanol ratio from 2 to 10 at T_{REF} = 700˚C, T_{SOFC} = 800 ˚C is illustrated in Figure 6.7. From the simulation result, the oxygen in the system increases that results in preheater heat duty of air (Q_{AIRR}) is also increased. When the oxygen is raised, the reformer duty (Q_{POX}) decreases because the complete oxidation reaction is supported, resulting in the reduction of hydrogen content. Thus, the SOFC duty and cooler (Q_{COOL}) duty is slightly decreased. However, the total heat duty (Q_{TOTAL}) increases with increasing oxygen to ethanol ratio.

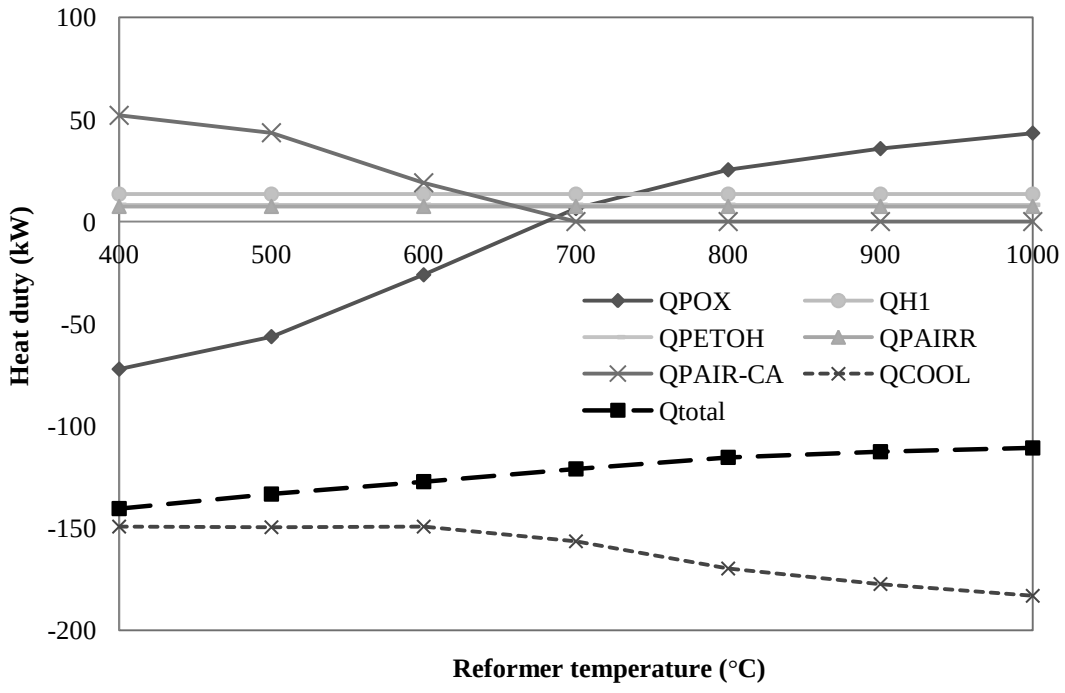

Figure 6.6 Effect of reformer temperature at O/E = 0.5, T_{SOFC} = 800 ˚C on heat duty of the SOFC-POX system.

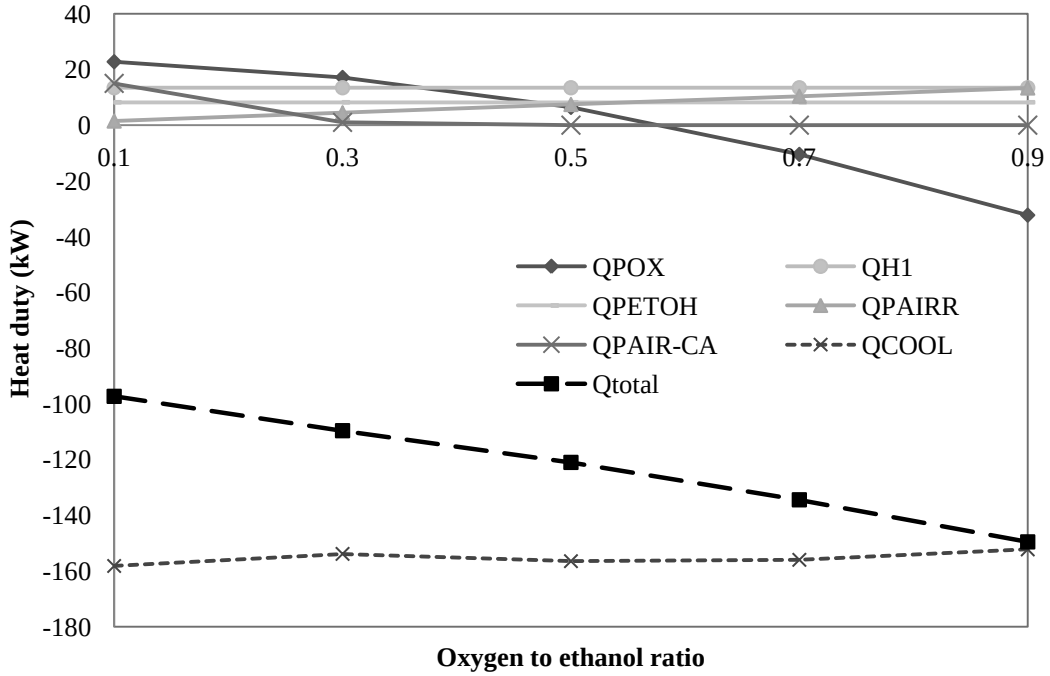

Figure 6.7 Effect of oxygen to ethanol ratio at T_{REF} = 700 ˚C, T_{SOFC} = 800 ˚C on heat duty of the SOFC-POX system.

Figure 6.8 presents the influent of SOFC temperature at T_{REF} = 700˚C, O/E = 0.5 on heat duty of the SOFC-POX system. Since an increase in cell operating temperature increases the reverse water gas shift reaction and the internal steam reforming of methane in the SOFC are supported that leads to decrease the heat duty of anode and cooler (Q_{COOL}). Therefore, the total heat duty (Q_{TOTAL}) decreases with decreasing the SOFC operating temperature.

The thermal efficiency ($\eta_{Thermal}$) of the SOFC-POX system as a function of reformer temperature and oxygen to ethanol ratio is shown in Figure 6.9. The $\eta_{Thermal}$ is enhanced with increasing O/E and decreasing reformer temperature. This can be explained by the complete oxidation reaction is supported although an increased the heat duty of preheating air inlet at reformer (Q_{AIRR}), so the energy is more produced in the reformer. Considering the effect of SOFC temperature on the thermal efficiency, it can be seen that a decrease in SOFC operating temperature can improve the $\eta_{Thermal}$ as shown in Figure 6.10. It is noted that at all the reformer temperature, SOFC temperature and S/E range considered, the value of $\eta_{Thermal}$ shows positive. This implies that the energy consumption is less than the energy production.

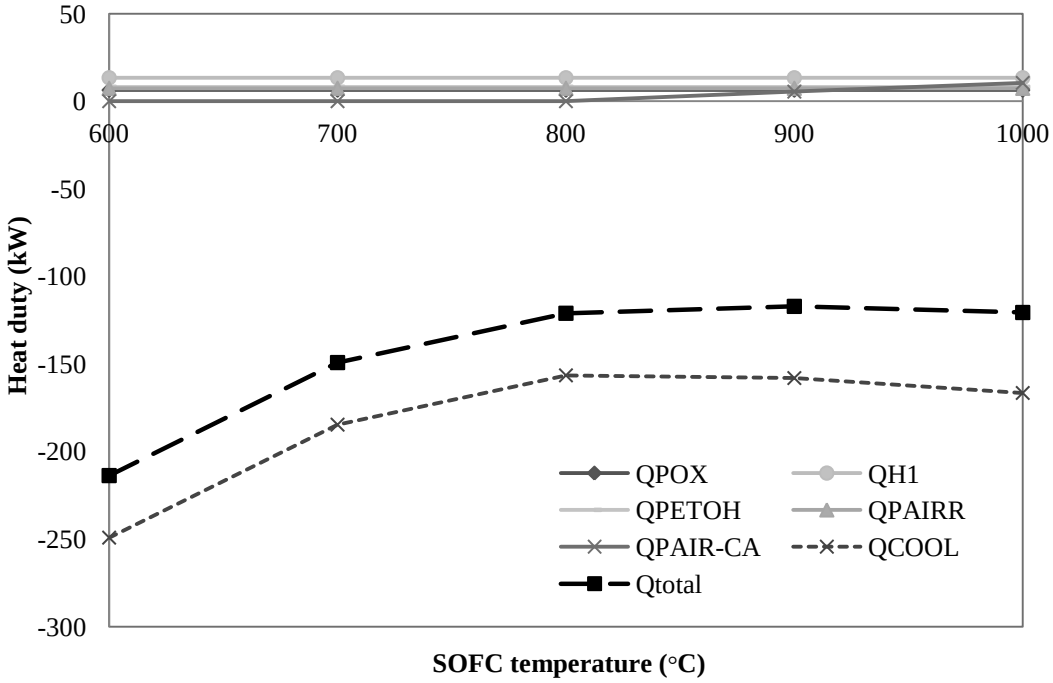

Figure 6.8 Effect of SOFC temperature at O/E = 0.5, T_{REF} = 700 ˚C on heat duty of the SOFC-POX system.

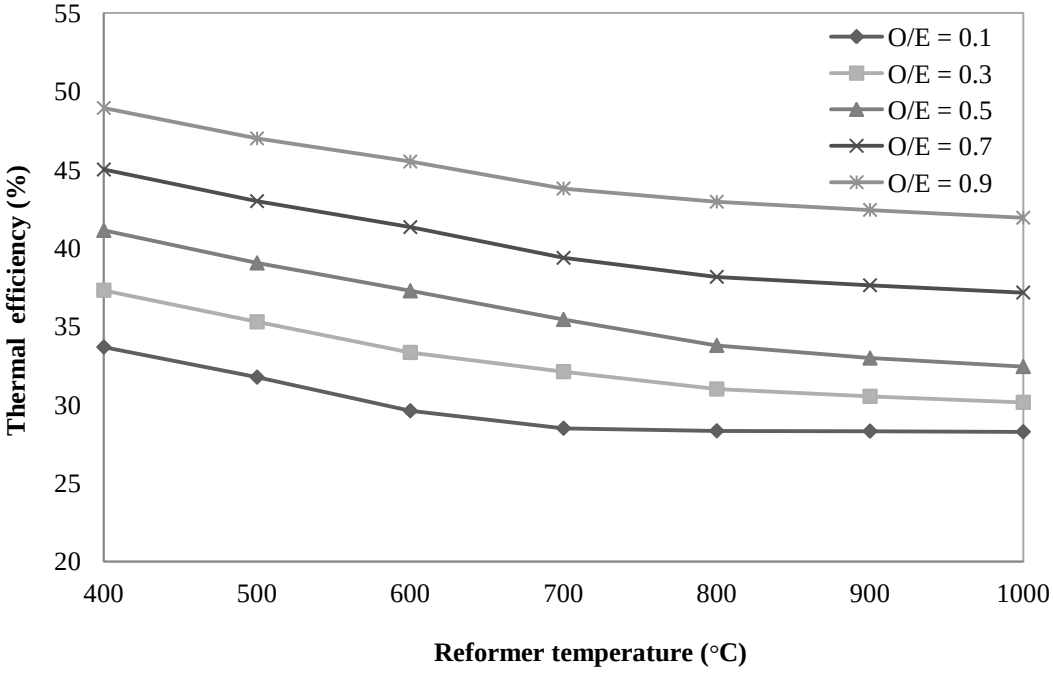

Figure 6.9 Effect of reformer temperature and oxygen to ethanol ration on thermal efficiency of the SOFC-POX system.

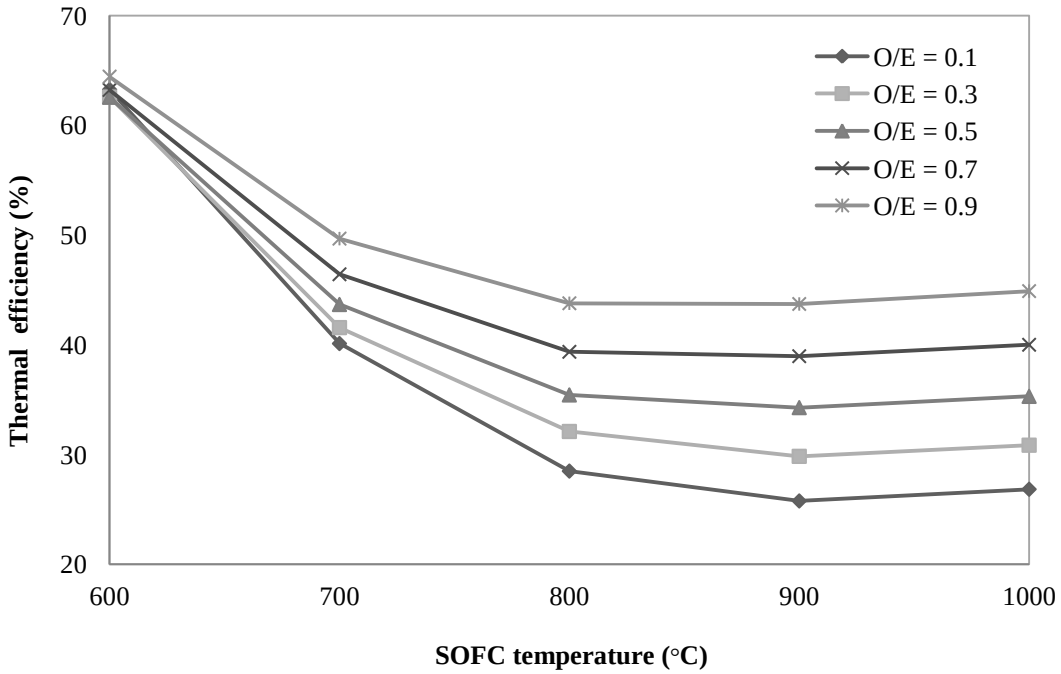

Figure 6.10 Effect of SOFC temperature and oxygen to ethanol ration on thermal efficiency of the SOFC-POX system.

6.2.3 The SOFC integrated with autothermal reforming process (SOFC-ATR)

In this section, a thermodynamic analysis of ethanol autothermal reforming process is presented. At the standard conditions, the inlet molar flow rate of ethanol is 1 kmol/h, steam to ethanol ratio (S/E) is 2 and oxygen to ethanol ration (O/E) is 0.5.

The effect of reformer temperature S/E = 2, O/E = 0.5, T_{SOFC} = 800 ˚C on heat duty of the SOFC-ATR system is shown in Figure 6.11. The simulation result shows that the increasing reformer temperature results in the increased reformer duty (Q_{ATR}) that means the increasing in energy demand. This is because at high reformer temperature, the steam reforming reaction is supported. The heat duty of air inlet to cathode preheating ($Q_{PAIR-CA}$) decreases that can explain by the heat duty of SOFC, which is more produced and has to control the SOFC temperature at constant. So the air inlet at the cell is raised, result in the cooler duty (Q_{COOL}) is increased. The total heat duty (Q_{TOTAL}) reduces with raising the reformer temperature. However, the increasing reformer temperature causes the constant of vaporizer and preheater heat duty of ethanol (Q_{H1}, Q_{PETOH}) and water (Q_{H2}, Q_{PH2O}) as well as preheater of air (Q_{AIRR}).

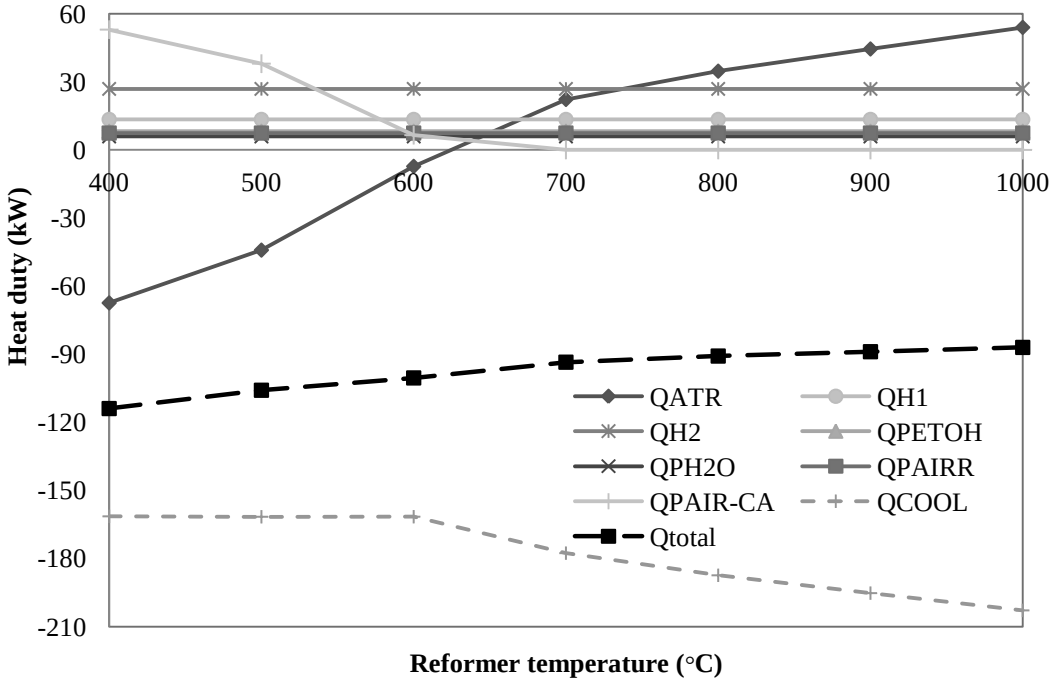

Figure 6.11 Effect of reformer temperature at S/E = 2, O/E = 0.5, T_{SOFC} = 800 ˚C on heat duty of the SOFC-ATR system.

Figure 6.12 and Figure 6.13 show the heat duty at different steam to ethanol ratio and oxygen to ethanol ratio, respectively. According to the Figure 6.12, the result shows that the preheater duty of water (Q_{PH2O}) and the reformer duty (Q_{SR}), especially vaporizer duty of water (Q_{H2}) increase. This is because the inlet water is increased, results in pronounced the steam reforming reaction. The cooler (Q_{COOL}) duty is also increased. So the heat duty in the system increases, the total heat duty (Q_{TOTAL}) produced in this system is decreased. From the Figure 6.13, the oxygen in the system increases that results in preheater heat duty of air (Q_{AIRR}) is also increased. When the oxygen is raised, the reformer duty (Q_{ATR}) decreases because the complete oxidation reaction is supported, resulting in the depleted fraction of hydrogen. Thus, the SOFC duty and cooler (Q_{COOL}) duty is slightly decreased. However, the total heat duty (Q_{TOTAL}) increases with increasing oxygen to ethanol ratio.

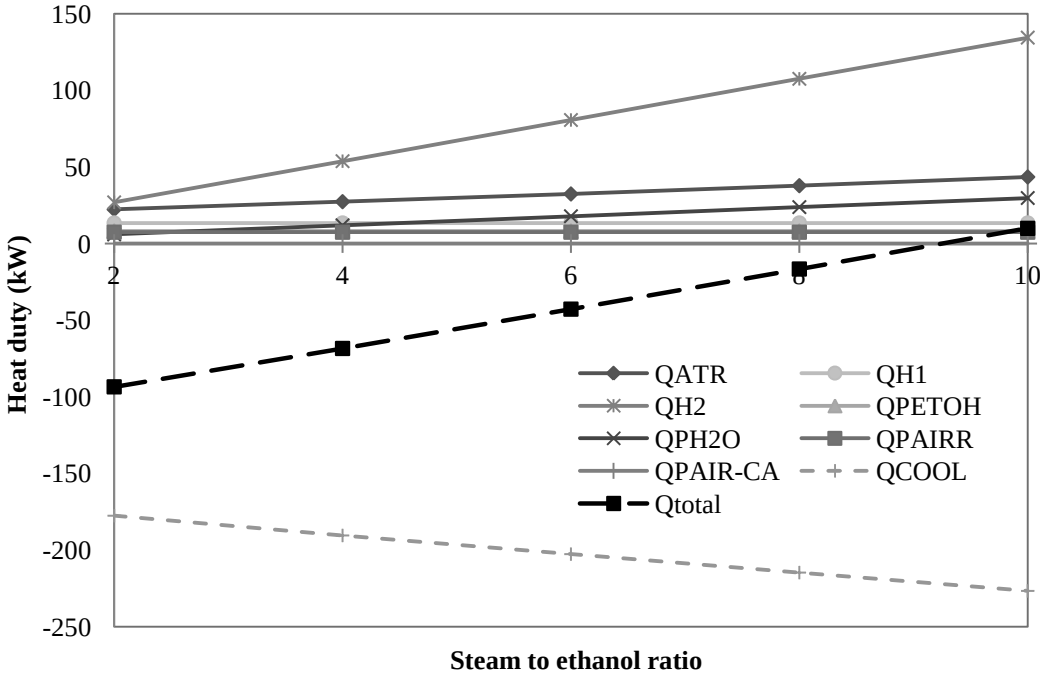

Figure 6.12 Effect of steam to ethanol ratio at O/E = 0.5, T_{REF} =700˚C, T_{SOFC} = 800˚C on heat duty of the SOFC-ATR system.

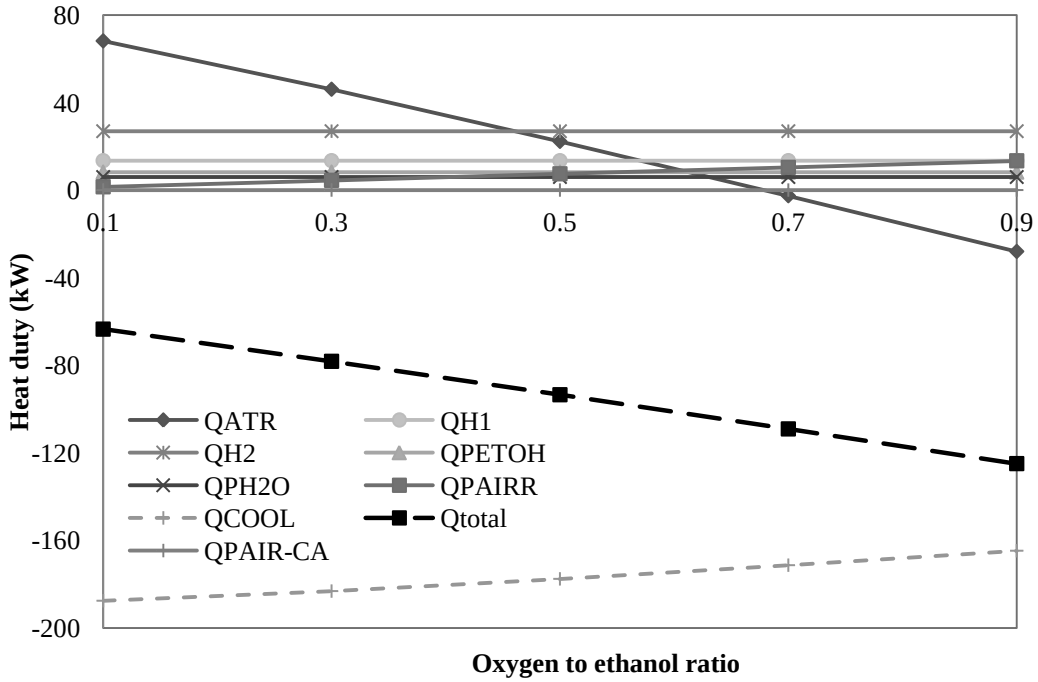

Figure 6.13 Effect of oxygen to ethanol ratio at S/E = 2, T_{REF} =700 ˚C, T_{SOFC} = 800˚C on heat duty of the SOFC-ATR system.

Figure 6.14 demonstrates that although the rate of electrochemical reaction increases with increasing in cell operating temperature, the methane steam reforming reaction is pronounced, so the heat duty of anode is reduced. An air flow into the cell is also decreased that causes cooler duty (Q_{COOL}) decrease. Therefore, the total heat duty (Q_{TOTAL}) decreases with decreasing the SOFC operating temperature. A similar trend is observed in SOFC-SR and SOFC-POX systems.

Figure 6.15 and Figure 6.16 show thermal efficiency ($\eta_{Thermal}$) of the SOFC-ATR system as a function of reformer temperature, SOFC operating temperature and steam to ethanol ratio. The $\eta_{Thermal}$ is slightly reduced when increased in reformer temperature. Similarly, an increase in SOFC operating temperature and S/E can decay the $\eta_{Thermal}$. This is due to the energy demand in the system increases such as the vaporizer and preheater heat duty of water (Q_{H2}, Q_{PH2O}) and the reformer duty (Q_{ATR}) are increased that causes the total heat duty (Q_{TOTAL}) decreases. Therefore, the $\eta_{Thermal}$ reduces.

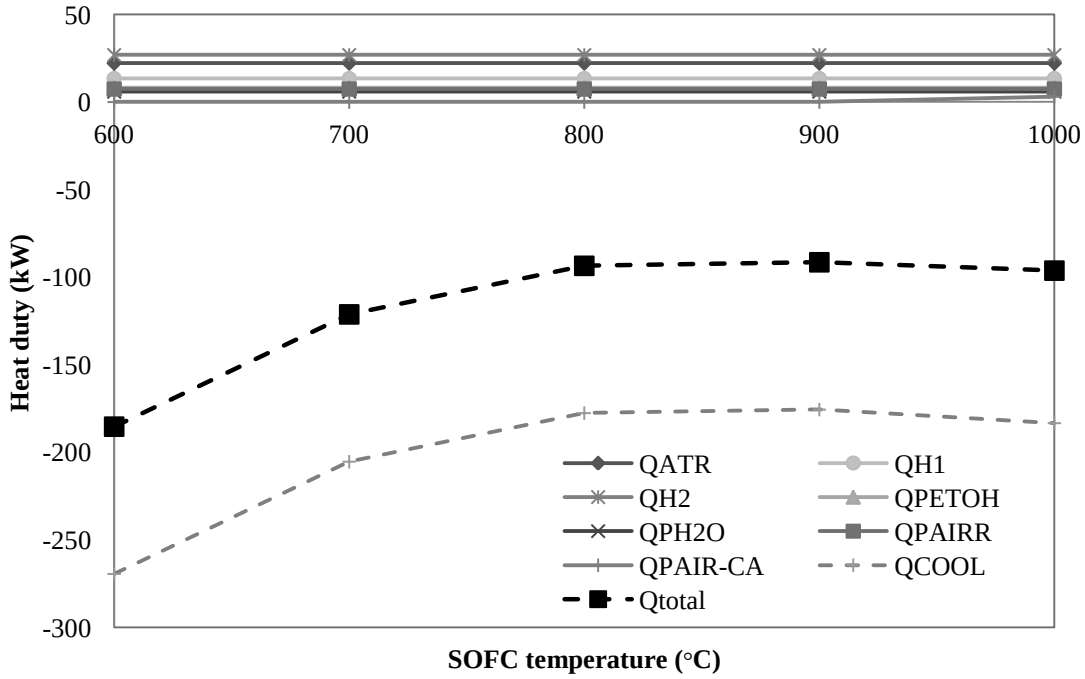

Figure 6.14 Effect of SOFC temperature at S/E = 2, O/E = 0.1, T_{REF} = 700 ˚C on heat duty of the SOFC-ATR system.

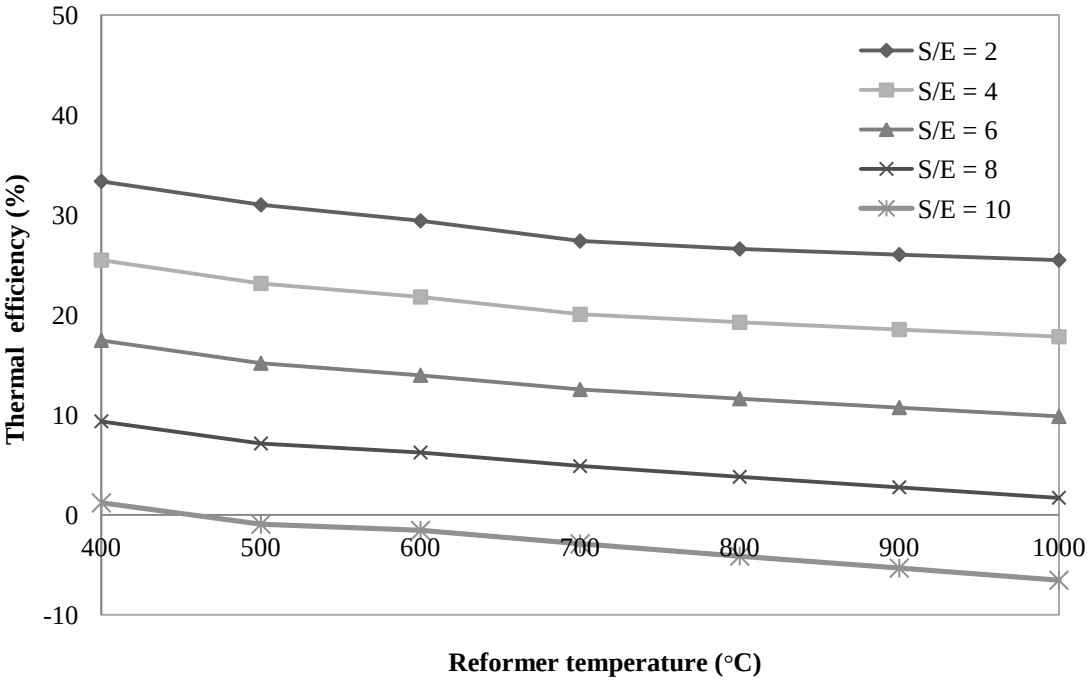

Figure 6.15 Effect of reformer temperature and steam to ethanol ration on thermal efficiency of the SOFC-ATR system.

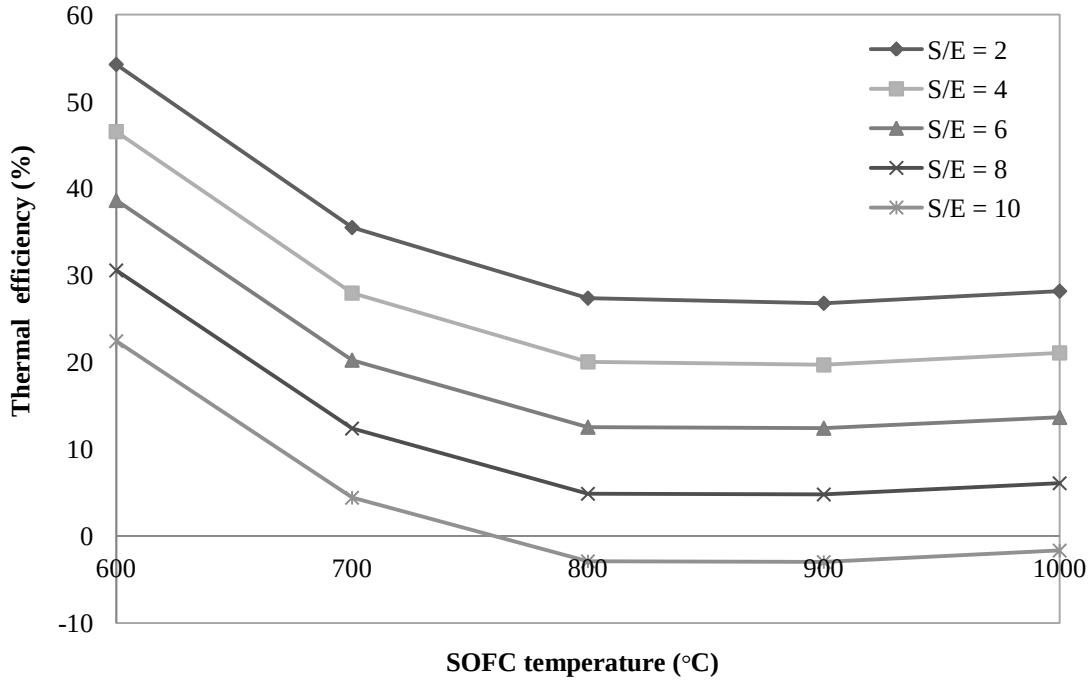

Figure 6.16 Effect of SOFC temperature and steam to ethanol ration on thermal efficiency of the SOFC-ATR system.

Considering the influent of reformer temperature and oxygen to ethanol ratio on the thermal efficiency ($\eta_{Thermal}$) of the SOFC-ATR system is shown in Figure 6.17. Raising O/E and decreasing reformer temperature can improve the $\eta_{Thermal}$. This can be explained by the complete oxidation reaction is supported although an increased the heat duty of preheating air inlet at reformer (Q_{AIRR}), so the energy is more produced in the reformer. From the Figure 6.18, the effect of SOFC temperature on the thermal efficiency, it can be seen that a decrease in SOFC operating temperature can improve the $\eta_{Thermal}$ that shows a similarly trend in other system.

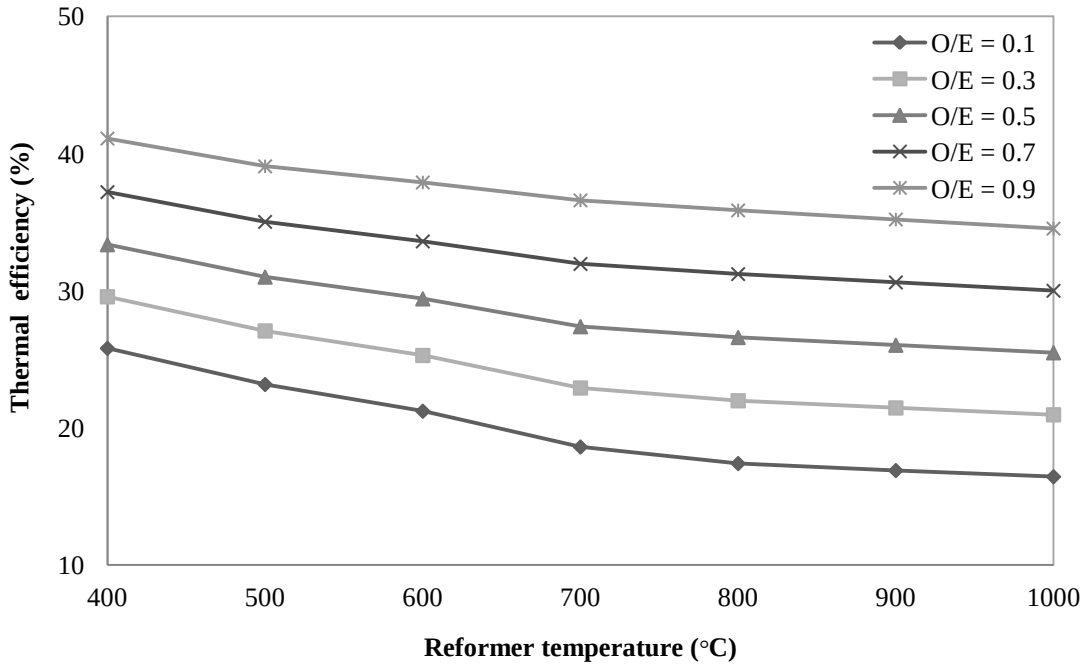

Figure 6.17 Effect of reformer temperature and oxygen to ethanol ration on thermal efficiency of the SOFC-ATR system.

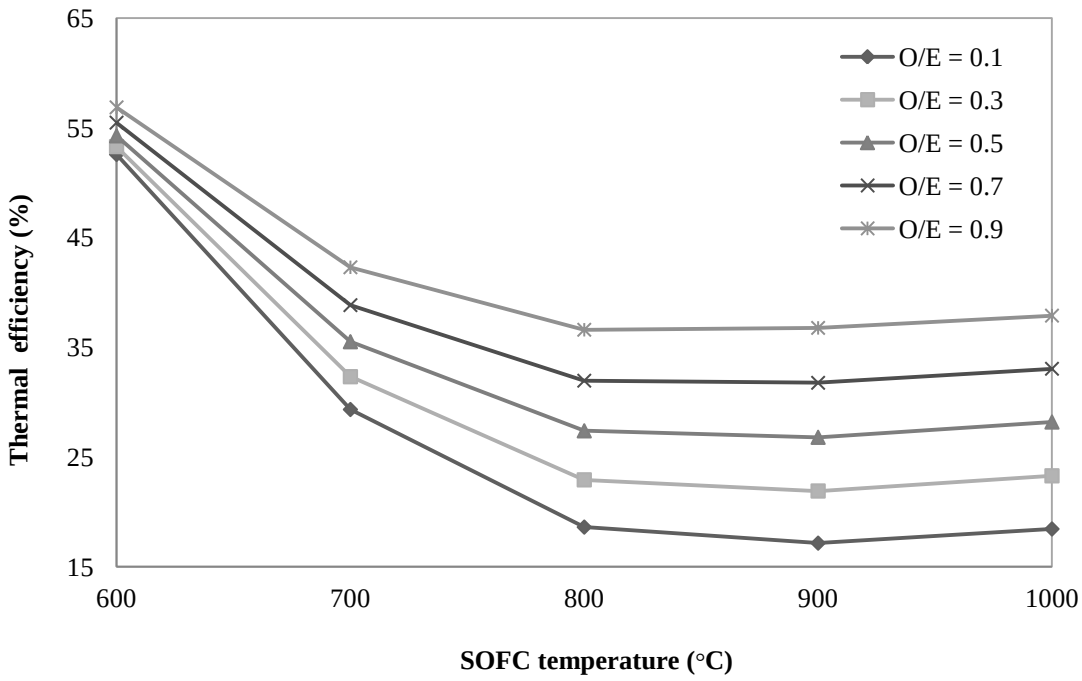

Figure 6.18 Effect of SOFC temperature and oxygen to ethanol ration on thermal efficiency of the SOFC-ATR system.

6.2.4 Performance comparisons of SOFC integrated with reforming process.

A performance analysis of solid oxide fuel cell (SOFC) integrated with different ethanol reforming processes by considering both the electrical and the thermal performances are summarized in Table 6.2. It can be seen that the electrical performance in all systems are slightly different whereas the thermal performance of SOFC-POX system provides highest thermal efficiency. However, a further thermal analysis is significant for used in real application. Furthermore, a design of heat exchanger network based on a pinch analysis is proposed in this study that is discussed in Section 6.3.

Table 6.2 The summary of the performance of the SOFC system

	SOFC-SR	SOFC-POX	SOFC-ATR
Steam to ethanol ratio	2	-	2
Oxygen to ethanol ratio	-	0.1	0.1
Reformer temperature (^{o}C)	700	700	700
SOFC temperature (^{o}C)	900	900	900
Voltage (V)	0.869	0.869	0.869
Current density (mA/cm^2)	273.39	264.28	264.28
Cell efficiency (%)	69.59	67.24	67.21
Thermal efficiency (%)	14.83	25.77	17.13

6.3 Results and discussion of heat exchanger network design

6.3.1 Thermal structure of the SOFC system

The thermal structure of a SOFC system integrated with different ethanol reforming processes such as steam reforming, partial oxidation, and autothermal reforming by using Aspen Plus are shown in Figure 6.19, Figure 6.20 and Figure 6.21, respectively. It consists of the vaporizer, preheater, reformer, SOFC stack, afterburner, and cooler as presented in Chapter 5 that differ in the color of streams.

The red stream represents the stream that need to be cool or hot stream. The blue stream represents the stream that need to be heat or cold stream. In addition, reformer is a requiring energy unit, so it represents in a cold stream.

6.3.2 Results and discussion of heat exchanger network design

A design of heat exchanger network of SOFC system based on a pinch analysis is proposed in order to minimize utility used in the SOFC systems. The operating condition examined in this study as shown in Table 6.2. The hot and cold streams are identified in the first step, the stream data, heat flows, supply and target temperatures are analyzed and the grand composite curve (GCC) is constructed and then the heat exchanger network is designed. The minimum temperature approach ($dT_{\text{min,set}}$) for overlapping the energy curves (hot and cold) is fixed at 40 ^{O}C.

6.3.2.1 Thermal management of a SOFC integrated with ethanol steam reforming process (SOFC-SR)

According to the Figure 6.19, it can be seen that the SOFC-SR system consists of 1 hot and 5 cold streams that the stream data is analyzed as shown in Table 6.3. From the stream data, the grand composite curve is constructed as shown in Figure 6.22. It is found that the only cold utility is required where only one utility is required is called a *threshold problem*. The GCC shows a near-pinch at 720 ◦C shifted temperature (740 ◦C for hot streams, 700 ◦C for cold streams) with a heat flow of only 2.07 kW. Here it is often advisable to treat the problem like a “double pinch” and design away from both the near-pinch and the non-utility end. Therefore, the heat exchanger network is shown in Figure 6.23. It is notable that, six heat exchangers exist in this network with a cold utility of 50.7 kW.

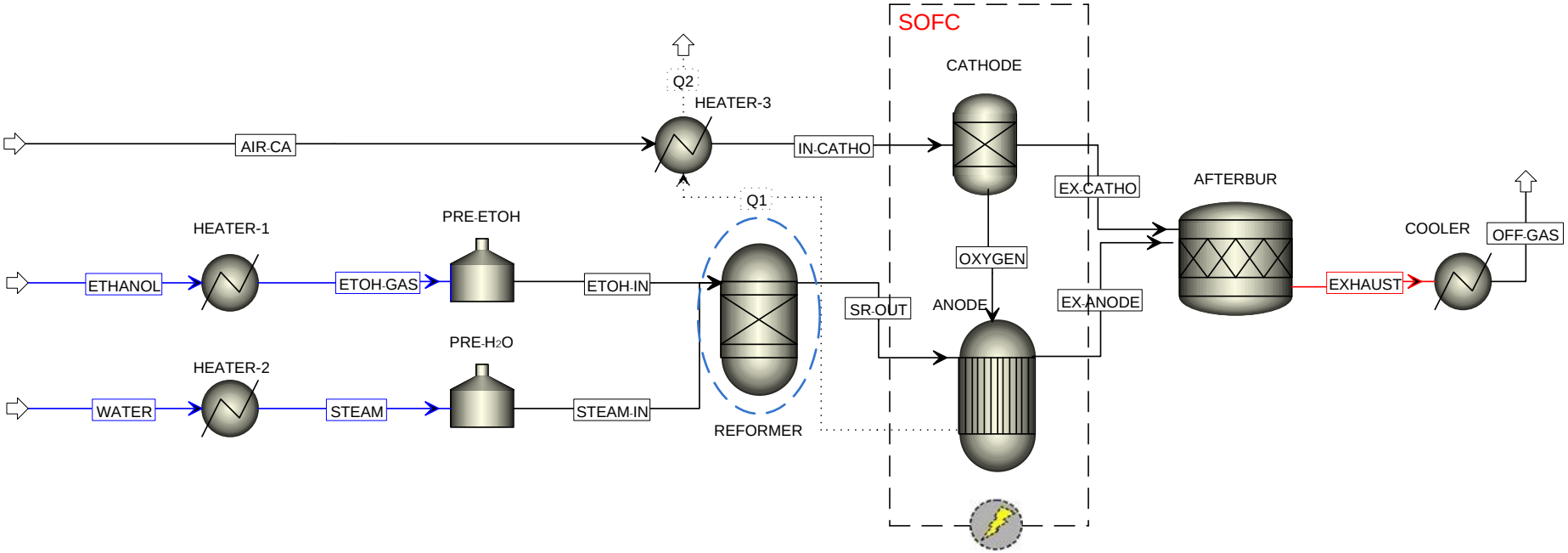

Figure 6.19 Thermal structure of a SOFC system with ethanol steam reforming process (SOFC-SR).

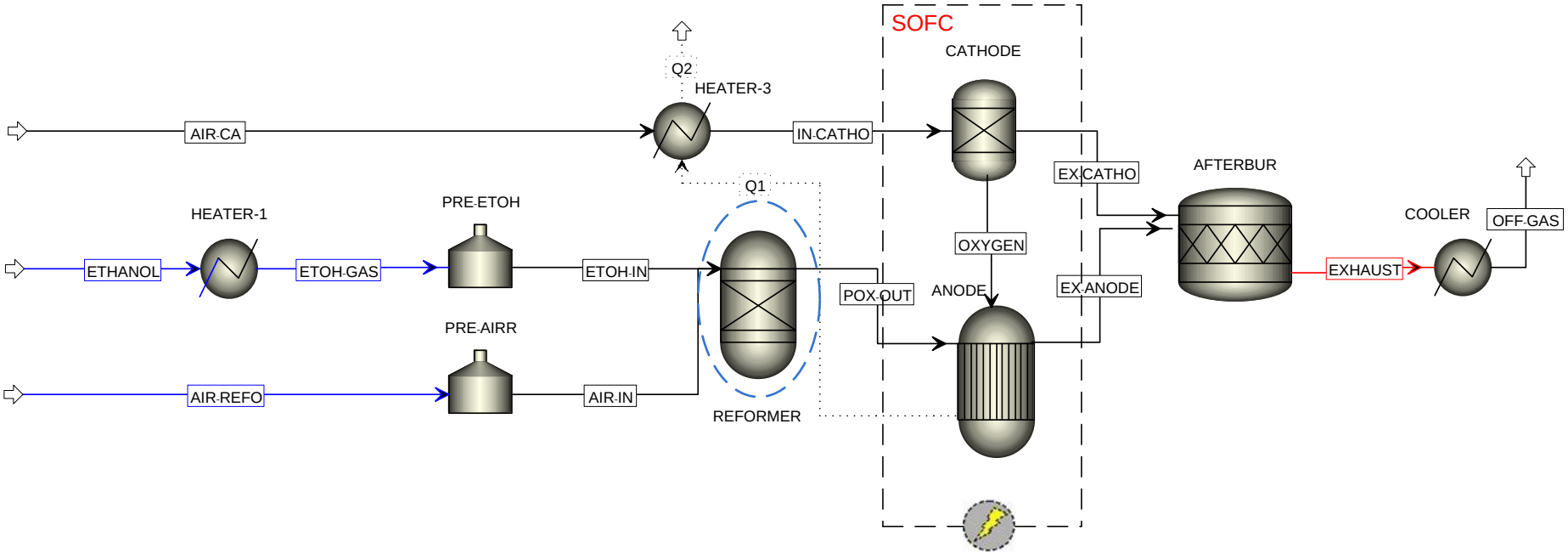

Figure 6.20 Thermal structure of a SOFC system with ethanol partial oxidation process (SOFC-POX).

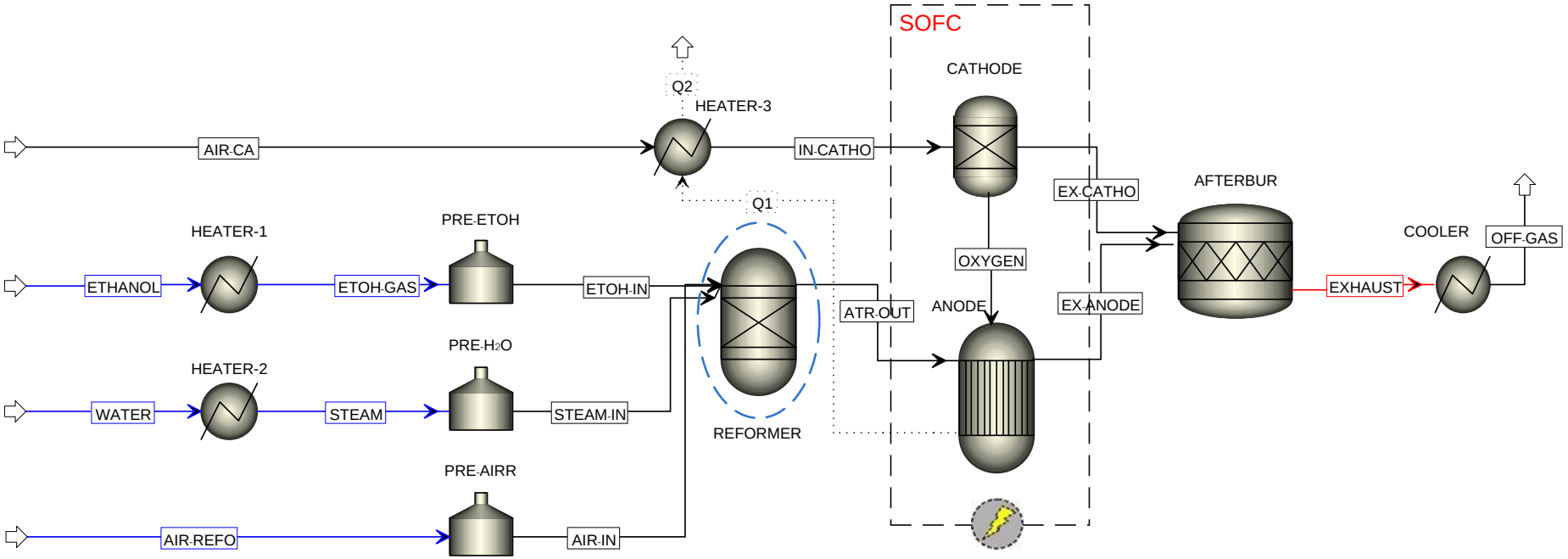

Figure 6.21 Thermal structure of a SOFC system with ethanol autothermal reforming process (SOFC-ATR).

Table 6.3 The stream data of the SOFC-SR system

No.	Type	Description	T_{in} (^{O}C)	T_{out} (^{O}C)	CP (kW/ ^{O}C)	Q (kW)
1	Hot	EXAUST	1161	200	0.191	183.44
2	Cold	ETHANOL	25	100	0.179	13.43
3	Cold	WATER	25	100	0.358	26.88
4	Cold	ETOH-GAS	100	400	0.027	8.21
5	Cold	STEAM	100	400	0.020	5.94
6	Cold	REFORMER	700	700	-	78.30

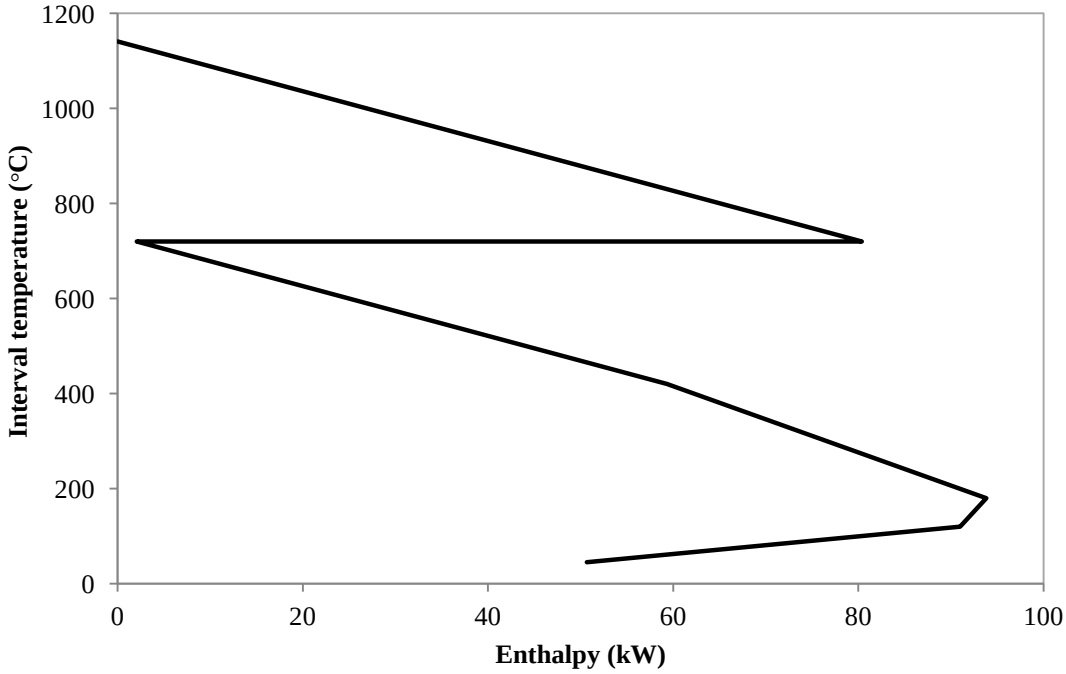

Figure 6.22 Grand composite curve for SOFC-SR system

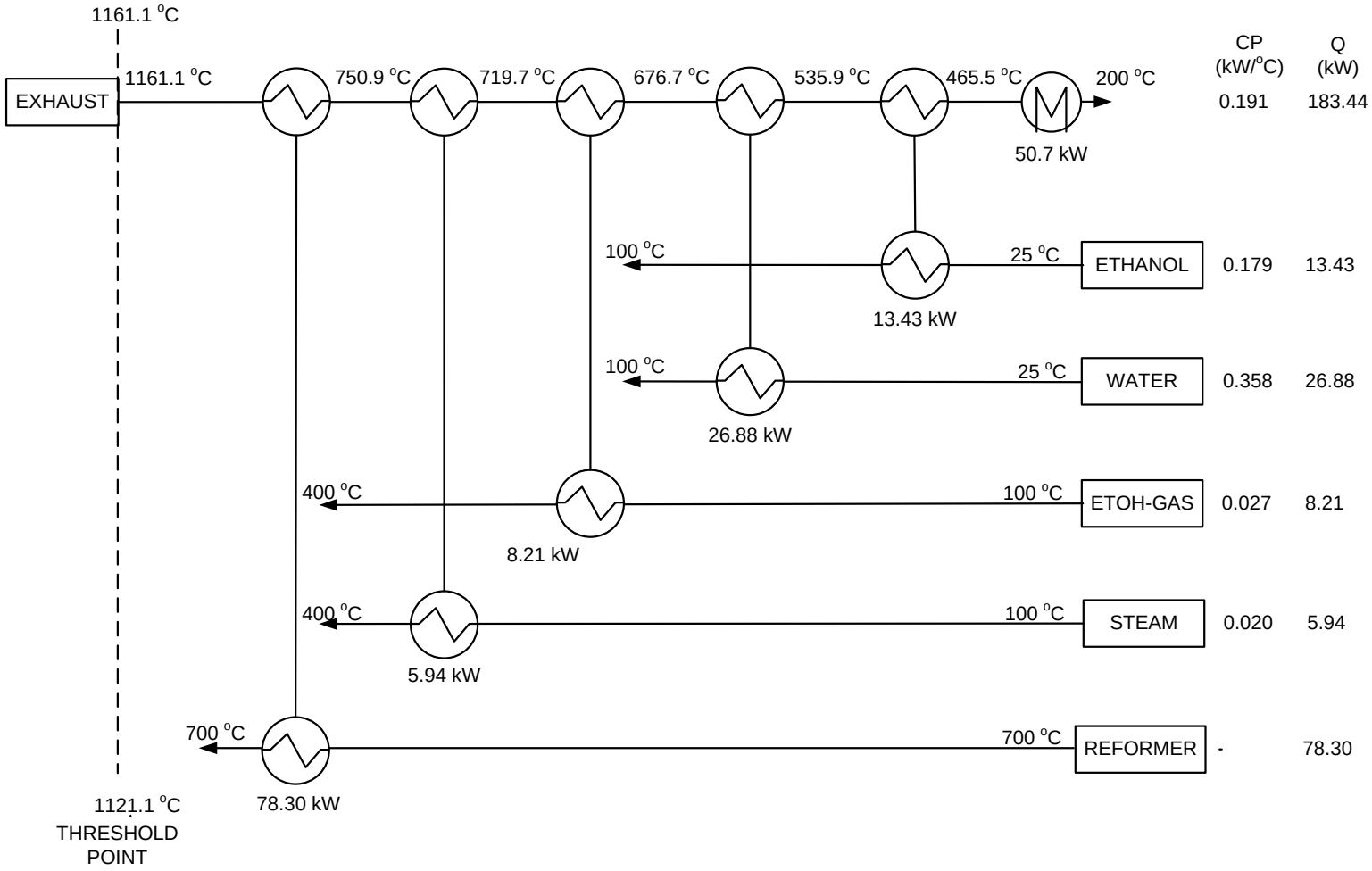

Figure 6.23 Heat exchanger network scheme for SOFC-SR system

6.3.2.2 Thermal management of a SOFC integrated with ethanol partial oxidation process (SOFC-POX)

The SOFC-POX system is compose of 1 hot and 5 cold streams. The thermal data extraction for each stream is explained in Table 6.4. From this table, it is shown that the heat used in the reformer is highest in this case. However, it is noted that the reformer duty in the SOFC-POX system is less than the SOFC-SR system. This is due to the partial oxidation reaction of ethanol consumed energy is less than the ethanol steam reforming reaction. The GCC is presented in Figure 6.24, shows hot utility is not required and 88.1 kW of cold utility, which is a *threshold problem*. In addition, the GCC shows the similarity to a true pinch, with zero heat flow. There are six heat exchangers in the network, as illustrated in Figure 6.25.

Table 6.4 The stream data of the SOFC-POX system

No.	Type	Description	T_{in} (^{O}C)	T_{out} (^{O}C)	CP (kW/ ^{O}C)	Q (kW)
1	Hot	EXAUST	1199.5	200	0.166	165.45
2	Cold	ETHANOL	25	100	0.179	13.43
3	Cold	AIR-REF	25	400	0.004	1.48
4	Cold	ETOH-GAS	100	400	0.027	8.21
5	Cold	REFORMER	700	700	-	22.77
6	Cold	PRE-AIR	25	300.6	0.114	31.5

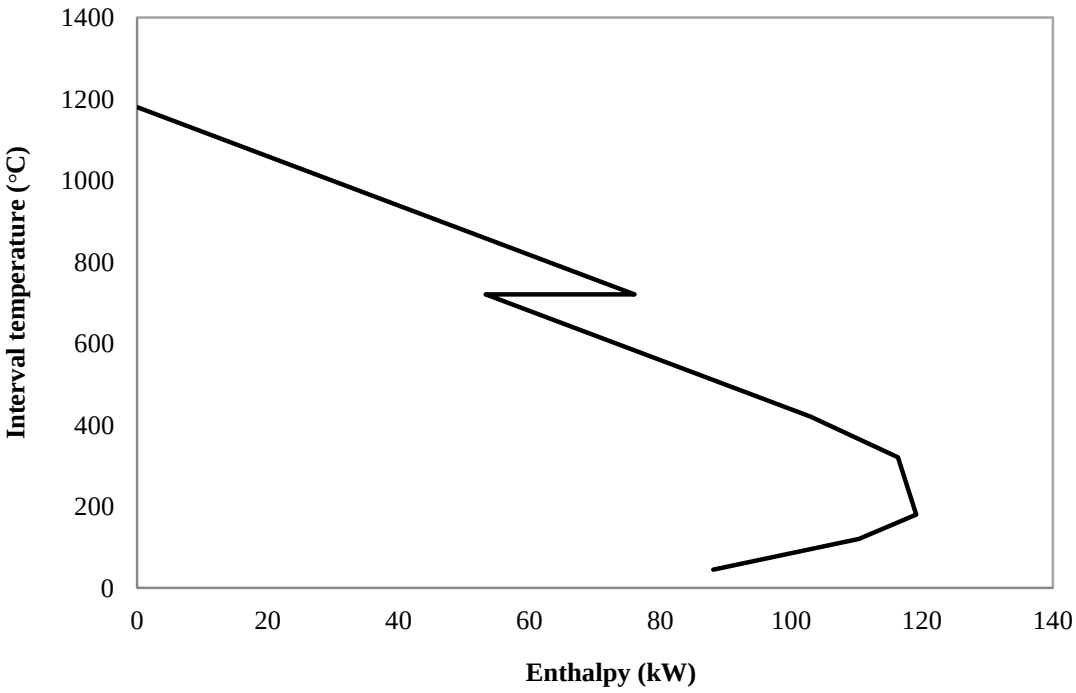

Figure 6.24 Grand composite curve for SOFC-POX system

6.3.2.3 Thermal management of a SOFC integrated with autothermal reforming process (SOFC-ATR)

From the Figure 6.21, seven streams are considered that fall into two type of streams; 1 hot and 6 cold streams. Table 6.5 demonstrates that details of each stream are examined in this case and then the GCC is created in Figure 6.26. It can be seen that the minimum temperature approach at threshold is found at 1129.5 ^{O}C shifted temperature. Therefore, the heat exchanger network is shown in Figure 6.27. The result shows that this system requires only cold utility of 58.5 kW.

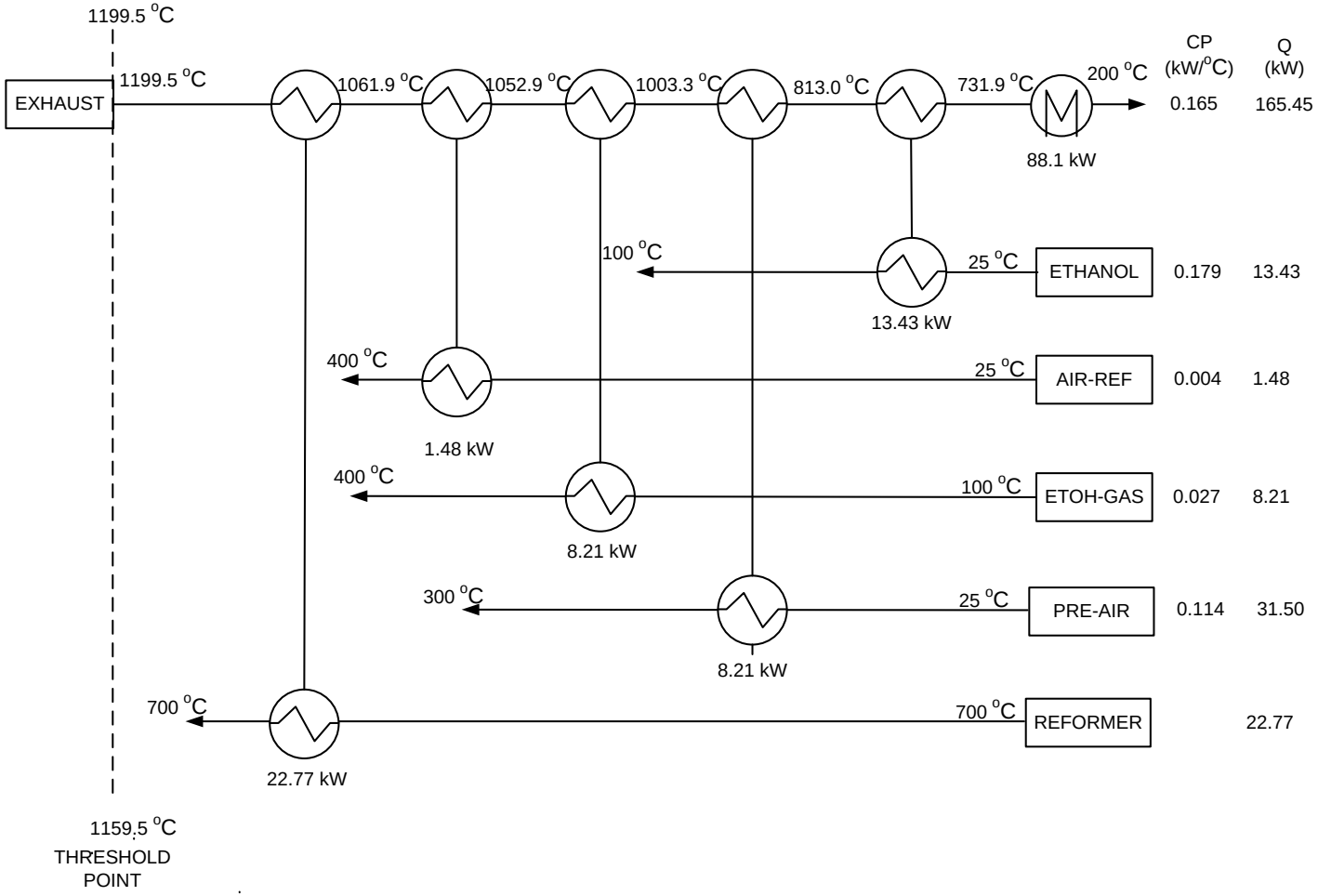

Figure 6.25 Heat exchanger network scheme for SOFC-POX system

Table 6.5 The stream data of the SOFC-ATR system

No.	Type	Description	T_{in} (^{O}C)	T_{out} (^{O}C)	CP (kW/ ^{O}C)	Q (kW)
1	Hot	EXAUST	937.1	200	0.493	363.32
2	Cold	ETHANOL	25	100	0.179	13.43
3	Cold	WATER	25	100	0.358	26.88
4	Cold	ETOH-GAS	100	400	0.027	8.21
5	Cold	STEAM	100	400	0.020	5.94
6	Cold	AIR-REF	25	400	0.004	1.48
7	Cold	REFORMER	700	700	-	68.15

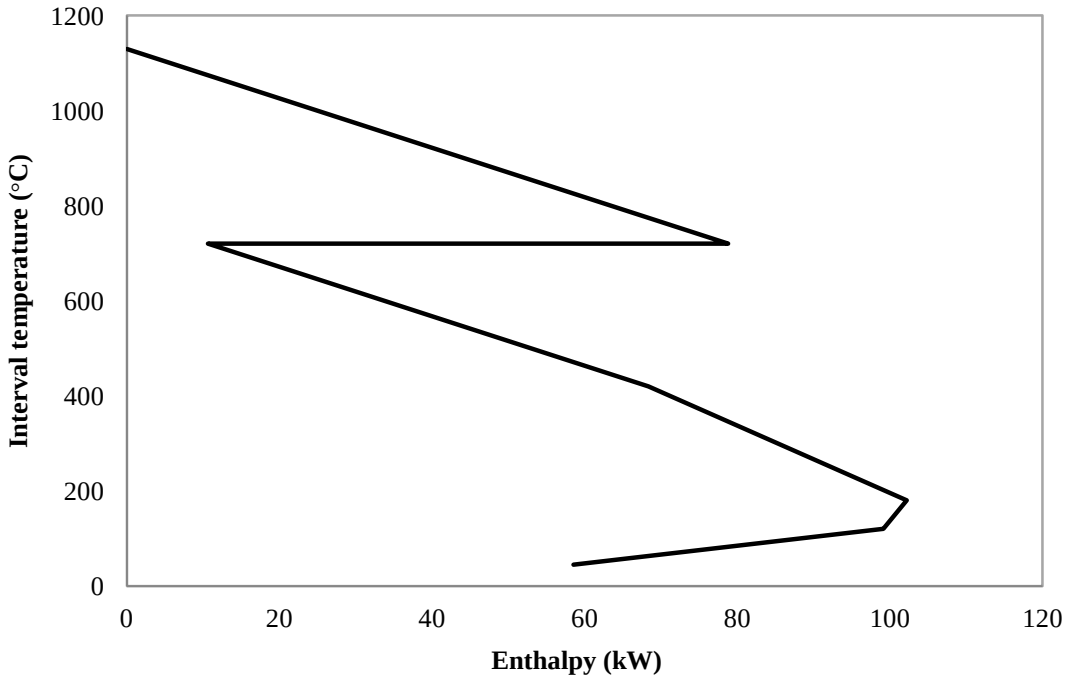

Figure 6.26 Grand composite curve for SOFC-ATR system

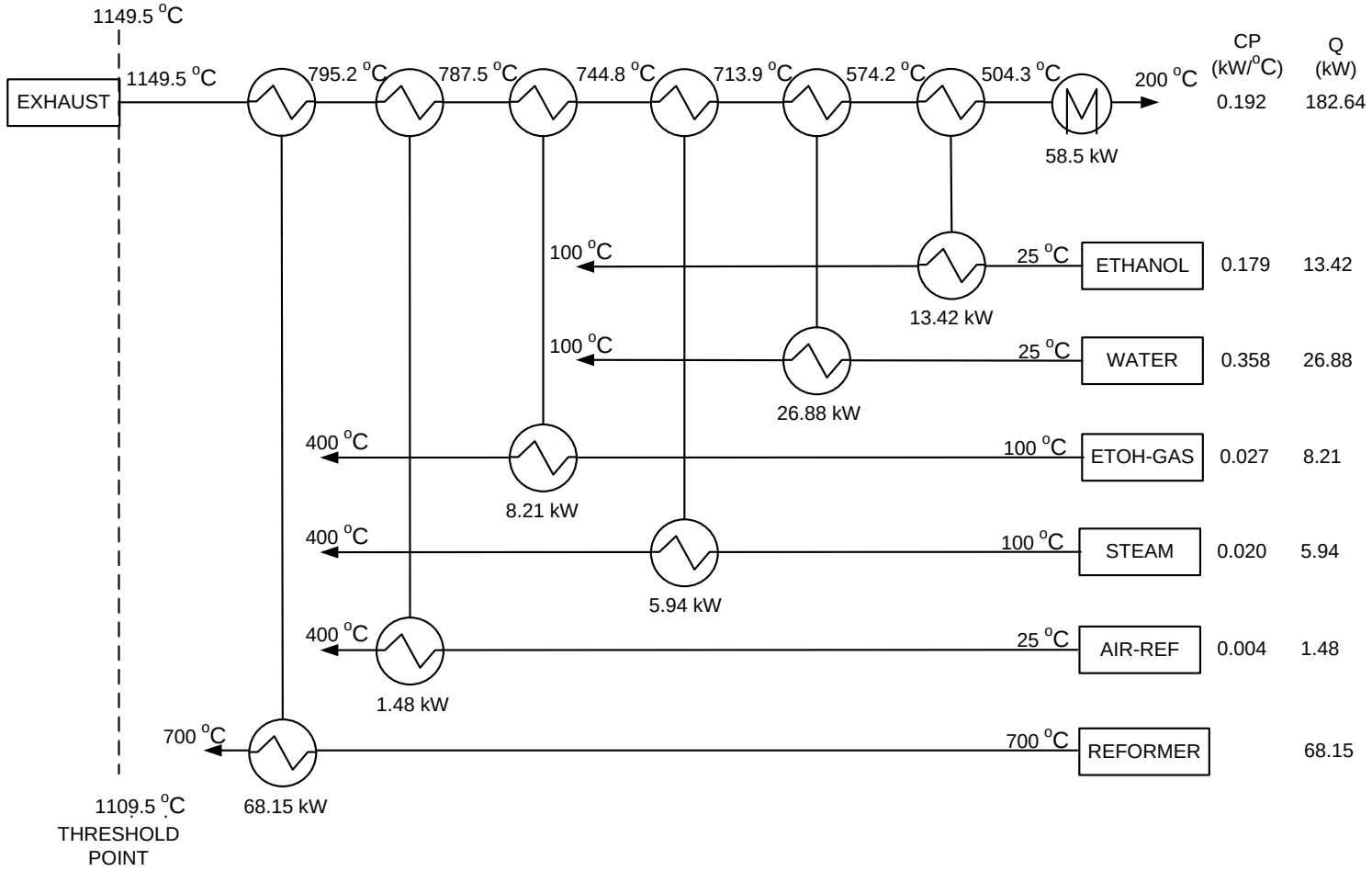

Figure 6.27 Heat exchanger network scheme for SOFC-ATR system

6.4 Conclusions

Thermal analysis of SOFC system cooperating with ethanol reforming process (i.e., steam reforming, partial oxidation and autothermal reforming) is presented in this study. The simulation result shows that the SOFC-POX system provides the thermal efficiency of 25.77% whereas a SOFC-ATR and SOFC-SR have the thermal efficiency of 17.17% and 14.83%, respectively. Therefore, the SOFC-POX system provides a higher thermal efficiency compared with other systems. The thermal efficiency of SOFC system at different reformer temperature, SOFC operating temperature, steam to ethanol ratio and oxygen to ethanol ratio is also investigated. It is found that decreasing the reformer temperature, SOFC operating temperature and steam to ethanol ratio as well as increasing oxygen to ethanol ratio can enhance the thermal performance of the system. Furthermore, a design of heat exchanger network based on a pinch analysis was proposed in this study to reduce utility used in the SOFC systems and apply the heat recovery in the real applications. The result demonstrates that the only cold utility is required in all systems. The SOFC-POX system provides the required cold utility of 88.1 kW whereas a SOFC-ATR and SOFC-SR demand cold utility of 58.5 kW and 50.7 kW, respectively. However, the required cold utility is considered as a heat that produces from the system, so the SOFC-POX system generates maximum heat.

CHAPTER VII

CONCLUSIONS AND RECOMMEDATIONS

7.1 Conclusions

The objective of this work is to analyze a performance of solid oxide fuel cell integrated with different ethanol reforming processes by considering both the electrical and the thermal performances. A detailed electrochemical model taking into account all voltage losses (i.e., activation, concentration and ohmic losses) was considered. Thermodynamic analysis of hydrogen production from ethanol by using three different reforming processes such as steam reforming (SR), partial oxidation (POX) and autothermal reforming (ATR), are presented and compared in order to select a ethanol reforming process suitable for SOFC system. The operating condition of the SOFC system is considered under steady state condition was performed using a flowsheet simulator. The effect of key operating parameters, i.e., reformer temperature, SOFC operating temperature, steam to ethanol ratio and oxygen to ethanol ratio are also presented. Furthermore, the designs of the heat exchanger network for the SOFC integrated with different ethanol reforming process are investigated by using of the pinch technology.

For the electrical efficiency analysis of a SOFC system integrated with ethanol reforming process, the simulation result showed that the operating condition provides the maximum electrical performance for each system at the reformer temperature of 700 °C, cell temperature of 900 °C steam to ethanol ratio of 2 and oxygen to ethanol ratio of 0.1. At this condition, the electrical performance of SOFC-SR shows its maximum value as equal to 69.59%. However, the electrical performance of the SOFC system with different reforming systems is slightly different because an internal reforming of methane was considered in this work. The electrical efficiency can be enhanced by either increasing in reformer and cell temperatures or decreasing steam to ethanol ratio and oxygen to ethanol ratio.

In case of the thermal analysis of SOFC system cooperating with ethanol reforming process, the result demonstrated that the SOFC-POX system provides the best thermal efficiency of 25.77%, whereas a SOFC-ATR and SOFC-SR have the thermal efficiency of 17.13% and 14.83%, respectively. The thermal efficiency can be improved with decreasing the reformer temperature, SOFC operating temperature and steam to ethanol ratio as well as increasing oxygen to ethanol ratio.

Moreover, for a design of heat exchanger network based on a pinch analysis, it was found that the only cold utility is required in all systems. The SOFC-POX system provides the required cold utility of 88.1 kW whereas a SOFC-ATR and SOFC-SR demand cold utility of 58.5 kW and 50.7 kW, respectively. However, the required cold utility is considered as a heat that produces from the system, resulting in the SOFC-POX system produces maximum heat.

As mentioned above, therefore, an appropriate ethanol reforming process for used in solid oxide fuel cell is partial oxidation process.

7.2 Recommendations

1.) Even if the heat exchange network of SOFC system coupled with ethanol reforming process was investigated, the remained energy was not considered. Therefore, the remained energy should further use to improve the electrical efficiency such as combined gas/steam turbine.
2.) Further economic analysis should take place by including cost of heat exchangers.

REFERENCES

Aguiar, P., Adjiman, C.S., and Brandon, N.P., Anode – supported intermediate temperature direct internal reforming solid oxide fuel cell. I: model – based steady – state performance. Journal of Power Sources 138 (2004) : 120 – 136.

Arpornwichanop, A., Chalermpanchai, N., Patcharavorachot, Y., Assabumrungrat, S., and Tade, M., Performance of an anode-supported solid oxide fuel cell with direct-internal reforming of ethanol. International Journal of Hydrogen Energy 34 (2009) : 7780–7788.

Arteaga, L.E., Peralta, L.M., Kafarov, V., Casas, Y., and Gonzales, E., Bioethanol steam reforming for ecological syngas and electricity production using a fuel cell SOFC system. Chemical Engineering Journal 136 (2008) : 256–266.

Arteaga-Perez, L.E., Casas, Y., Peralta, L.M., Kafarov, V., Dewulf, J., and Giunta, P., An auto-sustainable solid oxide fuel cell system fueled by bio-ethanol Process simulation and heat exchanger network synthesis. Chemical Engineering Journal 150 (2009) : 242 – 251.

Cai, W., Wang, F., Van Veen , A.C., Provendier, H., Mirodatos, C., Shen, W., Autothermal reforming of ethanol for hydrogen production over an Rh/CeO_2. Catalyst Catalysis Today 138 (2008) :152–156.

Casas, Y., Arteaga, L.E., Morales, M., Rosa, E., Peralta, L.M., and Dewulf, J., Energy and exergy analysis of an ethanol fueled solid oxide fuel cell power plant. Chemical Engineering Journal 162 (2010) : 1057–1066.

Chan, S.H., Low, C.F., and Ding, O.L., Energy and exergy analysis of simple solid-oxide-fuel-cell power systems. Journal of Power Sources 103 (2002) : 188–200.

EG&G Technical Services, Inc., Fuel Cell Handbook, 5th edition. U.S. Department of Energy. National Technical Information Service : Virginia, 2000.

EG&G Technical Services, Inc., Fuel Cell Handbook, 7th edition. U.S. Department of Energy. National Technical Information Service : Virginia, 2004.

Fierro, V., Akdim, O., Provendier, H., Mirodatos, C., Ethanol oxidative steam reforming over Ni-based catalysts. Journal of Power Sources 145 (2005) ;659–666.

Garaia, E. Y., and Laborde, M. A., Hydrogen production by the steam reforming of ethanol: thermodynamic analysis. International Journal of Hydrogen Energy 16 (1991) : 307-312.

Haseli, Y., Dincer, I. and Naterer, G.F., Thermodynamic modeling of a gas turbine cycle combined with a solid oxide fuel cell. International Journal of Hydrogen Energy 33 (2008) : 5811–5822.

Hayre, R.O., Cha, S.W., Colella, W., and Prinz, F.B., Fuel Cell fundamentals. New York : John Wiley & Sons, 2006.

Hernandez, L., and Kafarov, V., Use of bioethanol for sustainable electrical energy production. International Journal of Hydrogen Energy 34 (2009) : 7041–7050.

Hirschenhofer, J.H., Stauffer, D.B., Engleman, R.R., and Klett, M.G., Fuel Cell Handbook, 4th edition. U.S. Department of Energy. National Technical Information Service : Virginia, 1998.

Huang, B., Zhu, XJ., Hu, WQ., Yu, QU., and Tu, HY., Characteristics and performance of lanthanum gallate electrolyte-supported SOFC under ethanol steam and hydrogen. Journal of Power Sources 186 2009) : 29–36.

Ian C Kemp, Pinch Analysis and Process Integration, 2th edition. India : Charon Tec Ltd (A Macmillan Company), 2007.

Jamsak, W., Douglas, P.L., Croiset, E., Suwanwarangkul, R., Laosiripojana, N., Charojrochkul, S., and Assabumrungrat, S., Design of a thermally integrated bioethanol-fueled solid oxide fuel cell system integrated with a distillation column. Journal of Power Sources 187 (2009) : 190–203.

Lima da Silva, A., Malfatti, C. F., and Muller, I. L., Thermodynamic analysis of ethanol steam reforming using Gibbs energy minimization method: A detailed study of the conditions of carbon deposition. International Journal of Hydrogen Energy 34 (2009) : 4321–4330.

Lisbona, P., Corradetti, A., Bove, R., and Lunghi, P., Analysis of a solid oxide fuel cell system for combined heat and power applications under non-nominal conditions. Electrochimica Acta 53 (2007) : 1920–1930.

Mas, V., Kipreos, R., Amadeo, N., and Laborde, M., Thermodynamic analysis of ethanol/water system with the stoichiometric method. International Journal of Hydrogen Energy 31 (2006) : 21 – 28.

M. de Lima, S., da Cruz, I. O., Jacobs, G., Davis, B. H., Mattos, L. V., Noronha, F. B., Steam reforming, partial oxidation, and oxidative steam reforming of ethanol over $Pt/CeZrO_2$. Catalyst Journal of Catalysis 257 (2008) 356–368.

Naidja, A., Krishna, CR., Butcher, T., and Mahajan, D., Cool flame partial oxidation and its role in combustion and reforming of fuels for fuel cell systems. Progress in energy and combustion science 29 (2003) : 155–191.

Ni, M., Leung, D.Y.C., and Leung, M.K.H., A review on reforming bio-ethanol for hydrogen production. International Journal of Hydrogen Energy 32 (2007) : 3238 – 3247.

Ni, M., Leung, M. K.H., Leung, D. Y.C., Parametric study of solid oxide fuel cell performance. Energy Conversion and Management 48 (2007) : 1525‑1535.

Palsson, J., Selimovic, A., and Sjunnesson, L., Combined solid oxide fuel cell and gas turbine systems for efficient power and heat generation. Journal of Power Sources 86 (2000) : 442–448.

Perna, A., Hydrogen from ethanol: Theoretical optimization of a PEMFC system integrated with a steam reforming processor. International Journal of Hydrogen Energy 32 (2007) : 1811 – 1819.

Piroonlerkgul, P., Assabumrungrat, S., Laosiripojana, N., Adesina, A.A., Selection of appropriate fuel processor for biogas-fuelled SOFC system. Chemical Engineering Journal 140 (2008) : 341–351.

Rabenstein, G., and Hacker, V., Hydrogen for fuel cells from ethanol by steam-reforming, partial-oxidation and combined auto-thermal reforming: A thermodynamic analysis. Journal of Power Sources 185 (2008) : 1293–1304.

Riensche, E., Stimming, U., and Unverzagt, G., Optimization of a 200 kW SOFC cogeneration power plant Part I: Variation of process parameters. Journal of Power Sources 73 (1998) : 251–256.

Rossi, C.C.R.S., Alonso, C.G., Antunes, O.A.C., Guirardello, R., and Cardozo-Filho, L., Thermodynamic analysis of steam reforming of ethanol and glycerine for hydrogen production. International Journal of Hydrogen Energy 34 (2009) : 323–332.

Srisiriwat, A., High Temperature Solid Oxide Fuel Cell Integrated with Autothermal Reformer. 2nd IEEE International Conference on Power and Energy (PECon 08). Johor Baharu, Malaysia; 1-3 December 2008.

Srisiriwat, N., Therdthianwong, S., Therdthianwong, A., Oxidative steam reforming of ethanol over Ni/Al_2O_3 catalysts promoted by CeO_2, ZrO_2 and CeO_2–ZrO_2**.** International journal of hydrogen energy 34 (2009) :2224–2234.

Srisiriwat, N., Therdthianwong, A., and Therdthianwong, S., Thermodynamic analysis of hydrogen production from ethanol in three different technologies. The 2nd joint international conference on "Sustainable Energy and Environment (SEE 2006)". Bangkok, Thailand; 21-23 November 2006.

Sunggyu, Lee., Speight, James G., and Loyalka, Sudarshan K., Handbook of Alternative Fuel Technologies. New York : Taylor & Francis Group, 2007.

Tsiakaras, P., Demin, A., Thermodynamic analysis of a solid oxide fuel cell system fuelled by ethanol. Journal of Power Sources 102 (2001) : 210–217.

Vasudeva, K., Mitra, N., Umasankar, P., and Dhingra, S. C., Steam reforming of ethanol for hydrogen production: thermodynamic analysis. International Journal of Hydrogen Energy 21 (1996) : 13–18.

Vourliotakis, G., Skevis, G., and Founti, M.A., Detailed kinetic modelling of non-catalytic ethanol reforming for SOFC applications. International Journal of Hydrogen Energy 34 (2009) : 7626–7637.

Wang, W., and Wang, Y., Thermodynamic analysis of hydrogen production via partial oxidation of ethanol. International Journal of Hydrogen Energy 33 (2008) : 5035–5044.

Yang, W.J., Park, S.K., Kim, T.S., Kim, J.H., Sohn, J.L. and Ro, S.T., Design performance analysis of pressurized solid oxide fuel cell/gas turbine hybrid systems considering temperature constraints. Journal of Power Sources 160 (2006) : 462–473.

Zhang, W., Croiset, E., Douglas, P.L., Fowler, M.W., Entchev, E., Simulation of a tubular solid oxide fuel cell stack using AspenPlus™ unit operation models. Energy Conversion and Management 46 (2005) : 181–196.

APPENDICES

APPENDIX A

THERMODYNAMIC DATA

Table A.1 Heat capacities of selected component ($C_{p)}$

Components	$C_p = a + bT + cT^2 + dT^3 + eT^4$[J/mol.K]				
	a	$b\times10^{-3}$	$c\times10^{-5}$	$d\times10^{-8}$	$e\times10^{-13}$
Ethanol	27.091	110.55	10.957	-15.046	466.01
Methane	34.942	-39.957	19.184	-15.303	393.21
Carbon monoxide	29.556	-6.5807	2.013	-1.2227	22.617
Carbon dioxide	27.437	42.315	-1.9555	0.39968	-2.9872
Water	33.933	-8.4186	2.9906	-1.7825	36.934
Hydrogen	25.399	20.178	-3.8549	3.188	-87.585
Nitrogen	29..342	-3.5395	1.0076	-4.3116	2.5935
Oxygen	29.526	-8.8999	3.8083	-3.2629	88.607

Table A.2 Heat of formation (H_f^0) and entropy (S^0) of selected component at standard state (298 K, 1 atm)

Components	H_f^0 (kJ/mol)	S^0 (J/mol.K)
Ethanol	-234.95	283.00
Methane	-74.52	186.27
Carbon monoxide	-110.53	197.70
Carbon dioxide	-393.51	213.80
Water	-241.82	188.80
Hydrogen	0.00	130.70
Nitrogen	0.00	191.60
Oxygen	0.00	205.20

APPENDIX B

DETERMINING GIBBS ENERGY AND EQUILIBRIUM CONSTANT

B1. Determining Gibbs energy (G) at any temperatures by equations below:

$$G = H - TS \quad \text{(B1)}$$

$$dG = dH - d(TS) \quad \text{(B2)}$$

Take integration to the equation above:

$$\int dG = \int dH - \int d(TS) \quad \text{(B3)}$$

$$G_T - G_{STD} = \int_{298}^{T} dH - \int_{298}^{T} d(TS) \quad \text{(B4)}$$

$$H_f(T) = H_f^0 + \int_{298}^{T} C_p dT \quad \text{(B5)}$$

$$S(T) = S^0 + \int_{298}^{T} \frac{C_p}{T} dT \quad \text{(B6)}$$

B2. Determining the equilibrium constant (*K*)

$$G_T = RT \ln K \quad \text{(B7)}$$

Rearrange the above equation;

$$K = exp\left(-\frac{G_T}{RT}\right) \quad \text{(B8)}$$

And from thermodynamic concept

$$K = \prod a_i^{vi} \tag{B9}$$

For gas phase is considered, we can substitute activity with partial pressure term

$$K = \prod \left(\phi_i y_i \frac{P}{P^0} \right)^{vi} \tag{B10}$$

Since it was studied at the pressure of 1 atm, the equation (B10) became the following equation:

$$K = \prod (y_i)^{vi} \tag{B11}$$

From equation (B11), the converted moles associated to the reactions involved in the production of hydrogen from steam reforming (x_1, x_2, and x_3) can be calculated.

APPENDIX C

DETAIL OF DESIGN SPEC

C1. Determining the cell efficiency

The electrochemical model of SOFC is solved by determining the cell efficiency for given the fuel utilization (U_f) at 85%. The flow diagram of numerical solution for calculating the cell performance is shown in Figure C1.

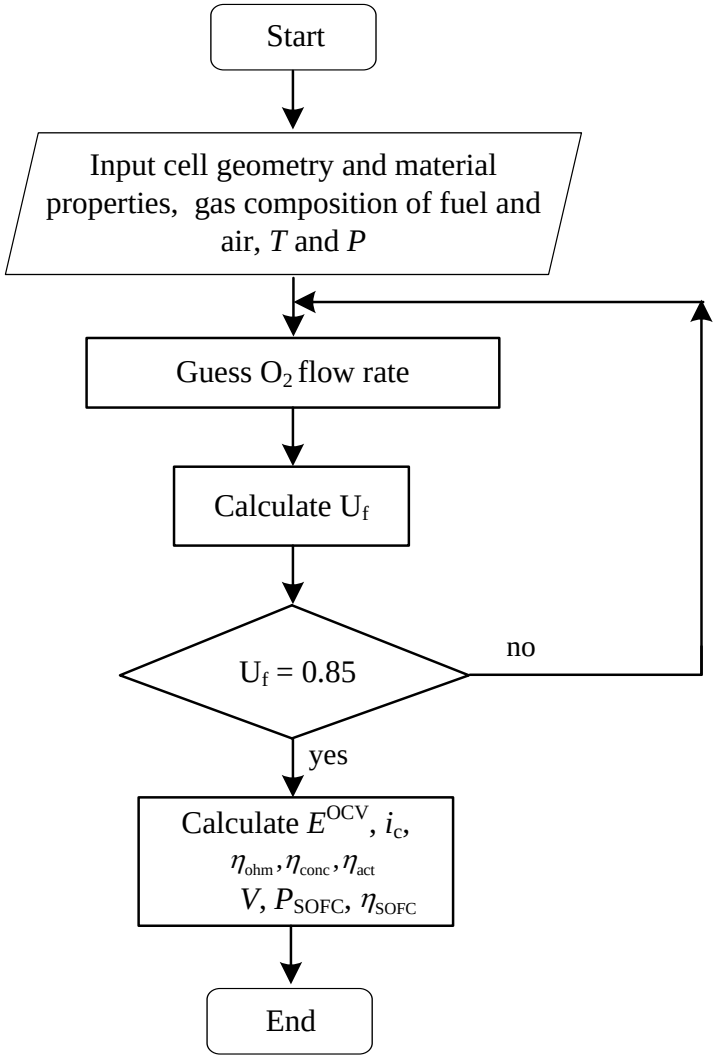

Figure C1. Flow diagram of numerical solution for calculating the cell performance.

C2. Determining air flow rate to cathode side

To control the cell operating temperature operated an isothermal temperature, the requested air flow can be determined by using an AspenPlus™ *Design-spec* satisfying the heat released from the cell. The flow diagram of numerical solution for calculating an air flow rate is shown in Figure C2.

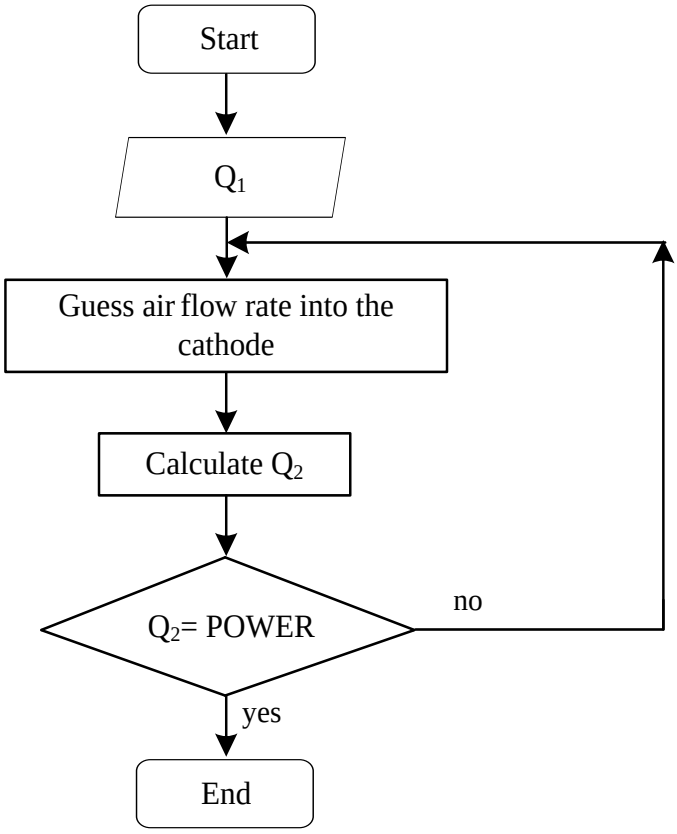

Figure C2. Flow diagram of numerical solution for calculating an air flow rate.

VITA

Miss Chollaphan Thanomjit was born on October 13, 1986 in Kamphaeng Phet, Thailand. After finished high school from Takhliprachason School, she entered King Mongkut's University of Technology Thonburi in May 2005 and received her Bachelor's Degree of Engineering in Chemical Engineering in April 2010. She began her graduate studies in May 2010 when she entered the Graduate School of Chulalongkorn University and joined the process control engineering group in the Department of Chemical Engineering, Faculty of Engineering, Chulalongkorn University.